COMPARATIVE STUDY OF THE MODULATED STRUCTURES IN Rb_2ZnBr_4 AND IN RELATED COMPOUNDS

COMPARATIVE STUDY OF THE MODULATED STRUCTURES IN Rb_2ZnBr_4 AND IN RELATED COMPOUNDS

Proefschrift

Ter verkrijging van de graad van
doctor in de technische wetenschappen
aan de Technische Hogeschool Delft,
op gezag van de Rector Magnificus,
prof.dr. J.M. Dirken,
in het openbaar te verdedigen
ten overstaan van het College van Dekanen
op dinsdag 13 mei 1986 te 14.00 uur

door

ARNOLDUS CORNELIS RUDOLPHUS HOGERVORST
geboren te Pijnacker
natuurkundig ingenieur

Dit proefschrift is goedgekeurd door de promotoren
prof.dr.ir. F. Tuinstra en prof.dr.ir. P.M. de Wolff

This work is part of the research program of the Stichting voor Fundamenteel Onderzoek der Materie (Foundation for Fundamental Research on Matter) and was made possible by financial support from the Nederlandse Organisatie voor Zuiver-Wetenschappelijk Onderzoek (Netherlands Organization for the Advancement of Pure Research).

aan Marleen
en aan mijn ouders

TABLE OF CONTENTS

Chapter 1

INTRODUCTION.

'The term "modulated structure" can be used to describe any periodic, or partially periodic perturbation of a crystal structure with a repetition distance appreciably greater than the basic unit cell dimensions.' Cowley et al. (1978) used this definition in defining the limits of the subject matter for one of the two international symposia entirely devoted to modulated structures. (The proceedings of the other one were edited by Tsakalakos, 1984.) The periodic perturbation is ment to be static. So a phonon, for instance, is not included in this definition.

The perturbation mentioned in the definition is found to apply to different physical quantities, for instance the direction of magnetic dipole moments (*magnetic modulation), the probability that in certain disordered* structures a crystallographic site is occupied by a given kind of atom (occupational modulation) or the atomic positions (displacive modulation, discussed in section 1.1).
Examples are abundant. They are found in organic crystals and in inorganic ones, in minerals and in synthetic crystals, in magnetic crystals and in non-magnetic ones, in insulators, in semiconductors and in conducting solids.

Structures with a partially periodic perturbation will not be considered here. The discussion will be restricted to structures with long range order perturbations.
Though there are structures of which the perturbation must be described by a *superposition of waves with different modulation wave vectors, in the present study only so-called 1-dimensionally modulated structures occur.*
A further restriction is made in that only structures with a displacive modulation will be considered.

Examples of structures with a displacive modulation are found in the structures of Rb_2ZnBr_4 and related compounds. These modulated structures on one hand show a variety of symmetries and modulation wavelengths, on the other hand their diffraction patterns - in particular those of different phases of the same compound - are strikingly similar. So one can assume that the modulation in all these phases has a common origin.

Indeed the purpose of the present work is to verify and substantiate that assumption. The approach chosen to achieve this is to study the modulated crystal structures in detail.

The scheme of this thesis is as follows. Chapter 2 describes the principles of a computer program by which details of the modulation in incommensurate as well as in commensurate crystals can be determined from diffraction data. Chapter 3 describes the determination of the modulated structures of three phases in Rb_2ZnBr_4. In chapter 4 these modulated structures are compared with the structures of related compounds, of which the structure determinations have been published, mostly in the last few years. Chapter 5 presents a model concerning the origin of the modulation in crystals of Rb_2ZnBr_4 and related compounds.

The rest of chapter 1 provides an introduction on several items. Section 1.1 introduces the concept of displacive modulation, whereas section 1.2 deals with the comparison of incommensurately versus commensurately modulated structures. Section 1.3 discusses the symmetry of incommensurate structures. Section 1.4 deals with the β-K_2SO_4 type structure. The modulated structures discussed in this thesis are modifications of this structures type.

1.1. Displacive modulation.

The crystal structures discussed in this thesis are modulated by a displacement wave. Figure 1.1.1 shows a simple structure with a displacive modulation, together with a non-modulated one. In the normal structure (figure 1.1.1a) $\underline{a}$ and $\underline{c}$ are two of the three unit cell vectors of the crystal structure. The position of the atom in unit cell n is given by

$$\underline{x}_n = \underline{n} + \underline{x}_o \qquad (1.1.1)$$

where $\underline{n}$ is the position vector of unit cell n, and $\underline{x}_o$ is the vector that gives the position of the atom within the unit cell.
In the modulated structure the position of the atom in the unit cell is not equal for all unit cells. The displacive modulation wave causes the position of the atom in cell n to become

$$\underline{x}_n' = \underline{n} + \underline{x}_o + \underline{d}((\underline{n}+\underline{x}_o).\underline{q}) \ . \qquad (1.1.2)$$

Vector $\underline{d}(t)$, the modulation displacement, has three components $d_i(t)$ (i=1,2,3) with respect to $\underline{a}$, $\underline{b}$ and $\underline{c}$, which are called the modulation functions of the atom. These modulation functions are periodic with period 1, and have zero mean value.

The cell spanned by $\underline{a}$, $\underline{b}$ (not shown in figure 1.1.1) and $\underline{c}$ is called subcell of the modulated structure. If more atoms are present in the subcell, then each of these atoms has its own modulation functions. In equation 1.1.2 $\underline{q}$ is the modulation wave vector, which can be written as

$$\underline{q} = \alpha\underline{a}^* + \beta\underline{b}^* + \gamma\underline{c}^* \ . \qquad (1.1.3)$$

$\underline{a}^*$, $\underline{b}^*$ and $\underline{c}^*$ are the vectors reciprocal to the set subcell vectors $\underline{a}$, $\underline{b}$ and $\underline{c}$. The wavelength of the modulation wave is equal to

$$\lambda = 1/|\underline{q}| \ . \qquad (1.1.4)$$

The modulation discussed here is a so-called 1-dimensional modulation: just one modulation wave vector is needed to describe the modulation. This is the most frequently occurring type of modulated structure, and it is the only type occurring in the group of compounds to be studied.

The extra periodicity in the structure is the origin of extra reflections in the diffraction pattern. The extra reflections are called satellite reflections. In contrast, the normal ones are called main reflections. Figures 1.1.1c and 1.1.1d show the diffraction patterns of the structures of figures 1.1.1a and 1.1.1b respectively. The reflections of the modulated structure are indexed using four integer indices h, k, l and m, instead of the usual three for non-modulated structures. The diffraction vectors are given by

$$\underline{H} = \underline{h} + m\underline{q} \ , \qquad (1.1.5)$$

$$\text{with } \underline{h} = h\underline{a}^* + k\underline{b}^* + l\underline{c}^*. \qquad (1.1.6)$$

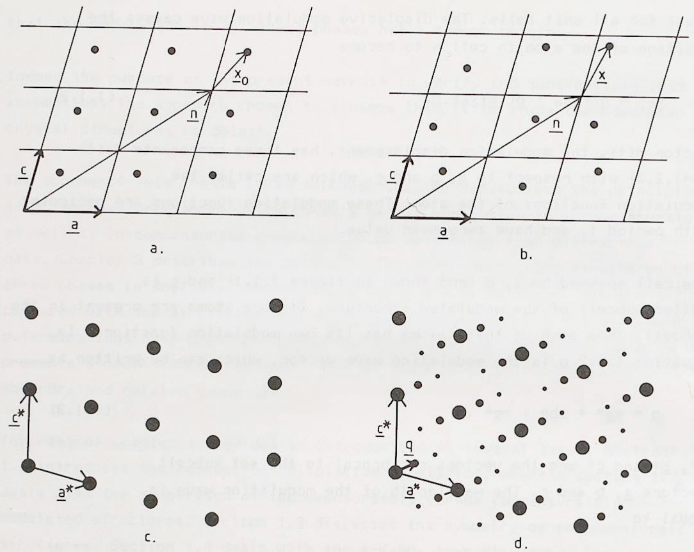

FIGURE 1.1.1. A non-modulated crystal structure (a), a structure with a displacive modulation (b), and the diffraction patterns of both structures (c and d respectively). In part d the large, medium size and small dots are main reflections, first order satellite reflections and second order satellites respectively. $\underline{q}$ is the modulation wave vector.

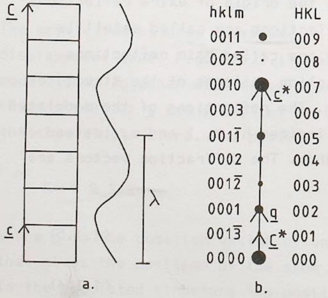

FIGURE 1.2.1. The basic structure and a modulation function of a modulated structure with a rational modulation wave vector ($\underline{q}=2\underline{c}^*/7$) (a) and its diffraction pattern (b). The reflections can be indexed either with respect to $\underline{a}^*$, $\underline{b}^*$, $\underline{c}^*$ and $\underline{q}$ (hklm), or with respect to the supercell vectors $\underline{a}^*$, $\underline{b}^*$ and $\underline{C}^*$ (HKL).

If for a reflection $m=0$, this reflection is a main reflection. If $|m|=n\neq 0$ then it is a n-th order satellite.

For a given structure the modulation wave vector $\underline{q}$ is not unique. It can be replaced by $\underline{q}+\underline{h}$, $\underline{h}$ being any reciprocal lattice vector (1.1.6). Of course, thereby both the functions $\underline{d}(t)$ and the satellite indices are changed, but 1.1.2 remains valid. For more information about the subject of equivalent wave vectors the reader is referred to De Wolff et al. (1984) and to subsection 4.2.1. of this thesis.

From a modulated structure two hypothetical normal structures can be derived. The first one is the so-called basic structure. This structure corresponds to the case $\underline{d}(t)=\underline{0}$ in equation 1.1.2. For the modulated structure of figure 1.1.1b the basic structure is the one of figure 1.1.1a. The second hypothetical structure is the so-called average structure, which has the same Bravais lattice as the basic structure. The contents of the unit cell of this structure can be obtained by averageing the contents of all subcells of the modulated structure. If a Fourier synthesis is performed, using only the main reflections, then one finds the average structure.

The atomic positions in the modulated structure are completely defined by equation 1.1.2 if the following data are known:

- the lengths of the unit cell vectors $\underline{a}$, $\underline{b}$ and $\underline{c}$ of the basic structure and the angles between them,
- the atomic positions $\underline{x}_0$ of the atoms in the basic structure,
- the modulation wave vector components α, β and γ (see equation 1.2.4) and
- the modulation functions $d_i(t)$ (i=1,2,3) for all atoms in the basic structure unit cell, for instance in terms of Fourier coefficients.

1.2. Incommensurate versus commensurate modulation.

In order to simplify the discussion, α and β in equation 1.1.3 will be assumed to be zero. The modulation wave vector is then parallel to $\underline{c}^*$:

$$\underline{q} = \gamma\underline{c}^* . \qquad (1.2.1)$$

This is the situation in the crystal structures discussed in this thesis. In the previous section nothing is mentioned about the properties of γ. Now an important distinction is introduced. We shall - at least formally - distinguish between cases where γ is rational and those in which γ is irrational.

If γ is rational, it can be written as

$$\gamma = u/v \ , \tag{1.2.2}$$

with u and v mutually prime positive integers and $u<v$. Then u modulation wavelengths fit exactly in v subcell periods. The modulation is commensurate with the basic structure in this case. This is illustrated in figure 1.2.1a for $\gamma=2/7$. A v-fold supercell can be chosen as unit cell of the structure, and this superstructure can be treated as a normal structure, without using the modulation concept. Hence for this superstructure the reflections can be indexed either by three indices based on the large unit cell, or with four indices, based on the description as a modulated structure. This is illustrated in figure 1.2.1b for the example with $\gamma=2/7$.

If, however, γ is irrational, the modulation is incommensurate with the basic structure, and the modulated structure is called incommensurate.

Crystals with modulated structures very often show the following behaviour as a function of temperature. Above a certain temperature T_i the crystal structure is normal (non-modulated). Below T_i the structure is modulated. Down to a certain temperature T_c this modulation is incommensurate and below T_c it is commensurate. The modulation wave vectors of the incommensurate structure and the superstructure usually do not differ much. In the incommensurate phase the modulation wave vector usually changes continuously; at T_c it jumps to the commensurate value. Temperature T_c is called the lock-in phase transition temperature, and the superstructure phase the lock-in phase.

Diffraction experiments can be used to examine whether a modulated structure is incommensurate or commensurate. If such an experiment shows that γ, in equation 1.2.1, for a certain crystal phase varies continuously as a function of temperature (or as a function of pressure or another physical condition), then is is almost certain that the structure of that phase is incommensurate. The possibility exist, however, that this conclusion is wrong, because such a behaviour of the modulation wave vector can be found also if the crystal has a few successive superstructure phases (with nearly the same modulation wave vector), while the phase transitions between these phases do not occur at the same moment for each part of the crystal. This can be caused by impurities or defects in the structure or by temperature gradients in the crystal. The measured modulation wave vector is the weighted average of the modulation wave vectors of the superstructure phases, the weight for each commensurate modulation wave vector being the volume fraction of te crystal occupied by the corresponding phase. For instance, Gesi and Iizumi (1978) first assumed a continuous behaviour for the modulation wave vector of Rb_2ZnBr_4 just above T_c. Later, however, they observed that γ changes stepwise (Iizumi and Gesi, 1983).

If γ does not change in a certain temperature region, and γ is equal to a simple rational value (e.g. 1/4, 2/7 or 3/10) within experimental error, then the structure is very probably a superstucture. But there is always the possibility that the measurements are not accurate enough to reveal that γ deviates from this rational value.

If γ is constant at a value that is not a simple fraction, then γ is either equal to a rational value with a large denominator (e.g. 23 or 29) or is irrational. In the last case the modulation wavelength may be pinned at a certain incommensurate value (e.g. the equilibrium value at the conditions under which the crystal has been grown or annealed) by defects in the crystal. More accurate measurements of γ or measurements on crystals that are prepared in another way may give more information.

In the definition mentioned at the beginning of chapter 1, it is not defined exactly how large the repetition distance in a crystal structure must be in order to consider it as a modulated structure. Often, a superstructure with a 3-fold or larger supercell is called a modulated structure. It will be shown in chapter 4 that it can be convenient to consider structures with smaller repetition distances also as modulated.

1.3. Symmetry in incommensurate crystal structures.

Because of the extra periodicity of the modulation, which destroys the periodicity in at least one dimension, the symmetry of an incommensurate crystal structure cannot be described by a normal 3-dimensional space group. 4-dimensional space groups can be used to give full account of the symmetry of incommensurate 1-dimensionally modulated structures. Only certain 4-dimensional space groups represent symmetries of such structures. These 4-dimensional space groups are called superspace groups by Janner and Janssen (1979). In this thesis the term "superspace group" will not be used further, because it can easely be confused with "superstructure space group" (the 3-dimensional space group of a superstructure), which will be used often. Instead, a 4-dimensional space group that represents the symmetry of an incommensurate structure will merely be called the 4-dimensional space group of that structure.

The reader is referred to De Wolff et al. (1981) for a full treatment on the symmetry of incommensurate 1-dimensionally modulated crystal structures and for a complete list of the 4-dimensional space groups of such structures. This section only provides a short introduction. It is only concerned with those items which are relevant for this thesis.

Consider an atom A with basic structure position $\underline{x}_0$ and modulation functions $\underline{d}(t)$ and atom A′ with basic structure position $\underline{x}_0'$ and modulation functions $\underline{d}'(t)$. A symmetry operation relating atom A′ to A has the form

$$\begin{pmatrix} \underline{x}_0' \\ t' \end{pmatrix} = \begin{pmatrix} R & 0 \\ 0 & \varepsilon \end{pmatrix} \begin{pmatrix} \underline{x}_0 \\ t \end{pmatrix} + \begin{pmatrix} \underline{s} \\ \tau \end{pmatrix} . \qquad (1.3.1)$$

The first part of this operation,

$$\underline{x}_0' = R\underline{x}_0 + \underline{s} \quad , \qquad (1.3.2)$$

transforms the basic structure position of atom A into that of A′. It is a normal 3-dimensional symmetry operation. The 3x3 matrix R is the point group operation and $\underline{s}$ is the additional shift.

The second part,

$$t' = \varepsilon t + \tau \, , \qquad (1.3.3)$$

tells us how the modulation functions are related, namely as

$$\underline{d}'(t) = R\underline{d}(\varepsilon(t-\tau)) \quad . \qquad (1.3.4)$$

ε can be 1 or −1 only. $\varepsilon=1$ if R transforms the modulation wave vector $\underline{q}$ into itself, and $\varepsilon=-1$ if $\underline{q}$ is transformed into $-\underline{q}$:

$$R\underline{q} = \varepsilon\underline{q} \quad . \qquad (1.3.5)$$

According to 1.3.4 the modulation functions of atom A′ can be found from those of atom A by shifting the modulation functions of A over $\tau\lambda$ (λ is the modulation wavelength). Moreover, if $\varepsilon=-1$ one has to change the sign of the argument of the modulation functions, so that those of A and A′ run in opposite directions. In both cases ($\varepsilon=1$ and $\varepsilon=-1$), the direction of the displacement vector is transformed by R.

Two operations will be illustrated: c(s) and n($\bar{1}$).

Figure 1.3.1a illustrates the operation c(s), which for a particular choice of axes and origin can be written as

$$c(s): \; (R,\underline{s},\varepsilon,\tau) = \left(\begin{pmatrix} -1 & 0 & 0 \\ 0 & 1 & 0 \\ 0 & 0 & 1 \end{pmatrix} , \begin{pmatrix} 1 \\ 0 \\ 0.5 \end{pmatrix} , 1 , 0.5 \right) . \qquad (1.3.6)$$

The c in the symbol c(s) indicates that the basic structure part of the symmetry operation is a c-glide plane. The s in the symbol means that $\varepsilon=1$ and that the modulation functions have to be shifted over 0.5λ. In figure 1.3.1a it can be seen that the modulation functions of atom A′ are shifted over 0.5λ with respect to those of atom A. Because $R_{11}=-1$, moreover the sign of $d_1(t)$ is reversed.

In figure 1.3.1b the operation

$$n(\bar{1}): \; (R,\underline{s},\varepsilon,\tau) = \left(\begin{pmatrix} 1 & 0 & 0 \\ 0 & 1 & 0 \\ 0 & 0 & -1 \end{pmatrix} , \begin{pmatrix} 0.5 \\ 0.5 \\ 1 \end{pmatrix} , -1 , 0.5 \right) \qquad (1.3.7)$$

is shown. The basic structure part of this operation is a n-glide plane. The $\bar{1}$ in symbol n($\bar{1}$) means $\varepsilon=-1$. In that case the value of τ cannot be derived from the symbol n($\bar{1}$), but it follows from the choice of the phase of the modulation wave with respect to the origin or, seeing it from another point of view, from the choice of origin in the modulated structure. Note that s_3 in this example and s_1 in the previous one are also origin-dependent. Figure 1.3.1b shows that the modulation functions of atom A′ are derived from those of atom A by changing the sign of the argument of

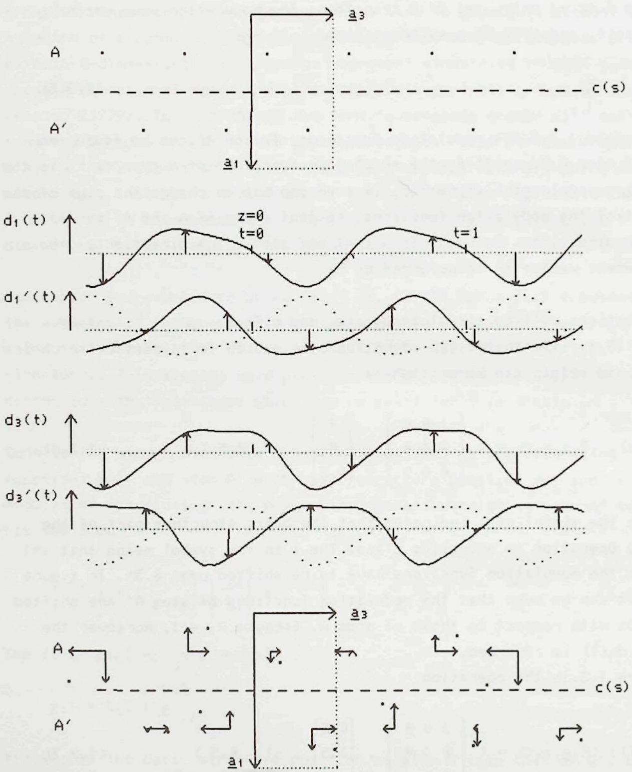

a.

FIGURE 1.3.1. Two examples of symmetry operations in a structure with displacement modulation. In each example the symmetry operation transforms atom A, with modulation functions $d_1(t)$ and $d_3(t)$, into atom A′, with modulation functions $d_1'(t)$ and $d_3'(t)$.
a. symmetry operation

$$c(s): (R,\underline{s},\varepsilon,\tau) = \left(\begin{bmatrix} -1 & 0 & 0 \\ 0 & 1 & 0 \\ 0 & 0 & 1 \end{bmatrix} , \begin{bmatrix} 1 \\ 0 \\ 0.5 \end{bmatrix} ,1 ,0.5 \right)$$

shown are: the undistorted structure, the modulation functions and the modulated structure;

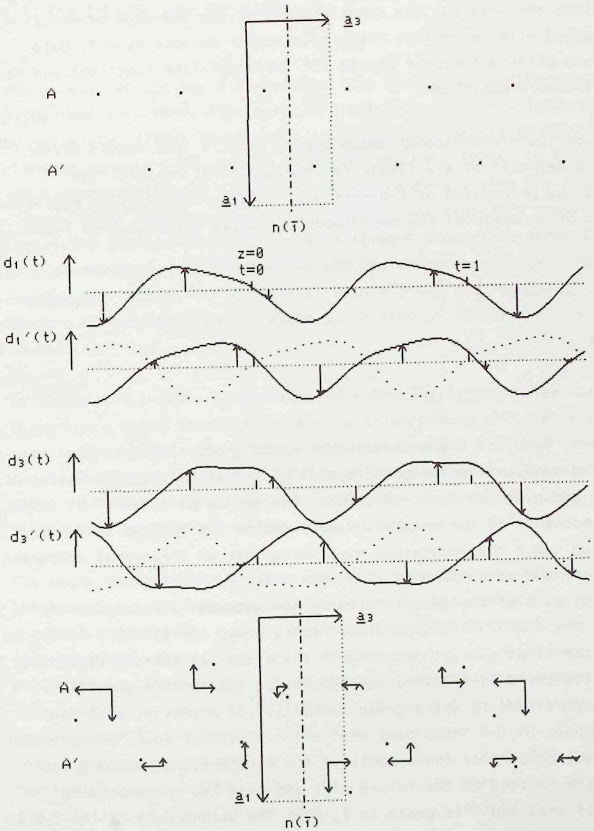

b.

Figure 1.3.1 b. Symmetry operation

$$n(\bar{1}): (R,\underline{s},\varepsilon,\tau) = \left(\begin{vmatrix} 1 & 0 & 0 \\ 0 & 1 & 0 \\ 0 & 0 & -1 \end{vmatrix} , \begin{vmatrix} 0.5 \\ 0.5 \\ 1 \end{vmatrix} ,-1 ,0.5 \right)$$

The dotted functions show $d_1'(t)$ and $d_3'(t)$ before the shift $\tau\lambda$ is applied.

these functions and shifting the functions over 0.5λ. The sign of $d_3'(t)$ has been changed with respect to the sign of $d_3(t)$ because $R_{33}=-1$. Note that there are different mirror planes for the modulation functions and for the basic structure positions.

The symbols of the 4-dimensional space groups used in this thesis differ from those in De Wolff et al. (1981) for typographical reasons. The notation and the properties of 4-dimensional space groups will be explained with the aid of an example: The most important space group in this thesis is

$$P\,\frac{2_1}{c}\,\frac{2_1}{m}\,\frac{2_1}{n}\,(00\gamma)\,(\frac{\bar{1}}{s}\,\frac{\bar{1}}{s}\,\frac{1}{\bar{1}}) \qquad (1.3.8a)$$

or in short:

$$Pcmn(00\gamma)(ss\bar{1}). \qquad (1.3.8b)$$

The first part, Pcmn, of the 4-dimensional space group symbol is the (standard) 3-dimensional space group symbol (International Tables Volume A) of the space group of the basic structure. The second part in 1.3.8, (00γ), gives the components of the modulation wave vector (as defined in 1.1.3). In space group 1.3.8 the modulation wave vector has an irrational component parallel to $\underline{c}^*$, and no components along the other two directions. The third and last part of the symbol tells us how modulation functions are transformed. The symbol of an individual space group operation is formed by a symbol of the first part, together with the symbol at the corresponding position in the third part. Hence the symbols of the three 4-dimensional space group operations in space group symbol 1.3.8b are c(s), m(s) and n($\bar{1}$). The symbols in the third part of the 4-dimensional space group symbol (and in the second part of the symbols of the 4-dimensional space group operations) are related to the values of ε and τ of the corresponding operations. If ε=+1 and τ is equal to 0, then the second part of the symbol of the 4-dimensional space group is (1) (example: $2_1(1)$ in 1.3.8a). If ε=+1 and τ=0.5 then the second part of the symbol is (s) (examples: c(s) and m(s) in 1.3.8a and 1.3.8b). If ε=-1, the second part of the symbol of the 4-dimensional space group operation is always ($\bar{1}$).

Rules for systematically absent reflections for incommensurate crystal structures also involve the satellite reflections (De Wolff et al., 1981).

1.4. The β-K_2SO_4 type structure.

The crystal structures discussed in this thesis are modifications of the β-K_2SO_4 type structure. (The structure determination of β-K_2SO_4 has been done by McGinnety ,1972.) The β-K_2SO_4 type structure occurs in many compounds of chemical formula A_2BX_4 (see e.g. Muller and Roy, 1974). In this formula B and X represent single atoms while A can represent also NH_4 or $N(CH_3)_4$ (Tetra Methyl Ammonium, TMA). The β-K_2SO_4 type structure consists of negatively charged BX_4 groups and positive A atoms (NH_4 and $N(CH_3)_4$ will also be designated as "A atoms"). The BX_4 groups are in good approximation regular tetrahedra. The X atoms of such a group are located at the four corners of the tetrahedron, while the B atom is located at the barycentre of it.

In figure 1.4.1 three projections of a β-K_2SO_4 type structure are shown. This figure shows the contents of the orthorhombic unit cell: four BX_4 groups and eight A atoms. Of each BX_4 group the B atom and two X atoms (X_1 and X_2 in figure 1.4.1) are located on a mirror plane. The other two X atoms (X_3 and X_4) are related to each other by te mirror plane operation. The A atoms are all located on mirror planes.

The space group of the β-K_2SO_4 type structure is Pcmn. Figure 1.4.1d shows the symmetry operations of this space group. The symbol Pcmn corresponds to the choice of axes $\underline{a}$, $\underline{b}$ and $\underline{c}$ as shown in figure 1.4.1. If the axes would have been labelled in another way, as is often done in other publications, then another space group symbol should have been used. In this thesis the axes will be labelled throughout in the manner followed by De Pater (1978) and Rasing (1982) shown in figure 1.4.1d.
The symmetry-independent atoms are A_1, A_2, B, X_1, X_2 and X_3. If A represents NH_4 or $N(CH_3)_4$, then the position of this group is defined to be the position of the nitrogen atom.

More information about the β-K_2SO_4 type structure can be found in Muller and Roy (1974) and Eysel (1971).

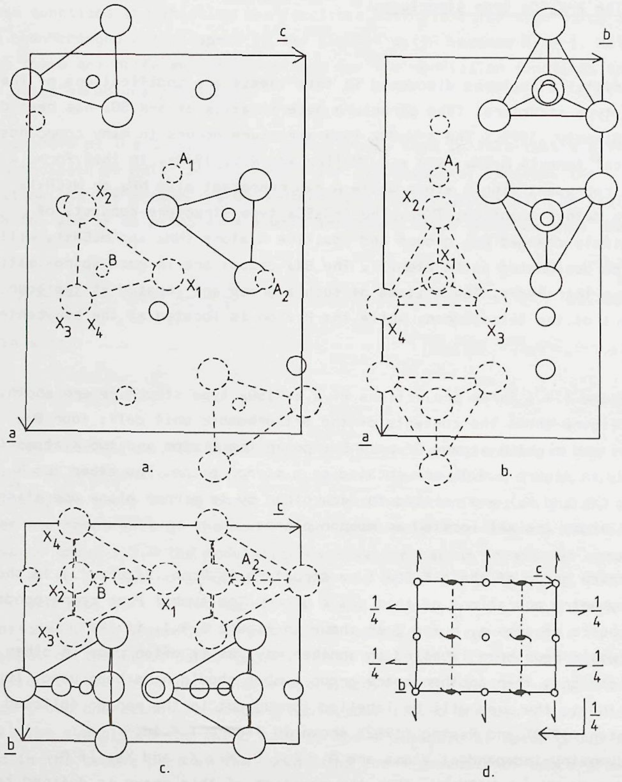

FIGURE 1.4.1. Three projections of a β-K_2SO_4 type crystal structure (a, b and c) and its space group operations (d). The structure shown is that of $(NH_4)_2ZnCl_4$ at 418K (Matsunaga, 1982).

Chapter 2

DETERMINATION OF MODULATED STRUCTURES.

2.1. Introduction.

Whereas many computer programs are available for normal crystal structures, at the beginning of the work described in this thesis, none was available for incommensurate structures . Therefore a computer program has been written for the most frequently occurring type of incommensurate crystal structures (1-dimensional modulation).
In 1983 a computer program for modulated structures written by Yamamoto became available. This program has a larger scope than the program discussed in this chapter. For instance, it is not limited to the case of 1-dimensional modulation. For the structure determinations of this thesis (chapter 3), the program discussed in this chapter has been used.

Additional features are needed in a computer program for modulated crystal structures because

- extra parameters are necessary for modulated structures in order to describe the modulation,
- the symmetry is more extended for modulated structures: it also involves the modulation functions,
- the structure factor calculation is more complex for modulated structures,
- moreover, the number of reflection indices is different: 4 for structures with a 1-dimensional modulation and 3 for normal structures.

The computer program discussed in this chapter can handle structures with a displacive modulation (discussed in section 1.1) as well as structures with a so-called occupational modulation, or structures with a combination of the two types of modulations. The discussion in this chapter will be limited to the first type of modulation.

Two refinement methods are incorporated in the computer program: the least squares procedure and the simplex method (Nelder and Mead, 1965; not used for this thesis). Both methods minimize the sum of weighted squared differences between calculated and observed structure amplitudes:

$$\sum_{r} w_r(F_{or}-|F_{cr}|)^2 \quad , \tag{2.1.1}$$

where F_{or} is the observed structure amplitude, $|F_{cr}|$ is the calculated structure amplitude, w_r is the weight and the summation is over all measured X-ray or neutron reflections.
The simplex method has the advantage that the starting values of the parameters need not be close to the values of the solution, but the disadvantage that it needs very much more computation time than the least squares procedure.

In section 2.2 a new derivation of the structure factor formula for modulated structures is given. Section 2.3 will show how the symmetry of modulated structures is treated in the program. Section 2.4 will explain how superstructures can also be handled with the computer program.

2.2. The structure factor.

In this section the unit cell vectors $\underline{a}$, $\underline{b}$ and $\underline{c}$ of the basic structure are denoted as $\underline{a}_i$ with i=1,2,3 respectively, for convenience. Also, the reflection indices h, k and l are denoted as h_1, h_2 and h_3, and the components α, β and γ of the modulation wave vector (defined in equation 1.1.3) as q_1, q_2 and q_3.

For a modulated structure, the structure factor $F(\underline{H})$ can be written as

$$F(\underline{H}) = \sum_{a} f_a(|\underline{H}|).T_a(\underline{H}).G_a(\underline{H}) \quad . \tag{2.2.1}$$

The summation is over all atoms in the unit cell of the basic structure. The atomic scattering factor $f_a(|\underline{H}|)$ of atom a is as for normal structures (including the dispersion correction). $\underline{H}$ is given by equation 1.1.5.
The expression for the temperature factor $T_a(\underline{H})$ is identical to the one for normal structures:

$$T_a(\underline{H}) = \exp(-2\pi^2 U_a|\underline{H}|^2) \tag{2.2.2}$$

for the isotropic temperature factor, whereas for the anisotropic temperature factor:

$$T_a(\underline{H}) = \exp(-2\pi^2 \sum_{i=1}^{3} \sum_{k=1}^{3} U_{aik}\, H_i\, a_i^*\, H_k\, a_k^*) \quad . \tag{2.2.3}$$

U_a and U_{aik} (i,k=1,2,3) are the isotropic temperature parameter and the anisotropic temperature parameters respectively and $H_i=h_i+mq_i$ (i=1,2,3) are the components of the diffraction vector $\underline{H}$.
It is not possible to modulate the temperature factor in the computer program discussed here. This means that the thermal motion of an atom is taken to be the same as that of the equivalent atom in any other subcell.
The geometrical part of the structure factor $G_a(\underline{H})$ for modulated structures differs from the geometrical part of the stucture factor for normal structures. De Wolff (1974) derived in a very elegant manner an expression for $G_a(\underline{H})$, using a crystal description in four dimensions.
In this section this expression will be derived via the expression for the geometrical part of the structure factor for superstructures. This has the advantage that the relation between both expressions becomes clear. The results will be used in section 2.4 to show how to calculate the structure factor for superstructures exactly, using the formula for incommensurate structures.

The geometrical part of the structure factor of reflection $\underline{h}$ of a normal (non-modulated) crystal structure is

$$G_a(\underline{h}) = \exp(2\pi i\underline{h}.\underline{x}_{oa}) \quad , \tag{2.2.4}$$

in which $\underline{x}_{oa}$ is the position of atom a:

$$\underline{x}_{oa} = \sum_{i=1}^{3} x_{oai}\underline{a}_i \tag{2.2.5}$$

and $\underline{h}$ is the diffraction vector:

$$\underline{h} = \sum_{i=1}^{3} h_i\underline{a}_i^* \text{ , } h_i \text{ integer .} \tag{2.2.6}$$

Though it is not conventional, the same (normal) structure can be described as a v-fold superstructure with supercell axes $v_1\underline{a}_1$, $v_2\underline{a}_2$ and $v_3\underline{a}_3$ (v_1,v_2,v_3: integer, $v=v_1v_2v_3$). The diffraction vectors $\underline{h}'$ of the superstructure are

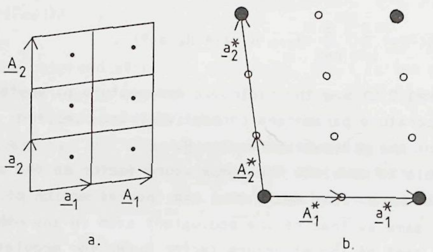

FIGURE 2.2.1.
a. Superstructure with six equal subcells. $\underline{A}_1$ and $\underline{A}_2$ are the superstructure unit cell vectors.
b. The corresponding reciprocal latice. *The full and open* circles are reflections with non-zero and zero intensity respectively.

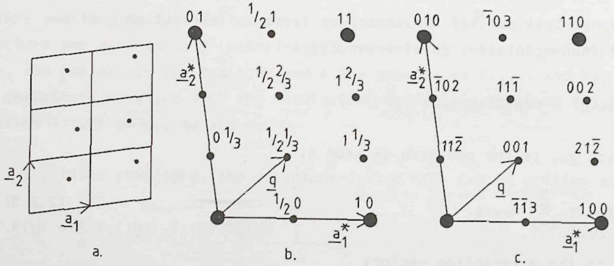

FIGURE 2.2.2.
a. The superstructure after modification by a displacive modulation with wave vector $\underline{q}$.
b. The corresponding reciprocal lattice. All indicated reflections have non-zero intensity.
c. As b, but with new indices. Three indices are *needed for* a 2-dimensional crystal in the new notation.

$$\underline{h}' = \sum_{i=1}^{3} j_i(\underline{a}_i^*/v_i) \quad . \qquad (2.2.7)$$

Here j_i can be any integer, but intensities are observed only if j_i is a multiple of v_i for $i=1,2,3$. The other positions in reciprocal space have zero intensities because all the subcells in this unusual superstructure are equal. The geometrical part of the structure factor of diffraction vector $\underline{h}'$ is

$$G_a(\underline{h}') = \frac{1}{v} \sum_{k=1}^{v} \exp(2\pi i \underline{h}'.[\underline{x}_{oa}+\underline{e}_k]) \quad , \qquad (2.2.8)$$

in which $\underline{e}_k$ are the v "centering translations" in the supercell (to which $\underline{0}$ is added), numbered by k in an arbitrary sequence:

$$\underline{e}_k = \sum_{i=1}^{3} e_{ki}\underline{a}_i \quad , \; e_{ki} \text{ integer with } 0 \le e_{ki} < v_i \quad . \qquad (2.2.9)$$

The factor $1/v$ in equation 2.2.8 makes $G(\underline{h}')=G(\underline{h})$ (equations 2.2.8 and 2.2.4).
Figure 2.2.1 gives a 2-dimensional example of such a superstructure.

Now consider the positions of the atoms to be displaced in a special manner, so that the artificial superstructure becomes a real one:

$$\underline{x}_{oa}+\underline{e}_k \quad \text{becomes} \quad \underline{x}_{oa}+\underline{e}_k+\underline{d}_a(\varphi_{ka}) \qquad (2.2.10)$$

$$\text{with } \varphi_{ka} = (\underline{x}_{oa}+\underline{e}_k).\underline{q} \qquad (2.2.11)$$

$$\text{and } \underline{q} = \sum_{i=1}^{3} \frac{u_i}{v_i}\underline{a}_i^* \quad , \; u_i, v_i\text{: positive integers .} \qquad (2.2.12)$$

$\underline{d}_a(\varphi_{ka})$ is the displacement of atom a in subcell k according to a static displacement wave with wave vector $\underline{q}$. The functions $\underline{d}_a(t)$ are periodic with period 1 ($\underline{d}_a(t)=\underline{d}_a(t+1)$). The wave vector $\underline{q}$ is commensurate with the original lattice according to equation 2.2.12. u_i and v_i are mutually prime integers with $u_i<v_i$ for each i. It can be verified that the unit cell vectors of the superstructure, $v_i\underline{a}_i$, are *translation vectors in the new structure. For the example of figure 2.2.1* the situation after displacing the atoms corresponding to a displacive modulation wave with $\underline{q}=\underline{a}_1^*/2+\underline{a}_2^*/3$ is given in figure 2.2.2.

The geometrical part of the structure factor is now

$$G_a(\underline{h}') = \frac{1}{v} \sum_{k=1}^{v} \exp(2\pi\underline{h}'.[\underline{x}_{oa}+\underline{e}_k+\underline{d}_a(\varphi_{ka})]) \quad . \qquad (2.2.13)$$

where in general all reflections, including those with one or more non-integer indices with respect to $\underline{a}_1{}^*$, $\underline{a}_2{}^*$ and $\underline{a}_3{}^*$, will have non-zero structure factors.

As shown in section 1.1, the diffraction vectors can be written in another way (equation 1.15):

$$\underline{H} = \underline{h}+m\underline{g} \quad , \text{ m integer } , \qquad (2.2.14)$$

where $\underline{h}$ is given by equation 2.2.6. Reflections with m=0 are main reflections, those with m≠0 are satellites. m is the order of the satellite. For a 3-dimensional crystal four indices are needed to denote a reflection in this notation: h_1, h_2, h_3 and m. If v_1, v_2 and v_3 are pairwise mutually prime, so that their smallest common multiple w is equal to $v=v_1v_2v_3$, then 2.2.14 gives all diffraction vectors of 2.2.7. If $w<v$, the new notation cannot cover *all* the reflections which are given by 2.2.7. In that case, apart from $\underline{0}$, also one or more of the other $\underline{e}_k$ are translations of the modulated structure. These centering translations give rise to systematically absent reflections, which are exactly those superstructure reflections which are not covered by 2.2.14. In appendix A this will be proved.
Figure 2.2.2b and 2.2.2c show the diffraction pattern for the example of figure 2.2.2a with the fractional indices of the old notation and with the new indices respectively.

In terms of the new notation, the geometrical part of the structure factor becomes

$$G_a(\underline{h}+m\underline{g}) = \frac{1}{v} \sum_{k=1}^{v} \exp(2\pi i(\underline{h}+m\underline{g}).[\underline{x}_{oa}+\underline{e}_k+\underline{d}_a(\varphi_{ka})]) \quad . \qquad (2.2.15)$$

This can be rewritten to give

$$G_a(\underline{h}+m\underline{g}) = \exp(2\pi i\underline{h}.\underline{x}_{oa})$$

$$. \frac{1}{v} \sum_{k=1}^{v} \exp(2\pi i[(\underline{h}+m\underline{g}).\underline{d}_a(\varphi_{ka})+m\varphi_{ka}+\underline{h}.\underline{e}_k]) \quad . \qquad (2.2.16)$$

Between the square brackets the last term is an integer, so it can be left out. In appendix A it will be proved that

$$\underline{e}_k.\underline{g} = r/w \quad (\text{mod } 1) \quad (r = 0,\ 1,\ 2,\ \dots\ w-1) \quad , \qquad (2.2.17)$$

and that each value of r occurs g times if k runs from 1 to v if

$$g = v/w \quad . \qquad (2.2.18)$$

(If the smallest common multiple w of v_1, v_2 and v_3 is v, then g=1 and every value of r occurs once.)
Hence equation 2.2.16 can be written as (see equations 2.2.11 and 2.2.17)

$$G_a(\underline{h}+m\underline{g}) = \exp(2\pi i\underline{h}.\underline{x}_{oa})$$

$$. \frac{1}{w} \sum_{r=1}^{w} \exp(2\pi i[(\underline{h}+m\underline{g}).\underline{d}_a(t_{ra})+mt_{ra}]) \qquad (2.2.19)$$

$$\text{with } t_{ra} = \underline{x}_{oa}.\underline{g} + r/w \quad . \qquad (2.2.20)$$

In order to approximate an incommensurate structure (in which $\underline{g}$ has non-rational components), a superstructure with a large supercell can be chosen. In the limit of an infinitely large supercell, the summation can be replaced by an integral, and the formula of De Wolff (1974) is obtained:

$$G_a(\underline{h}+m\underline{g}) = \exp(2\pi i\underline{h}.\underline{x}_{oa}) \int_0^1 \exp(2\pi i[(\underline{h}+m\underline{g}).\underline{d}_a(t)+mt])\,dt \quad . \qquad (2.2.21)$$

In this equation the boundaries of the integral are shifted with respect to those in the summation. This is allowed because the integrand is periodic with period 1.
Putting $\underline{d}_a(t)=\underline{0}$ for all atoms again gives the geometrical part of the structure factor for a normal crystal structure.

The periodic function $\underline{d}_a(t)$ can be written as a sum of fourier components (harmonics). In order to investigate the influence of the individual harmonics on the satellite reflections, the integral of 2.2.21 is written as

$$\int_0^1 \exp(2\pi i(\underline{h}+m\underline{g}).\underline{d}_a(t)) \exp(2\pi imt)\ dt \quad . \qquad (2.2.22)$$

For small $\underline{d}_a(t)$ the approximation $\exp(ix)=1+ix$ can be used for the first factor in the integrand, and 2.2.22 becomes

$$\int_0^1 (1 + 2\pi i(\underline{h}+m\underline{q}).\underline{d}_a(t)) \exp(2\pi imt)\,dt \;. \qquad (2.2.23)$$

In this expression the n-th harmonic of $\underline{d}_a(t)$ has a non-zero contribution only if m=n. Hence, the m-th harmonic of $\underline{d}_a(t)$ contributes only to m-th order satellites. If $\underline{d}_a(t)$ is larger, then the approximation is not valid. Usually, however, $\underline{d}_a(t)$ is small enough to state that the m-th harmonic of $\underline{d}_a(t)$ mainly contributes to m-th order satellites.

In the computer program the integral of 2.2.21 is approximated by a summation:

$$\frac{1}{n} \sum_{i=1}^{n} \exp(2\pi i[(\underline{h}+m\underline{q}).\underline{d}_a(t_{ia})+mt_{ia}]) \qquad (2.2.24)$$

$$\text{with } t_{ia} = \underline{x}_{oa}.\underline{q} + i/n \;. \qquad (2.2.25)$$

The value for n has to be chosen large enough to get a good approximation. For the room temperature structure of Rb_2ZnBr_4 (chapter 3 of this thesis) n=7 is found to be large enough.
In section 2.4 it will be discussed how 2.2.24 can be used for superstructures.
For incommensurate structures the first term on the right hand side of 2.2.25 can be left out.

2.3. Symmetry.

If symmetry is taken into account, equation 2.2.1 can be written as

$$F(\underline{H}) = \sum_a f_a(|\underline{H}|) \frac{1}{p_a} \sum_s T_{as}(\underline{H}).G_{as}(\underline{H}) \;. \qquad (2.3.1)$$

This equation contains two summations. The summation over a extends over all atoms which are symmetry non-equivalent in the basic structure. The summation over s is over all symmetry operations necessary to generate the contents of one subcell (including the unity operation). p_a is the so-called multiplicity of an atom. This is the number of times the atom is transformed into itself by the symmetry operations of the basic structure.

The geometrical part $G_{as}(\underline{H})$ of the structure factor for atom a and symmetry operation s can be written as (using equations 1.3.2, 1.3.4 and 2.2.21)

$$G_{as}(\underline{h}+m\underline{q}) = \exp(2\pi i\underline{h}.(R_s\underline{x}_{oa}+\underline{s}_s))$$

$$.\int_0^1 \exp(2\pi i[(\underline{h}+m\underline{q}).R_s\underline{d}_a(\varepsilon_s(t-\tau_s))])dt \qquad (2.3.2)$$

for symmetry operation $(R_s,\underline{s}_s,\varepsilon_s,\tau_s)$.
The anisotropic temperature parameters U_{aik} in the temperature factor (see 2.2.3) are transformed as normally in order to get $T_{as}(\underline{H})$.
Isotropic temperature factors are equal for symmetry-equivalent atoms.

In order to save computation time, two kinds of symmetry operations are not treated in the way shown above. The first is the inversion operation:

$$(R_i,\underline{s}_i,\varepsilon_i,\tau_i) = \left(\begin{pmatrix} -1 & 0 & 0 \\ 0 & -1 & 0 \\ 0 & 0 & -1 \end{pmatrix} , \begin{pmatrix} 0 \\ 0 \\ 0 \end{pmatrix} , -1 , 0 \right) \;. \qquad (2.3.3)$$

As for normal crystal structures expression 2.3.1 can be written more economically by combining pairs of terms in the summation over s. If one of the symmetry operations is an inversion operation, then the symmetry operations can be divided into two sets with an equal number of operations. The first set contains the unity operation. The operations in the second set can be derived by combining each operation of the first set with the inversion operation:

$$(R_2,\ \underline{s}_2,\ \varepsilon_2,\ \tau_2) = (-R_1,\ -\underline{s}_1,\ -\varepsilon_1,\ -\tau_1) \;. \qquad (2.3.4)$$

Indices 1 and 2 denote operations of the first set and the second set respectively. If the origin in the basic structure and the phase of the modulation wave are chosen such that $\underline{s}_i=\underline{0}$ and $\tau_i=0$, as is assumed in 2.3.3, then the structure factor can be written as

$$F(\underline{H}) = \sum_a f_a(|\underline{H}|) \frac{1}{p_a} 2\,\mathrm{Re}[\sum_s{}' T_{as}(\underline{H}).G_{as}(\underline{H})], \qquad (2.3.5)$$

where the summation Σ' is only over the first set of symmetry operations. Hence the calculation of $T_{as}(\underline{H})$ and $G_{as}(\underline{H})$ for the symmetry operations of the second set is not necessary. Equation 2.3.5 can be deduced by substitution, using the fact that $T_{as}(\underline{H})$ is real.

The second type of symmetry operations which is treated separately is the centering translation:

$$(R_c,\underline{s}_c,\varepsilon_c,\tau_c) = \left(\begin{bmatrix} 1 & 0 & 0 \\ 0 & 1 & 0 \\ 0 & 0 & 1 \end{bmatrix} , \begin{bmatrix} s_{c1} \\ s_{c2} \\ s_{c3} \end{bmatrix} , 1 , \tau_c \right) \quad , \qquad (2.3.6)$$

where s_{c1}, s_{c2}, s_{c3} and τ_c are not all zero.
If n_c centering translations (excluding $\underline{0}$) are present in the structure, then the symmetry operations can be divided into two sets. The operations in the second set can be derived by combining each operation of the first set (which includes the unity operation) with each of the centering translations. Hence the number of operations in the second set is a factor n_c larger than in the first set.
For a structure with centering translations the structure factor can be written as

$$F(\underline{H}) = [\ 1 + \sum_c \exp(2\pi i[\underline{h}.\underline{s}_c])\ ]$$
$$. \sum_a f_a(|\underline{h}|) \frac{1}{p_a} \sum_s{}'' \, T_{as}(\underline{H}).G_{as}(\underline{H}) \quad , \qquad (2.3.7)$$

in which the summation Σ" is over the symmetry operations of the first set only, and the summation over c is over all centering translations (excluding $\underline{0}$). The summation over a is over all symmetry non-equivalent atoms.

If an atom is transformed into itself by a symmetry operation (not the unity operation), then there will be restrictions on some of the parameters of that atom. Consider for example the symmetry operation

$$m(s): (R,\underline{s},\varepsilon,\tau) = \left(\begin{bmatrix} 1 & 0 & 0 \\ 0 & -1 & 0 \\ 0 & 0 & 1 \end{bmatrix} , \begin{bmatrix} 0 \\ 0.5 \\ 0.5 \end{bmatrix} , 1 , 0.5 \right) \quad . \qquad (2.3.8)$$

An atom a at position $(x_{oa1}, 0.25, x_{oa3})$ in the basic structure is situated on this mirror plane. As for normal crystal structures with this situation, x_{oa2} has to be 0.25, and the anisotropic temperature parameters U_{a23} and U_{a12} have to vanish, as can be found in the tables of Peterse and Palm

(1966). But there are also restrictions on the modulation functions. The modulation functions of the atom on the mirror plane must be equal to those of the reflected atom. Thus, according to 1.3.6:

$$\underline{d}_a(t) = R\underline{d}_a(\varepsilon(t-\tau)) \quad . \qquad (2.3.9)$$

Hence, substituting 2.3.8:

$$\begin{aligned} d_{a1}(t) &= d_{a1}(t-0.5) \ , \\ d_{a2}(t) &= -d_{a2}(t-0.5) \qquad\qquad (2.3.10) \\ \text{and}\quad d_{a3}(t) &= d_{a3}(t-0.5) \ . \end{aligned}$$

From this it follows that $d_{a2}(t)$ can have odd harmonics only, and $d_{a1}(t)$ and $d_{a3}(t)$ can have even harmonics only.
Van Aalst et al. (1976) give more examples of this kind of restrictions.
When treating a structure with such symmetry operations with the computer program, one has to indicate which parameters are restricted and which ones are allowed to vary.

2.4. Superstructures as modulated structures.

It is often advantageous to describe a superstructure as a modulated structure rather than as a normal one. There can be several reasons for doing so:
- If satellite reflections of only low orders occur, then the structure can be described using modulation functions with only a few harmonics. This description needs fewer parameters than the normal description, and in the structure determination process, the reflections of the orders with zero intensities need not be used.
The 17-fold superstructure of Rb_2ZnBr_4 provides a good illustration (chapter 3). The satellite reflections of second and higher order have negligible intensities; only the first harmonics of the modulation functions are needed in the structure description.
- It may be possible to describe the superstructure by a 4-dimensional space group which gives an excellent description of it, whereas it needs fewer parameters than a description by a 3-dimensional space group. The room temperature structure of Rb_2ZnBr_4, for instance, can be very well

described by space group Pcmn(00γ)(ss$\bar{1}$). As will be shown in section 4.2, the operators of this space group cannot exist all in one 3-dimensional space group.

- In the process of structure determination one may more easily get convergence to the correct parameters (avoiding false minima) in the structure model if in the refinement procedure fourier coefficients of modulation functions and basic structure positions are used as parameters instead of superstructure positions. (Yamamoto, 1981).
- It is nearly impossible to interrelate different superstructures and/or incommensurate structures (chapter 4) without using the modulation description.

The description of a superstructure as a modulated structure may give rise to two ambiguities. The first one concerns the choice of the modulation wave vector. Apart from the question whether to choose $\underline{q}$ or one of its equivalents $\underline{q}+\underline{h}$ (treated for incommensurate structures in section 1.1 and subsection 4.2.1), there remains the question which satellite reflections should be chosen as first order satellites. For incommensurate structures this problem does not exist because there is only one modulation wave vector (apart from its equivalents) for which equation 1.1.5 covers all satellite reflections. For 5-fold or larger superstructures, however, more choices are possible: In equation 1.2.2 every value of u with $u<v/2$ which has no divisor common with v gives a possible modulation wave vector. For example, for a superstructure with a 7-fold $\underline{c}$-axis, three non-equivalent modulation wave vectors are possible: $\gamma=1/7$, $\gamma=2/7$ and $\gamma=3/7$. Often a compound with such a superstructure, in another temperature region has an incommensurate structure with a diffaction pattern very similar to that of the superstructure. Then the obvious choice of the modulation wave vector in the superstructure is the one for which corresponding satellite reflections in both diffraction patterns have the same set of four indices. In other cases it is elegant to choose the modulation wave vector such that the strongest group of satellite reflections are of first order.
The second ambiguity concerns the indices of the satellite reflections for a given modulation wave vector. For example, in a 7-fold superstructure in which the modulation wave vector has been chosen to be $(2/7)\underline{c}^*$, reflection 0003 can also be indexed as 002-4. In general, for a structure with modulation vector $(u/v)\underline{c}$, a reflection with indices hklm can also be indexed with indices h,k,l+nu,m-nv, in which n may be any integer. A simple convention avoids this ambiguity: the absolute value of the fourth index m should be as small as possible, and if two choices result with the same absolute value, then the positive one should be preferred.

The 4-dimensional space group used in the modulation description of the superstructure can be derived from the 3-dimensional space group of the superstructure and that of the average structure.
The 3-dimensional part of the 4-dimensional space group (see section 1.3) is identical with the space group of the average structure. The second part of the symbol of each 4-dimensional space group can be obtained as follows. If R of the 3-dimensional part of the operation transforms $\underline{q}$ into $-\underline{q}$, then the second part is ($\bar{1}$). If R transforms $\underline{q}$ into itself, then the second part of the symbol is determined by the selection rules of the reflections for the chosen modulation wave vector.

Because for a superstructure the phase of the modulation wave cannot be chosen freely (in contrast to incommensurate structures), the value of τ in the symmetry operations with $\varepsilon=-1$ must be chosen properly:
Take for example a n-glide plane normal to $\underline{c}$ in a structure with $\underline{q}=\gamma\underline{c}^*$ and $\gamma=u/v$. The z coordinates of the atoms in the superstructure are inverted with respect to the z coordinate z_n of this plane. In the description as a modulated structure this means that the z coordinates of the atoms in the basic structure and the "running direction" of the modulation functions are both inverted with respect to this z_n.
Hence τ has to fulfil the condition

$$s_3c = \tau\lambda \pmod 1 \quad \text{or} \quad \tau = \gamma s_3 \ . \qquad (2.4.1)$$

Such a condition does not exist for incommensurate structures, as can be seen in the second example in section 1.3.

Now the calculation of the structure factor. Consider a structure with a modulation wave vector given by 2.2.12. From the comparison of equations 2.2.19 and 2.2.24 it can be concluded that the structure factor of reflections of this superstructure can be calculated by using the same formula as for incommensurate structures. In the case of the superstructure, n in equation 2.2.24 has to be chosen equal to w if w is given by 2.2.18.
The fact that the same formula can be used for incommensurately and commensurately modulated structures is due to the term $\underline{x}_{0a}\cdot\underline{q}$ in equation 2.2.25. This term is not necessary for incommensurate structures, but is essential for commensurately modulated structures (compare 2.2.25

with 2.2.20).

Chapter 3

3. STRUCTURE DETERMINATION OF THREE MODULATED PHASES IN Rb_2ZnBr_4.

3.1. Introduction.

In Rb_2ZnBr_4 five phase transformations are observed at atmospheric pressure, at temperatures T_i=374, T_c=190, T_3=112, T_4=77 and T_5=50K (see e.g. Yamaguchi et al., 1982 and Nomoto et al., 1983). The values found in literature for these temperatures scatter around the above mentioned values. Rb_2ZnBr_4 melts at 753K according to Sawade et al. (1977). The six solid phases are denoted as N (normal), I (incommensurate), F (ferroelectric), IV, V and VI from high to low temperatures. T_c has a hysteresis of about 10K. This value strongly depends on the sample: De Pater (1978) observed that part of a crystal remained in phase I even at 4K, and De Boer (1984) observed that a crystal remained in phase I at temperatures below 100K. No hysteresis has been observed for the other phase transitions.

In phase N (above T_i) Rb_2ZnBr_4 has the β-K_2SO_4 type structure with unit cell dimensions a=13.386(3), b=7.679(2) and c=9.753(2) at 373K (De Pater, 1979).

In phase I (between T_i and T_c) the crystal structure is modulated by a displacive modulation wave with the modulation wave vector parallel to $\underline{c}^*$: $\underline{q}=\gamma\underline{c}^*$. The value of γ is constant at 5/17=0.294 within experimental error in the large temperature interval between T_i and T_c+10K (see De Pater et al., 1979 and Iizumi and Gesi, 1983). So here the structure of the so-called incommensurate phase is commensurate (section 4.6).

Below the so-called lock-in phase transition temperature T_c the value of γ is 1/3, and hence phase F has a 3-fold superstructure. It is not yet clear what happens between T_c+10K and T_c. Until recently is has been assumed that on lowering the temperature from T_c+10K, γ increases monotonously from 0.294 to about 0.31 at T_c, where it jumps to 1/3. Recent measurements of Iizumi and Gesi (1983), however, indicate a more complex behaviour. These measurements suggest that several extra phase transitions exist in that small temperature region, γ jumping at each transition temperature to a new value.

The symmetry of the 3-fold superstructure in phase F (between T_c and T_3) is $Pc2_1n$ according to De Pater (1979) and Ueda et al. (1982). Only little is known about the structures of phases IV, V and VI. According to Ueda et al (1982) these structures have the same 3-fold unit cell as phase F. They observed in phase IV the same rules for systematically absent X-ray reflections as in phase F, corresponding to a c-glide plane normal to a and a n-glide plane normal to c. In phases V and VI they only observed the n-glide plane. Yamaguchi et al. (1982) observed that the ferroelectricity along b, which appears on cooling at T_c (therefore, this temperature is often called Curie temperature), is present in all phases below this temperature. Only in phase IV they also observed a double D-E hysteresis loop along the a axis. This indicates that this phase is antiferroelectric along a.

Magnetic resonance measurements on Rb_2ZnBr_4 of Belobrova at al. (1981) show 3 ^{81}Br NQR frequencies in phase N, 12 in phase F and 32 in phase IV. In phase N the intensity of one of the 3 frequencies is twice as large as that of the other two. For phase N and phase F these results correspond nicely to the symmetry information mentioned above. The number of lines in phase IV, however, does not correspond to a 3-fold superstructure with symmetry $Pc2_1n$. The frequency peaks of phase IV do not have a normal shape. Belobrova at al. suggest that either several of the observed peaks are close doublets or the structure is incommensurate.

De Pater (1979) determined the structure of Rb_2ZnBr_4 in phase N at 373 K from a neutron diffraction powder diagram. He used the same technique to determine the average structure at 300K (phase I) and at 4K (phase VI). In all cases he fitted the measurements to a structure model with the unit cell size and symmetry of phase N. He used split atoms to account for the thermal motion at 373K and for the modulation displacements in the other cases.

De Jager (1980) determined the structure of Rb_2ZnBr_4 at 300K in a 3-fold superstructure approximation, using 730 X-ray reflections, of which 78 are satellites. His structure model has the same unit cell size and symmetry as the structure of phase F: a 3-fold supercell and space group $Pc2_1n$.

Several other compounds exist of which the crystals have the phase sequence normal - incommensurate - 3-fold superstructure. The phase transition temperatures T_i and T_c are 553K and 403K for K_2ZnCl_4 (Gesi and Iizumi, 1979a), 303K and 194K for Rb_2ZnCl_4 (Quilichini and Pannetier, 1983) and

129K and 94K for K_2SeO_4 (Iizumi et al., 1977).

Many other A_2BX_4-compounds show incommensurately and commensurately modulated structures related to the modulated structure of Rb_2ZnBr_4 (chapter 4).

In this chapter structure determinations of Rb_2ZnBr_4 at room temperature, 140K and 95K will be presented. At these temperatures Rb_2ZnBr_4 is in phase I, phase F, and phase IV. The structures at room temperature and 140K have been determined from single crystal X-ray measurements. For the structure at 95K single crystal neutron diffraction data have been used. The structures have been refined using the computer program described in chapter 2.

3.2. Experimental.

Transparent single crystals of Rb_2ZnBr_4 have been grown from aqueous solution containing RbBr and $ZnBr_2$ in the molar ratio 2:1 (RbBr: 99.9%, Alpha Products; $ZnBr_2$: 99.8%, Ventron GmbH). At room temperature, from a fresh solution first another compound crystallizes. The molar ratio of the two components in the solution changes then. Finally, clear Rb_2ZnBr_4 crystals appear. At 30°C only Rb_2ZnBr_4 crystals grow from a fresh solution. Attempts to make small spheres (diameter < 0.3mm) of Rb_2ZnBr_4 failed. Therefore the X-ray measurements have been performed on small ellipsoid-shaped crystals. Because of the strong absorption of X-rays in Rb_2ZnBr_4 (the linear absorption coefficient of Mo Kα radiation in Rb_2ZnBr_4 is $\mu=28200m^{-1}$), special care is necessary for the absorption correction (section 3.4).

Experimental details about the diffraction measurements at the three temperatures are given in table 3.2.1. The X-ray measurements have been performed with an Enraf Nonius CAD4 four circle diffractometer. During the measurements at 140K the crystal has been cooled by a controlled flow of N_2 vapour. The neutron diffraction measurements have been carried out by means of the four circle diffractometer at the HFR reactor in Petten. The crystal was mounted in a He-flow cryostat (Herbert and Campbell, 1977).

At the three temperatures the main reflections and the first order satellites have been measured in one octant. No higher order satellites

TABLE 3.2.1. Data on the structure determinations of Rb_2ZnBr_4.

temperature [K]	293(2)	140(3)	95(1)
stability [K]	±5	±3	±0.2
radiation	Mo $K\alpha$ 0.7107Å	Mo $K\alpha$ 0.7107Å	neutrons 1.304Å
monochromator	graphite	graphite	double Cu (220)
crystal shape	ellipsoid	ellipsoid	rough sphere
diameter [mm]	0.21 - 0.27	0.23 - 0.28	3.5
max. meas. time [s]	600	180	1800
max. θ	30°	30°	38.3°
space group	$Pcmn(00\gamma)(ss\bar{1})$	$Pc2_1n$	$Pc2_1n$
a [Å]	13.330(3) #	13.198(5) $	13.184(4)
b [Å]	7.656(2) #	7.594(4) $	7.599(2)
c [Å]	9.707(2) #	3x 9.614(3) $	3x 9.623(5)
γ ($\underline{q}=\gamma\underline{c}^*$)	0.293 &	1/3	1/3
number of refl.			
main	1512	1494	502
satellite	2654	3002	980
total	4166	4496	1482
removed reflections:			
extinction	0200, 0400, 1030, 4000	1030	-
$\lambda/2$ contamination	2000, 1100	2000, 1100	-
weighting scheme	$1/\sigma^2(F_o)$	$1/(\sigma^2(F_o)+(.05F_o)^2)$	$1/\sigma^2(F_o)$
number of parameters			
basic str. position	13	20	20
mod. four. coeff.	16	42	42
temperature param.	26	42	42
scale factor	1	1	1
total	56	105	105
largest parameter shift in last refinem. cycle	0.012σ	0.17σ	0.21σ
R_w of all reflections	0.080	0.119	0.050
R_w of main reflections	0.063	0.088	0.040
R_w of sat. reflections	0.167	0.154	0.073
D [Å] ⋇	0.037	0.047	0.025

# taken from De Pater (1979).
$ these lattice parameters have a larger error than the e.s.d. indicate, because of the strong absorption.
& taken from Iizumi and Gesi (1983).
⋇ D is defined in equation 3.4.2.

have been measured because they are not visible on precession photo's. Each reflection was measured until the desired accuracy ($\sigma(I) < 0.02I$) or the maximum measuring time was reached. In the neutron diffraction measurements the measurement of a reflection has been stopped after 900s in case the intensity was very low ($I < \sigma(I)$). For negative measured intensities I has been put to zero. All these weak reflections, however, take full part in the data set. The Lorentz-Polarization correction of the X-ray measurements have been applied according to Azaroff (1955). No *extinction correction* has been used.

During the refinements of the structures at room temperature and 140K, a few reflections have been removed from the data set (see table 3.2.1). The reflections suspected of *extinction* have small θ, a very high intensity and a calculated structure factor which is much higher than the observed one. The reflections with $\lambda/2$ contamination have a low intensity, a calculated structure factor which is much lower than the observed one and a very strong reflection at the position with double indices. It has been checked that the *$\lambda/2$ contamination* is indeed of the proper magnitude to explain the discrepancy.

The atomic scattering factors and the dispersion corrections of Rb(+), Zn(2+) and Br(-) for Mo $K\alpha$ radiation are taken from International Tables IV (1974). The neutron diffraction scattering amplitudes of Rb, Zn and Br, 0.708, 0.5680 and 0.679 respectively, are taken from Koester and Yelon (1982).

3.3. Symmetry.

Although the room-temperature phase of Rb_2ZnBr_4 is a commensurate superstructure (γ = 5/17, cf. section 4.6), it shows systematic extinctions which strongly suggest a (3+1)-dimensional space group as the best description of its symmetry. The reflection conditions which we observed on X-ray precession photographs are shown in table 3.3.1.
In our diffractometer results, these rules are obeyed as well. Since the three symmetry operations listed in table 3.3.1 generate the complete group $Pcmn(00\gamma)(ss\bar{1})$, it can be expected that this pseudo-"prototype symmetry" (cf. section 4.2.2) will lead to a satisfactory description of the

TABLE 3.3.1.

(i) $0klm$: $l+m$ = even ⇒ $c(s)$
(ii) $h0lm$: m = even ⇒ $m(s)$
(iii) $hk00$: $h+k$ = even ⇒ $n(\bar{1})$

structure. It has indeed turned out to be the best basis for refinement. The true symmetry of the superstructure has not been solved, in spite of considerable effort. For $\gamma=5/17$, only the elements $c(s)$ and $n(\bar{1})$ in the above symbol correspond to 3-dimensional elements, viz. c and n, in the required unit cell with $c_s=17c$. The element $m(s)$ is lost. This can be seen e.g. from the reflection condition (ii) which for the multiple cell ($L=17l+5m$) does not lead to a parity condition on L in $h0L$.
Accordingly, the true space group would become $Pc2_1n$ in the multiple cell. This is in flagrant contradiction with two observations:

- Crystals grown from aqueous solution at about 30 °C have a very pronounced 222 symmetry (De Pater, 1978; De Wolff, 1980). The same point group was also seen in experiments by Dam and Janner (1983). With a true symmetry $Pc2_1n$, however, the point group would be m2m; and m2m is not even a subgroup of 222.
- Neutron diffraction experiments of Iizumi and Gesi (1983) show that reflections 0210, 0201 and 022$\bar{1}$, at 25 °C, have intensities differing significantly from zero. These reflections are not allowed by condition (i), so they exclude the presence of a c-glide plane in the actual superstructure. It should be remarked, however, that their intensities are very small indeed. Therefore, it must be concluded that the structure almost has symmetry $Pcmn(00\gamma)(ss\bar{1})$. (The choice of a- and b axes was not stated by Iizumi and Gesi. Judging from other reflection intensities we concluded that their a (b) is our b (a), so in the indices mentioned above h and k have been interchanged with respect to those given in their paper.)

The two observations together suggest that the actual space group is $P2_12_12_1(00\gamma)(\bar{1}\bar{1}1)$.
Certain physical properties have been checked by other authors, mainly with a view to test a possible departure from centrosymmetry. All results, however, have been negative, so that no definite conclusion can be drawn:

- Smid (1984): no optical second harmonic generation (detection limit: 10^{-4} times the second harmonic generation level of quartz);
- Yamaguchi et el. (1982): no ferroelectricity or pyroelectricity.

A definite answer to the question what the space group of Rb_2ZnBr_4 in the room temperature phase is, cannot be given. Structure refinements have been done in three space groups (section 3.4). $Pcmn(00\gamma)(ss\bar{1})$ gives the best results. Hence, the room temperature structure of Rb_2ZnBr_4 can at least in good approximation be described by this space group.

The room temperature structure will be treated as incommensurate in the structure refinements, notwithstanding its rational modulation wavevector. Table 3.3.2 gives the symmetry operations of space group $Pcmn(00\gamma)(ss\bar{1})$. The atoms on the mirror plane ($m(s)$) are at special positions. As explained in section 2.3, the modulation functions $d_1(t)$ and $d_3(t)$ of such atoms, describing the displacement components in the $\underline{a}$ and $\underline{c}$ directions, cannot contain odd harmonics. The modulation functions $d_2(t)$ of these atoms cannot contain even harmonics. These symmetry restrictions exist together with the usual ones on the basic structure positions and the temperature parameters.

No inconsistencies exist concerning the space group of phase F: $Pc2_1n$. Rb_2ZnBr_4 is ferroelectric along $\underline{b}$ in this phase (Yamaguchi et al., 1982) and generates second harmonic light at a level of about 0.1 times that of quartz (Smid, 1984). The systematic absences for the c- and n-glide planes are clearly present (Ueda et al., 1982). A few apparent violations of these systematic absences in our measurements were shown to be caused by $\lambda/2$ contamination.

The space group of phase IV is still a puzzle. Despite the fact that the observations of Yamaguchi et al. (1982) and Belobrova et al. (1981) indicate that the structure of this phase is different from that of phase F, we could not find differences in the diffraction symmetry: the systematic absences of the c- and n-glide planes are still present (as has also been found by Ueda et al.,1982): no extra reflections could be found on the $\underline{a}^*$-, $\underline{b}^*$- or $\underline{c}^*$ axes; no tripling of $\underline{a}$ or $\underline{b}$ could be found; it has been checked that the modulation wavevector is $\underline{c}^*/3$, and not e.g. $3\underline{c}^*/8$ as suggested by the results of the magnetic resonance measurements of Belobrova et al. (1981). Moreover, just like in phase F, in this phase Rb_2ZnBr_4 is ferroelectric along $\underline{b}$ (Yamaguchi et al., 1982) and generates second harmonic light (Smid, 1984). Therefore it is concluded that the structure of this phase can be described as a 3-fold superstructure with space group $Pc2_1n$, like phase F. This symmetry has been used for the structure determination.

TABLE 3.3.2. Space group operations of $Pcmn(00\gamma)(ss\bar{1})$. For each operation, R, s̲, ε and τ are given.

$$
\begin{aligned}
c(s)&: \begin{pmatrix}-1&0&0\\0&1&0\\0&0&1\end{pmatrix}, \begin{pmatrix}1/2\\0\\1/2\end{pmatrix}, 1, 1/2 & \qquad 2_1(\bar{1})&: \begin{pmatrix}1&0&0\\0&-1&0\\0&0&-1\end{pmatrix}, \begin{pmatrix}1/2\\0\\1/2\end{pmatrix}, -1, 1/2\\
m(s)&: \begin{pmatrix}1&0&0\\0&-1&0\\0&0&1\end{pmatrix}, \begin{pmatrix}0\\1/2\\0\end{pmatrix}, 1, 1/2 & \qquad 2_1(\bar{1})&: \begin{pmatrix}-1&0&0\\0&1&0\\0&0&-1\end{pmatrix}, \begin{pmatrix}0\\1/2\\0\end{pmatrix}, -1, 1/2\\
n(\bar{1})&: \begin{pmatrix}1&0&0\\0&1&0\\0&0&-1\end{pmatrix}, \begin{pmatrix}1/2\\1/2\\1/2\end{pmatrix}, -1, 0 & \qquad 2_1(1)&: \begin{pmatrix}-1&0&0\\0&-1&0\\0&0&1\end{pmatrix}, \begin{pmatrix}1/2\\1/2\\1/2\end{pmatrix}, 1, 0\\
\bar{1}(\bar{1})&: \begin{pmatrix}-1&0&0\\0&-1&0\\0&0&-1\end{pmatrix}, \begin{pmatrix}0\\0\\0\end{pmatrix}, -1, 0 & \qquad 1(1)&: \begin{pmatrix}1&0&0\\0&1&0\\0&0&1\end{pmatrix}, \begin{pmatrix}0\\0\\0\end{pmatrix}, 1, 0
\end{aligned}
$$

TABLE 3.3.3. The 4-dimensional symmetry operations used to describe a 3-fold superstructure with space group $Pc2_1n$.

$$
\begin{aligned}
c(s)&: \begin{pmatrix}-1&0&0\\0&1&0\\0&0&1\end{pmatrix}, \begin{pmatrix}1/2\\0\\1/2\end{pmatrix}, 1, 1/2 & \qquad 2_1(\bar{1})&: \begin{pmatrix}-1&0&0\\0&1&0\\0&0&-1\end{pmatrix}, \begin{pmatrix}0\\1/2\\0\end{pmatrix}, -1, 1/3\\
n(\bar{1})&: \begin{pmatrix}1&0&0\\0&1&0\\0&0&-1\end{pmatrix}, \begin{pmatrix}1/2\\1/2\\1/2\end{pmatrix}, -1, -1/6 & \qquad 1(1)&: \begin{pmatrix}1&0&0\\0&1&0\\0&0&1\end{pmatrix}, \begin{pmatrix}0\\0\\0\end{pmatrix}, 1, 0
\end{aligned}
$$

TABLE 3.4.1. Comparison of refinements using reflections corrected for absorption with (A) and without (B) the anisotropic part.
N is the number of used reflections, w_r is the weighting scheme, R_w is the residual and D is the average of the differences between the maximum and minimum of the distance types $Zn\text{-}Br_i$ (i=1,2,3,4).

nr	temp [K]	used reflections	N	w_r	A R_w	A D[Å]	B R_w	B D[Å]
1	293	$I > 10\sigma(I)$	528*	$1/\sigma^2(F_o)$	.0640	.051	.0689	.051
2	293	$h^2+k^2+l^2 < 100$	1678*	$1/\sigma^2(F_o)$	.0771	.038	.0783	.037
3	293	all	4166	$1/\sigma^2(F_o)$	.0804	.037	-	-
4	140	$I > 10\sigma(I)$	890*	$1/\sigma^2(F_o)$	.0657	.067	.0730	.067
5	140	all	4498*	$1/\sigma^2(F_o)$	.0771	.052	.0796	.057
6	140	all	4496	$1/\sigma^2(F_o)$	.0735	.056	-	-
7	140	all	4498*	$1/(\sigma^2(F_o)+(.05F_o)^2)$	.1206	.047	.1242	.045
8	140	all	4496	$1/(\sigma^2(F_o)+(.05F_o)^2)$	.1188	.047	-	-

* including two reflections which are strongly contaminated by λ/2.

The 3-fold superstructures of Rb_2ZnBr_4 at 140K and 95K have been refined using space group $Pc2_1n(00\gamma)(s\bar{1}\bar{1})$, of which the symmetry operations are given in table 3.3.3. Condition 2.4.1 is fulfilled for operations $n(\bar{1})$ and $2_1(\bar{1})$, as can be checked in this table. As explained in section 2.4 this condition must be fulfilled for a proper description of a superstructure using 4-dimensional symmetry.

3.4. Absorption correction and refinement.

The refinements are carried out with the computer program described in chapter 2. The value of n in equation 2.2.24 has been 5 or 7 in the refinements of the room temperature structure. Only in the final stage of these refinements n=7 has been used. There is not much difference between using n=5 or n=7. n=7 gives a slightly lower residual, but needs more computation time. Because second and higher order satellite reflections are very much weaker than the first order ones (they were not seen by X-ray diffraction), only the first harmonics of the modulation functions are considered in the refinements.
The 3-fold superstructures have also been refined using the above mentioned computer program. In these cases, n=3 has been used, together with the symmetry operations mentioned in table 3.3.3.
All refinements are based on structure factors. The residual (R_w) is calculated using

$$R_w = \frac{\sum_r w_r(F_{or} - |F_{cr}|)^2}{\sum_r w_r F_{or}^2} \quad , \qquad (3.4.1)$$

in which the summations are over all used reflections, w_r is the weight of reflection r, F_{cr} is the calculated structure factor and F_{or} is the observed structure amplitude.

The linear absorption coefficient (μ) of Mo Kα radiation in Rb_2ZnBr_4 is $28200 m^{-1}$, that of neutrons (λ=1.304Å) is $8.2 m^{-1}$. For the neutron diffraction data no absorption correction is needed, but for the X-ray measurements a large correction is necessary. Because the absorption is very strong and because the crystals used for these measurements are not spheres, the usual isotropic correction (International Tables II, 1959) is not sufficient. Therefore, the reflection intensities have been corrected with the computer program CAMEL JOCKEY of Flack (1974, 1975).

The absorption correction is derived by this program from a separate set of measurements, consisting of 17 non-equivalent reflections and their symmetry equivalents, each measured for $\Psi=n\times20°$ ($n=-4,-3,-2,-1,0,1,2,3,4$; Ψ is the rotation angle around the reflection vector), as far as the geometry of the diffractometer allowed. In total, 1227 of these measurements were done at room temperature (some of them are double) and 1160 at 140K. If the crystal would have been a sphere, then for each of the 17 non-equivalent reflections all the measurements should give the same intensity within experimental error. The program calculates the average for each of the 17 groups of intensities, and calculates the correction necessary to make the eight measurements at $\Psi=0°$ in each group equal to this average. This correction, which is a function of the diffractometer angles, is applied to the intensities in the main data set, together with the usual isotropic correction.

Because the crystals are not spheres, the choice of the radius (R) for the isotropic part of the absorption correction is ambiguous, as pointed out by Flack (1974). For both crystals used for X-ray measurements, $\mu R=3.5$ has been chosen. For the room temperature measurements, also $\mu R=3.8$ has been tried, in order to investigate the effect of a different choice of radius. Using 1678 reflections (those with $h^2+k^2+l^2<100$), after the refinement the residuals were $R_w=0.07713$ and $R_w=0.07719$ for $\mu R=3.5$ and $\mu R=3.8$ respectively. In the case of $\mu R=3.8$, the diagonal temperature parameters were about 0.002 larger than in he case of $\mu R=3.5$, while the other parameters did not show noticable differences. Therefore it can be concluded that the only effect of choosing a different radius is that the refinements result in slightly different temperature parameters.

For the crystal used for the room temperature measurements, the program used 4 nonzero coefficients (including a scale factor) in the function that describes the transmission factor. For the crystal of the 140K measurements, 9 nonzero coefficients have been used.

The effect of the absorption correction can be evaluated by comparing results of refinements using reflections which are corrected as described, with the results of refinements using the same reflections corrected only by the isotropic part of the absorption correction. These results are shown in table 3.4.1. It can be concluded from the residuals in this table, that the absorption correction according to Flack is significantly better than the mere isotropic correction. The correction has more effect on the stronger reflections because the corrections are larger for stronger

reflections.

Besides the residual, another quantity is used to obtain information about the quality of the model. This quantity (D) is calculated from the Zn-Br distances within the rather rigid $ZnBr_4$ tetrahedra. The use of this quantity is based on the fact that all Zn-Br distances of a certain type (e.g. $Zn-Br_1$) will be equal in good approximation. This is true because the tetrahedra in different subcells have about the same surroundings since the deviation of the structure from the symmetry of the normal phase (N) is small. D is defined by

$$D = \frac{1}{4}\sum_{i=1}^{4}\left[\,(Zn-Br_i)_{max} - (Zn-Br_i)_{min}\,\right]. \qquad (3.4.2)$$

The structures at room temperature and at 95K indeed have quite small values of D: 0.037Å and 0.025Å respectively. However, the resulting structure at 140K (using weighting scheme $w_r=1/\sigma^2(F_o)$) has a quite large value: D=0.056Å. Assuming that perhaps the absorption correction for the measurements at this temperature is not as good as desirable, weighting scheme $w_r=1/(\sigma^2(F_o)+(0.05F_o)^2)$ has been used. This weighting scheme gives a lower weight to stronger reflections. If something is wrong with the absorption correction, then those reflections will be more affected than weaker ones. The result is shown in table 3.4.1: the value of D is smaller for the new weighting scheme. Therefore, the structure of this refinement is considered to be the better approximation of the real crystal structure of Rb_2ZnBr_4 at 140K.

Many attempts have been made to refine the room temperature structure with space group $Pc2_1n(00\gamma)(s\bar{1}\bar{1})$, using 1678 reflections ($h^2+k^2+l^2<100$) or 1359 reflections (the 557 main reflections with $h^2+k^2+l^2<100$ and the 802 satellites with $h^2+k^2+l^2<80$). These refinements have not been done with more reflections because that would not change the results much (compare D of refinements 2 and 3 in table 3.4.1), and it would require much more computation time. The number of parameters in these refinements is 100: 20 position parameters, 42 modulation parameters, 37 temperature parameters (isotropic temperature factor for Zn) and 1 scale factor. Several sets of starting parameters have been tried, several refinement strategies have been used and also soft constraints on the Zn-Br distances by using a penalty function (Yamamoto, 1983) in the first stage of refinements have been used. The residuals resulting from these refinements are about 0.063. According to Hamilton (1965) these values are significantly lower than the

TABLE 3.5.1. The atomic fractional coordinates of the basic structure ($\times 10^4$) and the fourier coefficients of the modulation functions ($\times 10^4$).

			293K			140K			95K	
at.	i	x_{oi}	d_{ic}	d_{is}	x_{oi}	d_{ic}	d_{is}	x_{oi}	d_{ic}	d_{is}
Rb_1	1	3234(1)	0	0	3229(1)	23(3)	-24(3)	3223(1)	3(5)	-15(4)
	2	2500	-11(5)	-147(4)	2476(8)	149(3)	167(3)	2489(10)	174(4)	204(4)
	3	5153(1)	0	0	5127(1)	0(4)	-14(5)	5120(2)	23(6)	-3(6)
Rb_2	1	5968(1)	0	0	5970(2)	20(5)	53(4)	5970(2)	27(6)	50(6)
	2	2500	110(5)	91(5)	2530(9)	-195(4)	-34(4)	2519(12)	-223(5)	-28(5)
	3	8730(1)	0	0	8759(2)	16(5)	-28(5)	8765(2)	6(7)	-25(6)
Zn	1	5777(1)	0	0	5785(1)	-6(3)	10(4)	5789(1)	-7(6)	-8(6)
	2	2500	-30(4)	93(4)	2491	-17(3)	-137(3)	2497	-16(4)	-132(4)
	3	2746(1)	0	0	2766(1)	1(5)	-11(5)	2772(2)	37(7)	-18(6)
Br_1	1	5831(1)	0	0	5803(1)	-27(3)	-46(3)	5792(1)	-27(5)	-52(5)
	2	2500	-60(6)	349(5)	2479(8)	-169(5)	-508(4)	2497(10)	-172(6)	-560(5)
	3	5184(1)	0	0	5224(1)	40(4)	7(4)	5234(2)	20(5)	-16(6)
Br_2	1	4126(1)	0	0	4146(1)	-1(3)	13(3)	4157(1)	-3(5)	6(4)
	2	2500	-516(5)	59(7)	2603(8)	545(5)	-438(5)	2619(9)	593(6)	-490(7)
	3	1802(1)	0	0	1756(2)	4(5)	-23(4)	1740(2)	-2(6)	-33(6)
Br_3	1	6593(1)	-252(2)	1(3)	6687(2)	291(3)	-178(3)	6704(3)	316(4)	-218(4)
	2	5012(1)	183(3)	62(4)	4966(6)	-243(5)	62(4)	4941(8)	-243(7)	107(6)
	3	1839(1)	-118(3)	-92(3)	1910(3)	240(4)	58(4)	1922(3)	283(4)	46(4)
Br_4	1				6569(2)	-297(3)	182(3)	6580(3)	-315(4)	200(4)
	2				-47(6)	-278(5)	85(5)	-64(8)	-276(6)	105(6)
	3				1858(3)	-184(4)	-9(3)	1888(3)	-203(4)	-46(4)

TABLE 3.5.2. The anisotropic temperature parameters [10^{-4} Å^2], corresponding to temperature factor $\exp(-2\pi^2\Sigma_{ik}U_{ik}h_ih_ka_i{}^*a_k{}^*)$.

		293K			140K			95K	
atom	U_{11} U_{23}	U_{22} U_{13}	U_{33} U_{12}	U_{11} U_{23}	U_{22} U_{13}	U_{33} U_{12}	U_{11} U_{23}	U_{22} U_{13}	U_{33} U_{12}
Rb_1	354(6)	593(9)	367(6)	254(6)	369(8)	172(6)	118(9)	232(11)	120(9)
	0	29(5)	0	-22(18)	9(5)	-1(13)	22(29)	2(8)	-22(21)
Rb_2	1170(14)	696(11)	369(8)	654(12)	450(11)	176(7)	444(13)	396(13)	112(10)
	0	-55(8)	0	-8(19)	-6(7)	90(21)	60(28)	0(9)	-8(32)
Zn	296(7)	279(7)	292(7)	217(6)	210(7)	140(6)	90(11)	104(11)	60(10)
	0	-4(5)	0	4(18)	0(5)	-2(16)	23(27)	1(9)	-27(33)
Br_1	602(9)	1152(18)	240(6)	376(8)	540(13)	119(6)	178(12)	345(17)	65(9)
	0	-74(6)	0	-23(15)	-36(6)	-81(16)	0(24)	-23(9)	-79(25)
Br_2	338(7)	1165(22)	414(8)	258(7)	581(12)	200(7)	137(10)	441(17)	126(11)
	0	-121(6)	0	-10(17)	-54(6)	53(15)	30(23)	-60(9)	69(24)
Br_3	982(11)	378(7)	631(8)	604(16)	237(13)	291(13)	340(18)	146(21)	164(17)
	-46(6)	250(9)	-316(8)	-25(12)	133(13)	-165(12)	-37(17)	78(17)	-126(18)
Br_4				549(15)	266(14)	306(14)	382(19)	73(20)	195(19)
				10(12)	71(13)	90(12)	-8(19)	118(17)	54(17)

value of 0.0771 for space group $Pcmn(00\gamma)(ss\bar{1})$, but the corresponding structures have values of D above 0.09Å (mostly about 0.12Å). Moreover, parameters which are zero because of symmetry in space group $Pcmn(00\gamma)(ss\bar{1})$, and in principle unequal to zero in $Pc2_1n(00\gamma)(s\bar{1}\bar{1})$, have strongly varying values: the x_{o2} parameters of the atoms on the pseudo-m(s) plane vary more than 0.01 and the modulation parameters more than 0.005. This could be caused by systematic errors in the observed structure factors, which remained after the absorption correction. The above mentioned parameters are adapted to these errors, thus lowering R_w. They get values deviating strongly from $Pcmn(00\gamma)(ss\bar{1})$ symmetry, because they can compensate each others R_w-increasing effects, due to the very strong correlations between these parameters in the least squares procedure. The same is observed during refinements in space group $P2_12_12_1(00\gamma)(\bar{1}\bar{1}1)$.
Because the initial stages of refinements in this space group resulted in much smaller drops of R_w than in space group $Pc2_1n(00\gamma)(s\bar{1}\bar{1})$, this space group has not been investigated further.
Therefore, the room temperature structure of Rb_2ZnBr_4 is supposed to be approximated best by the structure resulting from the refinement in space group $Pcmn(00\gamma)(ss\bar{1})$.

3.5. Results.

In the table 3.5.1 to 3.5.6 the results of the structure refinements are presented. The fractional coordinates of the basic structure and the fourier coefficients of the modulation functions are given in table 3.5.1 for the three structures. The actual position $\underline{x}$ of an atom in a given subcell of the modulated structure (incommensurate or commensurate) can be represented by

$$\underline{x} = \underline{n} + \underline{x}_o + \underline{d}((\underline{n}+\underline{x}_o).\underline{q}) \quad , \qquad (3.5.1)$$

in which $\underline{n}$ is the position of the subcell, $\underline{x}_o$ is the basic structure position of the atom, $\underline{q}$ is the modulation wavevector and $\underline{d}(t)$ is the displacement vector function, defined by its components $d_i(t)$, which are the modulation functions.
For the three structures described in this chapter, the modulation functions are given by

TABLE 3.5.3. The amplitudes (A_i, $\times 10^4$) and phases (φ_i) of the modulation functions. 5/12 has been added to the phases of the modulation functions in the room temperature structure to make them comparable to the phases of the two other structures.

at.	i	293K A_i	293K φ_i	140K A_i	140K φ_i	95K A_i	95K φ_i
Rb_1	1	0		33(3)	.87(1)	15(4)	.78(5)
	2	147(4)	.155(4)	223(3)	.134(2)	268(4)	.138(3)
	3	0		14(5)	.75(5)	23(6)	.98(4)
Rb_2	1	0		56(4)	.19(1)	57(6)	.17(2)
	2	143(5)	.527(5)	198(4)	.527(3)	225(5)	.520(3)
	3	0		32(5)	.84(2)	26(6)	.79(4)
Zn	1	0		12(4)	.33(5)	11(6)	.63(9)
	2	98(4)	.716(6)	138(3)	.730(4)	133(4)	.731(5)
	3	0		11(5)	.76(7)	41(7)	.93(3)
Br_1	1	0		53(3)	.67(1)	59(5)	.67(1)
	2	354(5)	.694(2)	535(4)	.699(1)	585(5)	.702(1)
	3	0		41(4)	.03(1)	26(5)	.89(3)
Br_2	1	0		13(3)	.27(4)	7(4)	.3(1)
	2	520(5)	.899(2)	699(5)	.892(1)	769(7)	.890(1)
	3	0		23(4)	.77(3)	33(6)	.74(3)
Br_3	1	252(2)	.916(1)	341(3)	.913(1)	383(4)	.904(2)
	2	193(3)	.468(2)	251(5)	.460(3)	265(7)	.434(4)
	3	150(3)	.022(3)	247(4)	.038(2)	286(4)	.026(2)
Br_4	1			348(3)	.413(1)	373(4)	.410(2)
	2			291(5)	.453(3)	295(6)	.442(3)
	3			184(4)	.508(3)	208(4)	.535(3)

Note that in chapter 5 subscript i of A_i and φ_i has a different meaning.

TABLE 3.5.4. The equivalent isotropic temperature parameters $U(eq)=(U_{11}+U_{22}+U_{33})/3$ [10^{-4}Å^2].

atom	293K	140K	95K
Rb_1	438(4)	265(4)	157(6)
Rb_2	745(6)	427(6)	317(7)
Zn	289(4)	189(4)	85(6)
Br_1	665(7)	345(6)	196(7)
Br_2	639(8)	346(5)	235(8)
Br_3	664(5)	377(8)	217(11)
Br_4		374(8)	217(11)

$$d_i(t) = d_{ic}\cos 2\pi t + d_{is}\sin 2\pi t \quad . \qquad (3.5.2)$$

In table 3.5.2 the anisotropic temperature parameters are given for the three structures. The parameters in tables 3.5.1 and 3.5.2 are the direct results of the refinements. The only exceptions are the x_{o2} parameters in the 140K and 95K structures, because the origin in these stuctures has been shifted in the b̲ direction in order to get the baricentre of the unit cell contents in the middle of the unit cell. In the room temperature structure the baricentre is automatically at this position because of the m(s) mirror plane.

The modulation functions can also be written as

$$d_i(t) = A_i\cos 2\pi(t-\varphi_i) \quad , \qquad (3.5.3)$$

with A_i and φ_i being respectively their amplitude and phase. The values of A_i and φ_i of the three structures are given in table 3.5.3. To the phases at room temperature we added 5/12 in order to make them comparable with the phases of the other structures.

Table 3.5.4 lists the equivalent isotropic temperature parameters.

For the two 3-fold superstructures the fractional coordinates of the asymmetric set of atoms are given with respect to the supercell axes in table 3.5.5. These coordinates are calculated from the parameters of table 3.5.1 using equations 3.5.1 and 3.5.2.

Table 3.5.6 gives the distances in the $ZnBr_4$ tetrahedra. These distances are not corrected for thermal motion.

In the tables, the numbers between brackets are the estimated standard deviations.

The residuals for the three structures are listed in table 3.2.1. The residuals for only the main reflections and only the satellites are also given. The residuals for only the satellites are larger than those for only main reflections because the satellites are much weaker, on the average, than the main reflections. This results in a smaller denominator in equation 3.4.1, and hence a larger R_w.

TABLE 3.5.5. The atomic fractional coordinates (x10^4) with respect to the supercell axes a, b and c_s=3c.

atom	140K x_{s1}	140K x_{s2}	140K x_{s3}	95K x_{s1}	95K x_{s2}	95K x_{s3}
Rb_{11}	3219(3)	2693(8)	1705(2)	3211(5)	2751(11)	1709(2)
Rb_{12}	3207(3)	2323(8)	5043(2)	3221(5)	2310(11)	5032(2)
Rb_{13}	3261(3)	2412(8)	8380(2)	3237(5)	2405(11)	8378(2)
Rb_{21}	6016(5)	2548(10)	2909(2)	6011(6)	2551(13)	2913(2)
Rb_{22}	5918(5)	2691(10)	6256(2)	5916(6)	2696(13)	6260(2)
Rb_{23}	5976(5)	2350(10)	9594(2)	5983(7)	2311(13)	9593(2)
Zn_1	5785(4)	2401(3)	920(2)	5779(6)	2411(4)	931(2)
Zn_2	5794(4)	2445(3)	4253(2)	5792(6)	2452(4)	4244(2)
Zn_3	5774(4)	2627(3)	7592(2)	5796(6)	2628(4)	7598(2)
Br_{11}	5750(4)	1950(9)	1750(1)	5733(5)	1921(11)	1743(2)
Br_{12}	5832(3)	2671(9)	5061(1)	5821(5)	2697(11)	5072(2)
Br_{13}	5827(4)	2815(9)	8413(1)	5821(5)	2874(11)	8419(2)
Br_{21}	4149(3)	2955(9)	584(2)	4156(5)	2998(11)	575(2)
Br_{22}	4155(3)	1904(9)	3913(2)	4163(5)	1849(12)	3907(2)
Br_{23}	4134(3)	2951(9)	7259(1)	4151(5)	3009(12)	7258(2)
Br_{31}	6886(4)	4766(8)	718(2)	6909(5)	4760(10)	733(2)
Br_{32}	6347(4)	5197(8)	3918(2)	6321(5)	5200(10)	3908(2)
Br_{33}	6828(4)	4934(8)	7274(2)	6881(5)	4864(10)	7281(2)
Br_{41}	6363(4)	-272(8)	561(2)	6367(5)	-278(10)	561(2)
Br_{42}	6915(4)	224(8)	3999(2)	6952(5)	220(10)	4007(2)
Br_{43}	6428(4)	-94(8)	7297(2)	6422(5)	-132(10)	7320(2)

TABLE 3.5.6. The interatomic distances in the $ZnBr_4$ tetrahedra [10^{-3}Å]. The estimated standard deviations are 0.004Å, 0.008Å and 0.01Å for the distances at 293K, 140K and 95K respectively. av is the average of the distances of a type and md is the maximum difference between two distances of a type.

distance type	293K distances	av	md	140K distances	av	md	95K distances	av	md
$Zn-Br_1$	2360 .. 2370	2365	10	2417 2337 2373	2376	80	2374 2397 2380	2384	23
$Zn-Br_2$	2378 .. 2409	2394	31	2404 2411 2381	2399	30	2414 2402 2398	2405	16
$Zn-Br_3$	2361 .. 2414	2388	54	2382 2416 2418	2405	35	2394 2405 2402	2401	11
$Zn-Br_4$	2361 .. 2414	2388	54	2403 2360 2396	2386	43	2433 2383 2393	2403	49
Zn-Br	2360 .. 2414	2384	54	2337 .. 2418	2392	81	2374 .. 2433	2398	59
Br_1-Br_2	3982 .. 4019	4000	38	4043 4026 4010	4026	34	4043 4062 4013	4039	49
Br_1-Br_3	3876 .. 3937	3907	61	3959 3876 3889	3908	84	3944 3916 3880	3913	64
Br_1-Br_4	3876 .. 3937	3907	61	3904 3858 3984	3915	126	3890 3900 3991	3927	101
Br_2-Br_3	3795 .. 3874	3827	79	3885 3824 3862	3857	61	3895 3818 3867	3860	76
Br_2-Br_4	3795 .. 3874	3827	79	3814 3868 3812	3831	56	3833 3890 3833	3852	57
Br_3-Br_4	3838 .. 3900	3869	61	3914 3857 3855	3875	59	3926 3885 3847	3886	79
Br-Br	3795 .. 4019	3890	224	3812 .. 4043	3902	231	3818 .. 4062	3913	244

3.6. Discussion.

By comparing the three structures in table 3.5.3, one can see that the modulation in these structures is very similar. The modulation amplitudes are larger for lower temperatures, but the same patterns of large and small amplitudes exist in all structures, and the phases are equal in very good approximation. This is the case despite the fact that the structure at 293K is incommensurate (or a 17-fold superstructure) and both others are 3-fold superstructures. In all three structures the largest amplitudes are A_2 of Br_1 and Br_2.

In the room temperature structure Br_4 is exactly the m(s) image of Br_3. In both other stuctures, this symmetry operation does not exist. However, in the 140K and 95K structures, Br_4 is in good approximation the m(s) image of Br_3, as can be seen from the modulation amplitudes and phases in table 3.5.3: $d_1(t)$ and $d_3(t)$ of Br_4 are in antiphase with those of Br_3 and $d_2(t)$ is in phase with $d_2(t)$ of Br_3.

Table 3.5.6 shows that $ZnBr_4$ tetrahedra are rather rigid. All Zn-Br distances are about equal. Also, all Br_i-Br_k distances are about equal for each set of i,k. But the Br_1-Br_2 distances are systematically larger than the other ones, and the Br_1-Br_3 and Br_1-Br_4 distances are systematically larger than Br_2-Br_3, Br_2-Br_4 and Br_3-Br_4. These systematic differences also exist in the normal phase (De Pater, 1979), and also in Rb_2ZnCl_4 (Quilichini and Pannetier, 1983), K_2ZnCl_4 (Mikhail and Peters, 1979), K_2CoCl_4 (Vermin et al., 1976), $(NH_4)_2ZnCl_4$ (Matsunaga, 1982), Cs_2CdBr_4 and Cs_2HgBr_4 (Altermatt et al., 1984).

Because apart from these systematic differences the variations in the distances in $ZnBr_4$ tetrahedra are much smaller than the modulation amplitudes of the Br atoms and because the Zn atoms have small modulation amplitudes, it can be concluded that the modulation consists mainly of rotations of the tetrahedra.

As will be shown in chapter 4 of this thesis, the modulation of the three structures of Rb_2ZnBr_4 discussed here are very similar to modulated structures in other A_2BX_4 compounds.

For each structure the equivalent isotropic thermal parameters (table 3.5.4) of the Br atoms are about equal. The thermal motion of these atoms (table 3.5.2) turns out to be strongly anisotropic, with the larger axes in directions normal to the Zn-Br bonds, while the thermal motion of Zn is much smaller than that of the Br atoms. From this it can be concluded that

the thermal motion ,too, consists mainly of rotational movements of the tetrahedra.
In each of the three Rb_2ZnBr_4 structures the thermal motion of Rb_2 is much larger than that of Rb_1. This corresponds to the fact that the cage of Br atoms around Rb_2 is considerably larger than the one around Rb_1. Rb_2 has more space to move in.

A few questions remain: what is the actual space group of the room temperature phase of Rb_2ZnBr_4; and what is the essential difference between phase F and phase IV? The results of the three structure determinations described in this chapter do not give a clue to answers.

Acknowledgements. The X-ray measurements have been performed in cooperation with dr. H. van Koningsveld. The neutron diffraction measurements have been carried out by dr. R.B. Helmholdt of the Netherlands Energy Research Foundation ECN. The investigations were supported in part by the Netherlands Foundation for Chemical Research (SON) with financial aid from the Netherlands Organization for the Advancement of Pure Research (ZWO). Dr. H.D. Flack has kindly sent us a copy of his computer program for the anisotropic absorption correction.

Chapter 4

COMPARISON OF DISTORTED β-K_2SO_4 TYPE STRUCTURES.

4.1. Introduction.

In this chapter the "distorted β-K_2SO_4 type structures" will be compared with each other. Distorted β-K_2SO_4 type structures are incommensurate structures or superstructures in which the atoms have coordinations analogous to the coordinations of the atoms in β-K_2SO_4. For the reasons given below, the term superstructure is understood to include "1-fold superstructures": structures with the same unit cell as β-K_2SO_4, but with lower symmetry. The space group of the basic structure of an incommensurately distorted β-K_2SO_4 type structure is Pcmn (the space group of β-K_2SO_4) or a subgroup of it. The space group of a distorted β-K_2SO_4 type superstructure is a proper subgroup of Pcmn. The β-K_2SO_4 type itself is not included in the group of distorted β-K_2SO_4 type structures. It occurs, however, often as a high temperature phase of compounds that have a phase with a distorted β-K_2SO_4 type structure.
In practice there is no problem in deciding whether a structure is of the distorted β-K_2SO_4 type or not. This statement can be illustrated by the following examples of structures that have some similarities with β-K_2SO_4, but very clearly do not belong to the β-K_2SO_4 type or the distorted β-K_2SO_4 type structures. In olivine type structures (Eysel, 1971) the coordinations of part of the atoms are very different from those in β-K_2SO_4. The incommensurate phases of K_2MoO_4, K_2WO_4 and Rb_2WO_4 (Tuinstra and Van den Berg, 1983) have a basic structure of wich the space group (Ccmm) is not Pcmn or a subgroup of it.
The modulated structures in Rb_2ZnBr_4 and related compounds, however, clearly are distorted β-K_2SO_4 type structures.

In this chapter, modulation wave vectors will be assigned also to 1-fold and 2-fold superstructures. Though these structures are not modulated structures according to the definition given in chapter 1, they will be regarded here as such. As will be shown in section 4.4, these structures have the same kind of local distortions as the other distorted β-K_2SO_4 type structures. Some of the 1-fold and 2-fold superstructures actually are structures of lock-in phases of compounds having an incommensurate structure.

In this thesis only distorted β-K_2SO_4 type structures with an incommensurate or commensurate modulation wave vector parallel to $\underline{c}$ are studied. Most distorted β-K_2SO_4 type structures obey this condition. Only a few exceptions are known. In these exceptional structures other axes are doubled or the modulation wave vector has another direction, as indicated behind the compound name:

- Cs_2MnI_4: $2\underline{a}$, $2\underline{b}$, $2\underline{c}$, below 105K (Zandbergen, 1981)
- Cs_2MgI_4: $2\underline{a}$, $2\underline{b}$, $2\underline{c}$, below 85K (Zandbergen, 1981)
- Cs_2HgBr_4: $2\underline{b}$, below 85K (Plesko, 1981)
- $(TMA)_2CuBr_4$: $\underline{q}=\gamma\underline{a}^*$, $0.38<\gamma<0.43$, between 242K and 272K,
  $2\underline{a}$, between 237K and 242K (Hasebe et al., 1982)
- Ca_2SiO_4 with part of Ca replaced by Ba or Sr or part of Si by B:
  $2\underline{a}$, $2\underline{b}$ (Suzuki and Yamaguchi, 1968)
- $6Ca_2Si0_4.1Ca_3(PO_4)_2$: $\underline{q}=0.267\underline{b}^*$ (Saalfeld and Klaska, 1981)

In $(TMA)_2CuBr_4$ the $CuBr_4$ groups are distorted considerably from a regular tetrahedron by the Jahn-Teller effect. This can be the cause of the exceptional behaviour of this compound in comparison with the other TMA compounds (see section 4.2). The last two examples strictly do not belong to the distorted β-K_2SO_4 type structures, because the compounds cannot be represented by the general chemical formula A_2BX_4.
The seven exceptions will not be considered further.

In section 4.2 the symmetry of the distorted β-K_2SO_4 type structures will be discussed. The structures reported in literature that will be compared are introduced in section 4.3. In section 4.4 the interatomic distances in these structures are compared. Section 4.5 compares the modulation functions of incommensurate structures and 3- and 4-fold superstructures. In section 4.6 the existence of large superstructures, in phases which have been supposed to be incommensurate until recently, will be discussed. Parts of this chapter have been published before (Hogervorst and De Wolff, 1982; Hogervorst, 1984).

4.2. Symmetry.

Many compounds, for instance Rb_2ZnBr_4 and Rb_2ZnCl_4, show phase transitions from an incommensurate structure to a superstructure. The diffraction patterns of both phases are almost identical. The incommensurate structures and the superstructures therefore cannot differ much, so their symmetries must be closely related. In this section, for the distorted β-K_2SO_4 type structures the relation between 4-dimensional space groups of incommensurate structures and 3-dimensional space groups of superstructures will be discussed.
Although the basic symmetry Pcmn allows two different 4-dimensional space groups with the modulation wave vector parallel to $\underline{c}$, it turns out that the symmetries of all observed distorted β-K_2SO_4 type structures are related to just one of them.
It also will be shown that symmetry can help to choose the correct modulation wave vectors in incommensurate structures and superstructures in order to obtain comparable modulation functions. This information will be used in section 4.5.
In section 4.6 the results of this section will be used in connection with large superstructures having a special kind of modulation wave vector.

4.2.1. 4-dimensional space groups.

A 4-dimensional space group can have different symbols, depending on the choice of the modulation wave vector.
As an illustration, figure 4.2.1 shows the same structure described as a modulated structure with wave vector $\underline{q}$, and as one with modulation wave vector $\underline{q}'=\underline{c}^*-\underline{q}$. In the description with $\underline{q}$ the two rows of atoms are related by symmetry operation c(s): the modulation functions have a phase difference of 0.5. In the other description (with $\underline{q}'$, dashed modulation functions) the two rows of atoms are related by c(1): the modulation functions do not have a phase difference.
Figure 4.2.1b shows the reciprocal lattice. The reflection conditions are different. If $\underline{q}$ is chosen, the reflection condition for the h0lm reflections is: $l+m$=even, whereas the condition is l=even if $\underline{q}'$ is chosen.
Choosing another wave vector in a modulated structure is analogous to choosing one of the crystallographic axes in another way in a normal

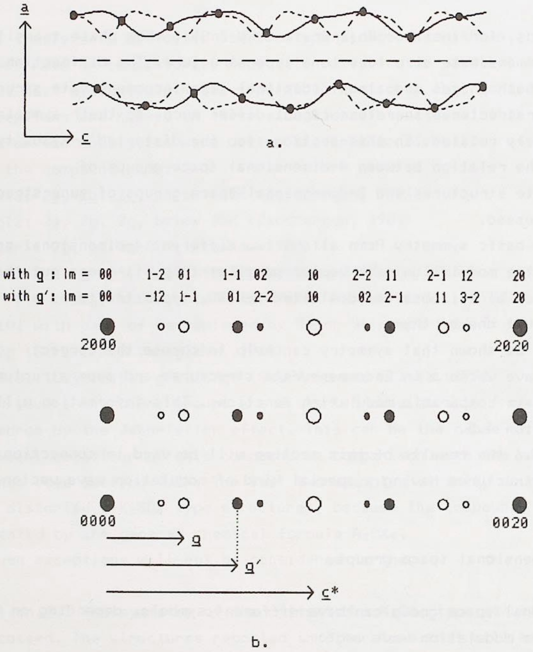

FIGURE 4.2.1. Two descriptions for the same modulated structure.
a. The atomic positions of the structure can be described by modulation functions corresponding to modulation wave vector $\underline{q}$ (full lines) or to $\underline{q}'=\underline{c}^*-\underline{q}$ (the dashed ones).
Note that these curves have the same shape, in spite of different wavelengths and an inversion in z.
The symbol for the c-glide plane normal to $\underline{a}$ is c(s) in the first case and c(1) in the second case.
b. The corresponding reciprocal lattice. The rule for systematic absences (open circles) is different in both cases for the h0lm reflections: l+m=odd and l=odd respectively.

structure. For example: if a space group has symbol P1n1 with respect to axes $\underline{a}$, $\underline{b}$ and $\underline{c}$, then it has symbol P1c1 with respect to axes $\underline{a}$, $\underline{b}$ and $\underline{a}+\underline{c}$. The reflection conditions change accordingly.

4-dimensional space groups are non-equivalent if their symbols cannot be transformed into a single symbol by a change of axes and/or a change of $\underline{q}$.
Just two non-equivalent 4-dimensional space groups exist for an incommensurate structure with Pcmn as basic structure space group and a modulation wave vector $\underline{q}$ parallel to $\underline{c}$ (De Wolff et al., 1981). The first of these is

$$P\,\frac{2_1}{c}\,\frac{2_1}{m}\,\frac{2_1}{n}\,(0\;0\;\gamma)\,(\frac{\bar{1}}{s}\,\frac{\bar{1}}{s}\,\frac{1}{\bar{1}})\text{ , or in short: }Pcmn(00\gamma)(ss\bar{1}). \tag{4.2.1}$$

If the equivalent modulation wave vector $\underline{q}'=\underline{c}^*-\underline{q}$ is chosen, then the symbol of the same space group is

$$P\,\frac{2_1}{c}\,\frac{2_1}{m}\,\frac{2_1}{n}\,(0\;0\;\gamma')\,(\frac{\bar{1}}{1}\,\frac{\bar{1}}{s}\,\frac{s}{\bar{1}})\text{ or }Pcmn(00\gamma')(1s\bar{1}),\ \gamma'=1-\gamma. \tag{4.2.2}$$

The second possible 4-dimensional space group is

$$P\,\frac{2_1}{c}\,\frac{2_1}{m}\,\frac{2_1}{n}\,(0\;0\;\gamma)\,(\frac{\bar{1}}{1}\,\frac{\bar{1}}{1}\,\frac{1}{\bar{1}})\text{ or }Pcmn(00\gamma)(11\bar{1}). \tag{4.2.3}$$

Choosing $\underline{q}'$ as modulation wave vector, the space group symbol is

$$P\,\frac{2_1}{c}\,\frac{2_1}{m}\,\frac{2_1}{n}\,(0\;0\;\gamma')\,(\frac{\bar{1}}{s}\,\frac{\bar{1}}{1}\,\frac{s}{\bar{1}})\text{ or }Pcmn(00\gamma')(s1\bar{1}),\ \gamma'=1-\gamma. \tag{4.2.4}$$

In this thesis the symbols 4.2.1 and 4.2.3 are chosen to represent the first and the second possible 4-dimensional space groups respectively. It should be noted that this choice implies that the modulation wave vector is not limited to the first Brillouin zone (see subsection 4.2.3).

4.2.2. Superstructure space groups.

Now we will investigate how superstructure space groups can be deduced from 4-dimensional space group 4.2.1 or 4.1.3.
In order to find the relation between the symmetry of an incommensurate structure and that of a superstructure, let us examine what happens with individual 4-dimensional symmetry operations if the modulation wave vector

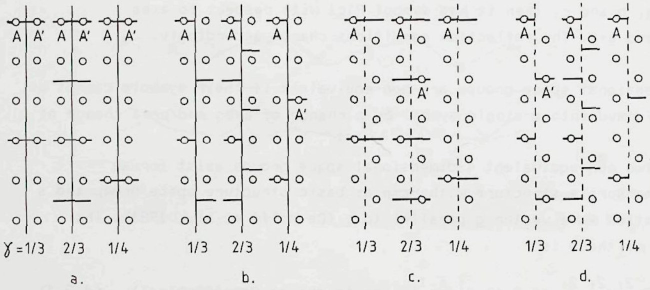

FIGURE 4.2.2. Modulation in superstructures with γ = odd/odd = *1/3; even/odd = 2/3; odd/even* = 1/4 in the presence of a symmetry element; a. the symmetry element is m(1); b. m(s); c. c(1); d. c(s).

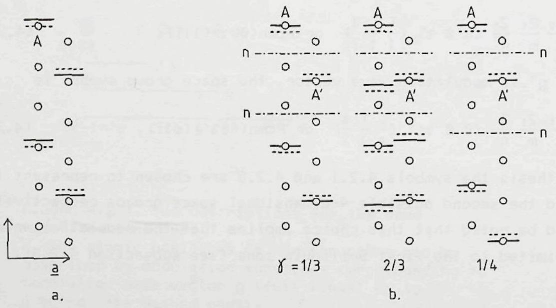

FIGURE 4.2.3.
a. Symmetry element n($\bar{1}$) does not appear in a superstructure if *the phase of the modulation wave* is chosen arbitrarily.
b. If the phase is chosen properly, symmetry element n($\bar{1}$) appears in the superstructure as a n-glide plane for any given rational value of γ.
Only two of the n-glide planes are drawn in each superstructure. The first superstructure is obtained from the structure in part a of this figure by shifting the complete modulation wave with respect to the basic structure.

becomes commensurate (something similar has been done independently by Yamamoto, 1982 and Janssen, 1985):

$$\underline{q} = \gamma\,\underline{c}^* \quad \text{with } \gamma = u/v \quad (u,\ v \text{ integer}). \qquad (4.2.5)$$

Suppose the symmetry of the basic structure and the symmetry relations between the modulation functions do not change during this imaginary lock-in process. Then many of these relations will condense into 3-dimensional symmetry elements, but not necessarilly all relations will do so. It will now be shown that some 4-dimensional symmetry elements can exist as a 3-dimensional Euclidian symmetry element in the superstructure only for certain parity combinations of u and v: for the relevant 4-dimensional symmetry operations, figure 4.2.2 shows the 3-dimensional symmetry *operations which can result. Each drawing in this figure shows two rows of* atoms, mutually related by the 3-dimensional part of the 4-dimensional symmetry operation. The modulation is represented by horizontal bars repeating with the modulation period c/γ, starting with a bar through the *top left atom A. The type of modulation (e.g. magnetic, occupational or* displacive) is not relevant in this discussion. For a rational value of γ, bars crossing an atom will occur again at the superstructure repeat distance c_s=vc. If the 4-dimensional symmetry operation involves a phase *difference in the modulation functions, the bars in the second row are* shifted accordingly. The symmetry operations of the superstructure, if any, are those which map the atom A on any other atom A′ crossed by a bar.
Figure 4.2.2a shows that a simple mirror operation m(1) is conserved *independently of the values of u and v. If the reflection is combined with* a shift 1/2 in the phase of the modulation (operation m(s)) the bars alternate as shown in figure 4.2.2b. Coincidences of bars with atoms in the second row now occur only if u=odd and v=even. In that case the m(s) operation appears in the superstructure as a c-glide plane relating, for instance, the atoms A and A′. For the other parity combinations, the 4-dimensional operation m(s) is completely lost.
Figure 4.2.2c depicts the situation for a c(1) element. Conservation of the point group element now requires u=even and v=odd. Then a c-glide plane results in the superstructure. Such a c-glide plane also appears for the element c(s): in figure 4.2.2d the alternating bars correspond to the phase shift of 1/2 of that element. But the condition now is: u and v both odd. The 4-dimensional symmetry operations 2_1(1) and 2_1(s) (not shown in the figure) impose the same parity conditions as c(1) and c(s) respectively. The resulting symmetry operation in the superstructure is a 2_1-screw axis

in both cases.

Thus far only 4-dimensional symmetry elements with $\varepsilon=1$ are considered (ε and R_{33} are defined in section 1.3). Symmetry elements with $\varepsilon=-1$ do not give rise to parity conditions. The phase of the modulation wave can always be chosen such that the symmetry operation exists in the superstructure. 4-dimensional symmetry element $n(\bar{1})$ becomes a n-glide plane then and $2_1(\bar{1})$ a 2_1-screw axis. Figure 4.2.3 shows the case of a $n(\bar{1})$ operation. In part a of this figure it is shown that if the phase of the modulation wave is arbitrary the $n(\bar{1})$ operation does not appear in the superstructure. In part b it can be seen that for a proper choice of the phase of the modulation wave, the $n(\bar{1})$ operation appears as a n-glide plane in the superstructure for all parity combinations of u and v.

Now, after the above discussion of individual symmetry operations, the relation between 4-dimensional space groups and superstructure space groups will be discussed. First we define a new concept, "rational subgroup". If each symmetry element of a superstructure space group can be deduced from an element of a certain 4-dimensional space group by the imaginary lock-in procedure described above, then this superstructure space group is a rational subgroup of that 4-dimensional space group. This 4-dimensional space group will then be called a prototype symmetry of that superstructure space group. In general, more than one prototype symmetry exists for one superstructure space group. A 4-dimensional space group will also be called a prototype symmetry of itself and of each of its proper subgroups.
With the information supplied above, for each space group of a superstructure with a multiple-$\underline{c}$ axis we will investigate whether it is a rational subgroup of the two 4-dimensional space groups mentioned in the previous subsection. In order to do this it is sufficient to consider the superstructure space group elements with $R_{33}=1$. If all these elements can originate from 4-dimensional symmetry elements of one of the two 4-dimensional space groups, then the superstructure space group is a rational subgroup of this 4-dimensional space group.
(It is always possible to choose the phase of the modulation wave such that one of the symmetry elements with $R_{33}=-1$ can be deduced from a 4-dimensional space group element. Then this is also true for all other elements with $R_{33}=-1$, since each of them is a product of the one just *mentioned and an element with* $R_{33}=+1$.)

The parity conditions for u and v, necessary for the relevant 4-dimensional symmetry operations to be present in a rational subgroup of the two possible prototype symmetries (4.2.1 and 4.2.3) are given in table 4.2.1. From this table it can be seen that for instance a rational subgroup of prototype symmetry 4.2.1 cannot contain both a c-glide plane normal to $\underline{a}$ and a 2_1-screw axis parallel to $\underline{c}$ because the parity conditions are different. It can also be seen that a rational subgroup of this prototype symmetry cannot contain a mirror plane normal to $\underline{b}$. Rational subgroups of the second prototype symmetry cannot contain a c-glide plane perpendicular to $\underline{b}$. Hence certain space groups can be a rational subgroup of only one of the prototype symmetries.
In table 4.2.2 one can find for each space group of a superstructure with a multiple-$\underline{c}$ axis wether it is a rational subgroup of $Pcmn(00\gamma)(ss\bar{1})$, or of $Pcmn(00\gamma)(11\bar{1})$, or of both.

Now we shall investigate whether there is a 4-dimensional space group that is a prototype symmetry of all known distorted β-K_2SO_4 type structures. All the commensurate distorted β-K_2SO_4 type structures published so far (see table 4.2.4) have a structure with a space group of row 1 or 2 of table 4.2.2 (underlined). Hence all these space groups are rational subroups of $Pcmn(00\gamma)(ss\bar{1})$. The observed space groups for the incommensurate structures are either $Pcmn(00\gamma)(ss\bar{1})$ or one of its subgroups.
Hence $Pcmn(00\gamma)(ss\bar{1})$ *is the only common prototype symmetry* of all observed distorted β-K_2SO_4 type structures with the modulation wave vector parallel to $\underline{c}^*$.

4.2.3. Standardization of the modulation wave vectors.

The standardization discussed in this subsection is based on a remarkable common feature of distorted β-K_2SO_4 type structures. They already share $Pcmn(00\gamma)(ss\bar{1})$ as a common prototype symmetry (see above), *which means that* at least some of the symmetry conditions for modulation functions imposed by $Pcmn(00\gamma)(ss\bar{1})$ are conserved as exact 3-dimensional symmetry relations. The new feature, to be called "pseudo prototype symmetry" manifests itself in the fact that those conditions which are not thus exactly fulfilled, are still satisfied in a very good approximation as non-crystallographic symmetries of the superstructure. Foremost among these pseudo-$Pcmn(00\gamma)(ss\bar{1})$ properties is the fact that (the first harmonics of) displacements of atoms lying in the mirror plane perpendicular to $\underline{b}$ in β-K_2SO_4 *(which are also the dominant displacements in all structures)* are

TABLE 4.2.1. Parity conditions for occurrence of symmetry elements in a rational subgroup.
x/-: the symmetry element can/cannot result from the indicated 4-dimensional space group for the indicated type of modulation wave vector $\underline{g}=(u/v)\underline{c}^*$ (o=odd, e=even).

symmetry element	$Pcmn(00\gamma)(ss\bar{1})$ = (4.2.1)			$Pcmn(00\gamma)(11\bar{1})$ = (4.2.3)		
	u/v= o/o	e/o	o/e	u/v= o/o	e/o	o/e
c11	x	-	-	-	x	-
1c1	-	-	x	-	-	-
112_1	-	x	-	-	x	-
1m1	-	-	-	x	x	x

TABLE 4.2.2. The possible space groups for distorted β-K_2SO_4 type superstructures.
x/-: the superstructure space groups are / are not rational subgroups of the indicated prototype symmetry. The space groups that are actually found (see table 4.2.4) are underlined.

row	superstructure space groups	prototype symmetry	
		$Pcmn(00\gamma)(ss\bar{1})$	$Pcmn(00\gamma)(11\bar{1})$
1	$\underline{P2_1cn}$, $\underline{P12_1/c1}$, $\underline{P1c1}$	x	-
2	$\underline{Pc2_1n}$, $\underline{P2_1/c11}$, $Pc11$, $\underline{P112_1/n}$, $\underline{P2_12_12_1}$, $P112_1$, $P11n$, $P2_111$, $P12_11$, $\underline{P\bar{1}}$, $P1$	x	x
3	$Pcmn$, $P2_1mn$, $Pcm2_1$, $P12_1/m1$, $P1m1$	-	x

TABLE 4.2.3. Possible combinations (x) of rational subgroups of $Pcmn(00\gamma)(ss\bar{1})$ and modulation wave vectors $\underline{g}=(u/v)\underline{c}^*$ giving modulation functions that correspond to those of incommensurate structures with space group symbol $Pcmn(00\gamma)(ss\bar{1})$.

rational subgroups	u/v=odd/odd	even/odd	odd/even
$Pc2_1n$, $P2_1/c11$, $Pc11$	x	-	-
$P112_1/n$, $P2_12_12_1$. $P112_1$	-	x	-
$P2_1cn$, $P12_1/c1$, $P1c1$	-	-	x
$P11n$, $P2_111$, $P12_11$, $P\bar{1}$, $P1$	x	x	x

parallel to $\underline{b}$ in good approximation, even in the many cases where there is no symmetry constraint for their direction. (In structures with the other space group, $Pcmn(00\gamma)(11\bar{1})$, the displacements of atoms in the mirror plane cannot have components parallel to $\underline{b}$!)

Figure 4.2.1 already demonstrated that the relations between modulation functions of symmetry-equivalent atoms depend on the choice of the modulation wave vector. For modulation wave vector $\underline{g}'=\underline{c}^*-\underline{g}$ other modulation functions are needed than for $\underline{g}$. This is the case for superstructures as well as for incommensurate structures. (The only exception is the 2-fold superstructure. In that case $\underline{g}'=\underline{g}$.)
Therefore, for comparison of modulation functions of different incommensurate structures and superstructures, it is important that the choices of the modulation wave vectors in different structures correspond to each other. The symmetry can guide us to the correct choice. As stated at the end of subsection 4.2.1, for incommensurate structures with the prototype symmetry, $\underline{g}$ is chosen such that the space group symbol is (4.2.1) rather then (4.2.2). This choice has also been made by Rasing (1982), and it corresponds to the choice of the modulation wave vector for Rb_2ZnBr_4, Rb_2ZnCl_4 and K_2ZnCl_4 made by De Pater (1979) and Gesi and Iizumi (1978, 1979a).
More generally the modulation wave vector in an incommensurate structure will be chosen here such that the symbol of the c-glide plane normal to $\underline{a}$ is c(s) and the symbol of the 2_1-screw axis parallel to $\underline{c}$ is $2_1(1)$. These are the symmetry elements of which the symbols change if the other modulation wave vector is chosen. Of course this recipe can only be used *if* at least *one of* these symmetry elements is present in the space group.
If both elements are absent, then a more detailed investigation is *necessary. In that case the c(s)-glide plane* is *not present*, so the 0klm reflections do not show the corresponding systematic absences.
Nevertheless, because of the pseudo-prototype symmetry, the reflections which correspond to those *systematically* absent *for the prototype* symmetry will be much weaker than the other reflections. This information can be used to find the modulation wave vector corresponding to symbol (4.2.1).

In superstructures, the results of subsection 4.2.2 can be used for the standardization of the modulation wave vectors. The relation between superstructure symmetry and prototype symmetry (4.2.1) can be found in table 4.2.1. From this table it can be concluded that if a c-glide plane

normal to $\underline{a}$ is present, then the modulation wave vector must be $\underline{q}=(u/v)\underline{c}^*$ with u and v both odd. If a 2_1-screw axis parallel to $\underline{c}$ is present, u must be even. The resulting modulation functions, found by fourier-analysis of the atomic coordinates of the superstructure, can be compared directly with those of the incommensurate structures discussed before. For all rational subgroups of Pcmn(00γ)(ss$\bar{1}$) the modulation wave vectors for which they can occur are listed in table 4.2.3.
If both the c-glide plane normal to $\underline{a}$ and the 2_1-screw axis parallel to $\underline{c}$ are absent, again that choice should be made for which the 0klm reflections with l+m=odd are weak.
(This is not possible in the case of a 1-fold or a 2-fold superstructure. For a 1-fold superstructure the satellite reflections are also main reflections: e.g. reflection 1231 is reflection 1240 for $\underline{q}=\underline{c}^*$ or 1230 for $\underline{q}=\underline{0}$. For a 2-fold superstructure the reflections with l+m=odd are the same as those with l+m=even: e.g. reflection 0231 is reflection 024$\bar{1}$ for $\underline{q}=(1/2)\underline{c}^*$. On the other hand: for a 1-fold superstructure the modulation functions are constants and for a 2-fold superstructure there is only one possible choice for $\underline{q}$ because $\underline{q}'=\underline{q}$. Therefore, in either case the choice does not matter anyhow.)

A consequence of the above described standardization of modulation wave vectors is that for some structures the standardized modulation wave vector is outside the first Brillouin zone. Now, solid state physicists prefer to choose wave vectors within this zone. The following example will show why it is convenient to neglect this preference here.
Consider an A_2BX_4 compound with a 2-fold superstructure phase between two incommensurate phases. On lowering the temperature, the modulation wave vector changes continuously from $0.46\underline{c}^*$ to $0.49\underline{c}^*$ in the high temperature phase. Then it jumps to $\underline{c}^*/2$ at the lock-in phase transition. On lowering the temperature further, a second phase transition occurs and the structure becomes incommensurate again. In this second incommensurate phase the modulation wave vector changes from $0.52\underline{c}^*$ to $0.57\underline{c}^*$. Using these modulation wave vectors, the two incommensrate *phases have the same 4-dimensional space group (e.g. Pcmn(00γ)(ss$\bar{1}$)), the* reflections with the same indices in both phases have about equal *intensities, and the rules for systematic extinctions are equal. In fact,* the two incommensurate phases can be interpreted as one incommensurate *phase, interrupted by the 2-fold superstructure phase.*
If in the second incommensurate phase the modulation wave vector would have been chosen within the first Brillouin zone, the space group symbol and the rules for systematic extinctions would have been completely different for both incommensurate phases. The relationship between these two phases would be hard to recognize in this situation.
It should be noted that the above comment, although illustrated for incommensurate structures, applies to superstructures as well, even including the 1-fold superstructures.

4.2.4. Application to observed structures.

In table 4.2.4 all distorted β-K_2SO_4 type structures which are mentioned in the literature are given, together with the standardized modulation wave vectors (expressed as γ in $\underline{q}=\gamma\underline{c}^*$).
The 4-fold superstructures in this table do not contain a c-glide plane normal to $\underline{a}$ or a 2_1-screw axis parallel to $\underline{c}$. As discussed above, in this case we have to rely on systematically weak intensities. The diffraction pattern of $(NH_4)_2ZnCl_4$ at room temperature (space group P1c1) shows very clearly that $\underline{q}=(1/4)\underline{c}^*$ should be chosen, and not $\underline{q}=(3/4)\underline{c}^*$: for $\underline{q}=(1/4)\underline{c}^*$ the 0klm reflections with l+m=odd *are very weak, and for the other choice they are strong. In section 4.4 it* will be shown that the resulting modulation functions of the P1c1- and the *$P2_1cn$ structure of $(NH_4)_2ZnCl_4$ are indeed very similar to the modulation functions of the other structures. According to Zandbergen (1981) Cs_2MnI_4 has space group $P2_1cn$ and is probably isomorphous with $(NH_4)_2ZnCl_4$.*
Table 4.2.4 includes 3-fold and 7-fold superstructures with space group *$P2_12_12_1$ or $P112_1/n$. The standardized modulation wave vectors, based on the* presence of the 2_1-screw axis parallel to $\underline{c}$ (originating from the $2_1(1)$ *operation of the prototype symmetry), have $\gamma=2/3$ or $\gamma=4/7$. For these* modulation wave vectors, the 0klm reflections with l+k=odd are very much weaker than those with l+m=even. Hence, they show pseudo-c(s) symmetry. The combination of this pseudo-c(s) operation and the $2_1(1)$ operation excludes Pcmn(00γ)(11$\bar{1}$) from being the prototype symmetry of these structures, and again confirms the pseudo-prototype symmetry.
The space group of the structure of $(NH_4)_2ZnCl_4$ with $\gamma=2/7$ is not given in the literature. This value of γ has been determined on the basis of pseudo-c(s) absences. Assuming that Pcmn(00γ)(ss$\bar{1}$) is the prototype symmetry of this superstructure, it can be concluded from this value of γ that the space group of this structure is $P112_1/n$, $P2_12_12_1$ or a subgroup of one of them (see table 4.2.3). Sato et al. (1984) observed that this structure is weakly ferroelectric along the $\underline{b}$ axis. This means that the space group

TABLE 4.2.4. Distorted β-K_2SO_4 type structures.
γ gives the length of the modulation wave vector: $\underline{q} = \gamma\,\underline{c}^*$.

sp.gr.	γ	compound	references
inc.1	0.31	K_2ZnCl_4	Gesi and Iizumi (1979a)
*	0.31	Rb_2ZnCl_4	Gesi and Iizumi (1979a)
	0.294	Rb_2ZnBr_4	this thesis (chapter 3)
	0.31	K_2SeO_4	Iizumi et al. (1977)
	0.384	Cs_2FeI_4	Zandbergen (1981, 1984))
*	0.48	$(NH_4)_2BeF_4$	Iizumi and Gesi (1977)
*	0.255	$(NH_4)_2ZnCl_4$	Sato et al. (1984)
*	0.255	$(NH_4)_2ZnBr_4$	Sato et al. (1983)
*	0.517	$(TMA)_2MnCl_4$	Mashiyama and Tanisaki (1981)
*	0.326	$(TMA)_2CuCl_4$	Gesi (1982), Sugiyama et al. (1980)
* %	0.56, 0.58	$(TMA)_2FeCl_4$	Mashiyama and Tanisaki (1982)
*	0.55	$(TMA)_2NiCl_4$	Mashiyama and Tanisaki (1982)
*	0.58	$(TMA)_2ZnCl_4$	Gesi (1982), Tanisaki and Mashiyama (1980)
* %	0.59, 0.61	$(TMA)_2CoCl_4$	Gesi (1982), Marion (1981)
inc.2	0.18	Cs_2CdBr_4	Maeda et al. (1983), Altermatt et al. (1984)
	0.15	Cs_2HgBr_4	Plesko (1981), Altermatt et al. (1984)
$P2_12_12_1$	4/7	$(TMA)_2FeCl_4$	Mashiyama and Tanisaki (1982), Hasebe et al. (1984)
		D-$(TMA)_2ZnCl_4$	Marion et al. (1981)
?	2/7	$(NH_4)_2ZnCl_4$	Sato et al. (1984)
$Pc2_1n$	3/5	$(TMA)_2FeCl_4$	Mashiyama and Tanisaki (1982)
		$(TMA)_2ZnCl_4$	Gesi (1982), Marion (1981)
		$(TMA)_2CoCl_4$	Gesi (1982), Marion (1981)
$P2_1cn$	1/4	Cs_2MnI_4	Zandbergen (1981)
#		Cs_2MgI_4	Zandbergen (1981)
		$(NH_4)_2ZnCl_4$	Matsunaga (1982)
#		$(NH_4)_2ZnBr_4$	Sato et al. (1983)
#		$(NH_4)_2CoCl_4$	Broda (1984)
P1c1	1/4	$(NH_4)_2ZnCl_4$	Van Koningsveld (1983)
$Pc2_1n$	1/3	K_2ZnCl_4	Mikhail and Peters (1979)
		Rb_2ZnCl_4	Quilichini and Pannetier (1983)
		Rb_2ZnBr_4	this thesis (chapter 3)
		K_2SeO_4	Iizumi et al. (1977)
		K_2CoCl_4	Vermin et al. (1976)
		Rb_2MgBr_4	Seifert and Wasel-Nielen (1977)
		Ba_2TiO_4	Gunter and Jameson (1984)
		$(NH_4)_2ZnCl_4$	Matsunaga et al. (1982)
#		$(NH_4)_2ZnBr_4$	Sato et al. (1983)
#		$(NH_4)_2CoCl_4$	Broda (1984)

TABLE 4.2.4. continued.

sp.gr.	γ	compound	references
$P2_1/c11$	1/3	$(TMA)_2CuCl_4$	Gesi (1982)
$P2_12_12_1$	2/3	$(TMA)_2ZnCl_4$	Gesi (1982)
		$(TMA)_2CoCl_4$	Gesi (1982)
$P112_1/n$	2/3	$(TMA)_2MnCl_4$	Mashiyama and Tanisaki (1981)
		$(TMA)_2FeCl_4$	Mashiyama and Tanisaki (1982)
		$(TMA)_2ZnCl_4$	Gesi (1982)
		$(TMA)_2CoCl_4$	Gesi (1982)
$P2_1cn$	1/2	Ba_2SnS_4	Suza and Steinfink (1971)
		Sr_2CrO_4	Wilhelmi (1966)
$		$(NH_4)_2BeF_4$	Misyul et al. (1980)
$P12_1/c1$	1/2	Cs_2FeI_4	Zandbergen (1981)
		$(TMA)_2MnCl_4$	Mashiyama and Tanisaki (1981)
$Pc2_1n$	1/1	$(NH_4)_2SO_4$	Schlemper and Hamilton (1966)
$P2_1/c11$	1/1	$(TMA)_2CuBr_4$	Hasebe et al. (1982)
		$(TMA)_2FeCl_4$	Mashiyama and Tanisaki (1982)
		$(TMA)_2ZnCl_4$	Gesi (1982)
		$(TMA)_2CoCl_4$	Gesi (1982)
		$(TMA)_2ZnBr_4$	Hasebe et al. (1984)
		$(TMA)_2CoBr_4$	Hasebe et al. (1984)
$P\bar{1}$	0/1	Cs_2HgBr_4	Plesko (1981), Altermatt et al. (1984)
		Cs_2CdBr_4	Plesko (1981), Altermatt et al. (1984)
$P112_1/n$	0/1	Cs_2CdBr_4	Plesko (1981), Altermatt et al. (1984)
		Cs_2HgBr_4	Plesko (1981), Altermatt et al. (1984)
		Ca_2SiO_4	Jost et al. (1977)
		Ba_2TiO_4	Wu and Brown (1973)
		Sr_2SiO_4	Catti et al. (1983)
		Cs_2MnI_4	Zandbergen (1981)
		Eu_2SiO_4	Muller and Roy (1974)
		Na_2BeF_4	Muller and Roy (1974)
		$(TMA)_2CuCl_4$	Gesi (1982)

inc.1: $Pcmn(00\gamma)(ss\bar{1})$
inc.2: $P112_1/n(00\gamma)(111/\bar{1})$
* symmetry not determined, but assumed by the author of this thesis.
# symmetry assigned on basis of similarities with the preceding compound
$ $(NH_4)_2BeF_4$ has the same symmetry as the other two compounds in this group, but the structure is different (see section 4.3).
% *two phases with such a structure exist.*
? space group unknown.

TABLE 4.2.5. Phase sequence of A_2BX_4 compounds with phases having distorted β-K_2SO_4 type structures. For each compound alternately structures and phase transition temperatures are given. Each structure is represented by its space group and the standardised modulation wave vector component γ (between brackets).

compound	phase sequence (temperatures in K)	references
K_2ZnCl_4	Pcmn 553 inc(0.31) 403 $Pc2_1n$(1/3) 213 ?(?) 145 ?(?)	Gesi and Iizumi (1979a), Shuvalov et al.(1983)
Rb_2ZnCl_4	Pcmn 303 inc(0.31) 194 $Pc2_1n$(1/3) 75 ?(1/3)	Quilichini and Pannetier (1983)
Rb_2ZnBr_4	Pcmn 347 inc(0.294) 190 $Pc2_1n$(1/3) 112 $Pc2_1n$(1/3) 77 Pc11(1/3)?	this thesis (chapter 3)
Cs_2CdBr_4	Pcmn 252 inc(0.18) 237 $P112_1/n$(0) 158 $P\bar{1}$(0)	Altermatt et al. (1984), Plesko (1981)
Cs_2HgBr_4	Pcmn 245 inc(0.15) 232 $P112_1/n$(0) 167 $P\bar{1}$(0) 85 $P\bar{1}(2\underline{b})$	Altermatt et al. (1984), Plesko (1981)
Cs_2FeI_4	Pcmn 152 inc(0.384) 123 $P12_1/c1$(1/2)	Zandbergen (1981)
Cs_2MnI_4	Pcmn 240 $P2_1cn$(1/4) 211 $p112_1/n$(0) 105 F1 or $F\bar{1}(2\underline{a},2\underline{b},2\underline{c})$	Zandbergen (1981)
K_2SeO_4	$P6_3/mmc$ 734 Pcmn 129 inc(0.31) 94 $Pc2_1n$(1/3) 56 ?(?)	Iizumi et al. (1977), Lopez Echarri et al. (1980)
Sr_2SiO_4	Pcmn 358 $P112_1/n$(0)	Catti et al. (1983)
Ba_2TiO_4	$Pc2_1n$(1/3) ? $P112_1/n$(0)	Gunter and Jameson (1984)
Ca_2SiO_4	$P6_3/mmc$ 1720 Pcmn 1430 ?(1/3) 943 $P112_1/n$(0) 700 olivine	Saalfeld (1975)
$(NH_4)_2SO_4$	Pcmn 223 $Pc2_1n$(1)	Schlemper and Hamilton (1966)
$(NH_4)_2BeF_4$	Pcmn 183 inc(0.48) 177 $P2_1cn$(1/2)	Onodera and Shiozaki (1979)
$(NH_4)_2ZnCl_4$	Pcmn 406 inc(0.255) 365 $P2_1cn$(1/4) 319 P1c1(1/4) 276 ?(2/7) 269 $Pc2_1n$(1/3)	Matsunaga (1982), Sato et al. (1984)
$(NH_4)_2CoCl_4$	Pcmn 323 $P2_1cn$(1/4)? 150? $Pc2_1n$(1/3)	Broda (1984)
$(NH_4)_2ZnBr_4$	Pcmn 432 inc(0.255) 395 $P2_1cn$(1/4) 217 $Pc2_1n$(1/3)	Sato et al. (1983)
$(TMA)_2FeCl_4$	Pcmn 282 inc(0.56) 271 $P2_12_12_1$(4/7) 267 inc(0.58) 266 $P112_1/n$(2/3) 240 $P2_1/c11$(1)	Mashiyama and Tanisaki (1982)
$(TMA)_2MnCl_4$	Pcmn 292 inc(0.517) 291 $P12_1/c1$(1/2) 267 $P112_1/n$(2/3) 175 ?(?)	Mashiyama and Tanisaki (1981)
$(TMA)_2CuCl_4$	Pcmn 299 inc(0.326) 291 $P2_1/c11$(1/3) 264 $P112_1/n$(0)	Gesi (1982)
$(TMA)_2NiCl_4$	Pcmn 285 inc(0.55) 275 ?(1/2) 223 ?(0 or 1)	Mashiyama and Tanisaki (1982)
$(TMA)_2ZnCl_4$	Pcmn 297 inc(0.58) 280 $Pc2_1n$(3/5) 275 $P112_1/n$(2/3) 168 $P2_1/c11$(1) 155 $P2_12_12_1$(2/3)	Gesi (1982)
$(TMA)_2CoCl_4$	Pcmn 294 inc(0.59) 281 $Pc2_1n$(3/5) 279 inc(0.61) 277 $P112_1/n$(2/3) 192 $P2_1/c11$(1) 122 $P2_12_12_1$(2/3)	Gesi (1982)
$(TMA)_2ZnBr_4$	Pcmn 288 $P2_1/c11$(1)	Hasebe et al. (1984)
$(TMA)_2CoBr_4$	Pcmn 288 $P2_1/c11$(1)	Hasebe et al. (1984)

is either $P11n$, $P12_11$ or $P1$.
The value of γ for the structures of Cs_2CdBr_4 and Cs_2HgBr_4 with space group $P\bar{1}$ is assigned on the basis of the similarity of these structures with the structures with space group $P112_1/n$ of the same compounds.

In table 4.2.5 the phase sequence is given for most of the compounds mentioned in table 4.2.4.

Conclusion: It is shown that the space groups of all reported distorted β-K_2SO_4 type structures are closely related to the 4-dimensional space group Pcmn(00γ)(ss$\bar{1}$). A recipe is given for choosing the modulation wave vectors in these structures such that the modulation functions are comparable.

4.3. Reported structure determinations.

Several structure determinations of distorted β-K_2SO_4 type structures have been published (mainly in the last few years). The results are used in this chapter to compare these structures. In the comparison, also some undistorted β-K_2SO_4 type structures are included.

Table 4.3.1a contains all determinations of distorted β-K_2SO_4 type structures reported in literature. For each of these structures the standardized modulation wave vector is given. The cell parameters of the structures listed in table 4.3.1a are given in table 4.3.1b.

- For the room temperature structure of $(NH_4)_2ZnCl_4$ two structure determinations have been reported independently. The results of the two *are not in good agreement* with each other. The positions of the N atoms differ by up to 0.26Å and those of the Cl atoms by up to 0.15Å. The structure found by Van Koningsveld (1983) is based on twice as many reflections, and the standard deviations of the atomic coordinates are much smaller in this structure. Moreover Van Koningsveld has taken into account that the crystals of $(NH_4)_2ZnCl_4$ at room temperature are twinned. Therefore his data are used in this thesis.
- *For the 2-fold superstructure phase of* $(NH_4)_2BeF_4$ also two structure determinations have been reported independently: one at 133K and the other at 153K. The differences in the atomic positions (after transformation to the average unit cell) are small (up to 0.054Å). The

TABLE 4.3.1a. Reported structure determinations of distorted β-K_2SO_4 type structures. T is the temperature at which the structure analysis has been performed (r.t.= room temperature). γ gives the standardized modulation wave vector: $\underline{q}=\gamma\underline{c}^*$.

no.	compound	space gr.	γ	T [K]	reference
1	$(NH_4)_2ZnCl_4$	$P2_1cn$	1/4	333	Matsunaga (1982)
2	$(NH_4)_2ZnCl_4$	$P1c1$	1/4	r.t.	Van Koningsveld (1983)
3	$(NH_4)_2ZnCl_4$	$P1c1$	1/4	r.t.	Matsunaga (1982)
4	$(NH_4)_2ZnCl_4$	$Pc2_1n$	1/3	223	Matsunaga et al. (1982)
5	K_2ZnCl_4	$Pc2_1n$	1/3	r.t.	Mikhail and Peters (1979)
6	K_2CoCl_4	$Pc2_1n$	1/3	r.t.*	Vermin et al. (1976)
7	Rb_2ZnCl_4	$Pc2_1n$	1/3	100	Quilichini and Pannetier (1983)
8	Rb_2ZnCl_4 $	$Pc2_1n$	1/3	60	Quilichini and Pannetier (1983)
9	Rb_2ZnBr_4	$Pc2_1n$	1/3	140	this thesis (chapter 3)
10	Rb_2ZnBr_4	$Pc2_1n$	1/3	95	this thesis (chapter 3)
11	Ba_2TiO_4	$Pc2_1n$	1/3	r.t.*	Gunter and Jameson (1984)
12	$(NH_4)_2BeF_4$	$P2_1cn$	1/2	153	Misyul et al. (1980)
13	$(NH_4)_2BeF_4$	$P2_1cn$	1/2	133	Onodera and Shiozaki (179)
14	Ba_2SnS_4	$P2_1cn$	1/2	r.t.	Suza and Steinfink (1971)
15	Sr_2CrO_4	$P2_1cn$	1/2	r.t.	Wilhelmi (1966)
16	Cs_2FeI_4	$P12_1/cn$	1/2	100	Zandbergen (1981)
17	$(NH_4)_2SO_4$	$Pc2_1n$	1	180	Schlemper and Hamilton (1966)
18	Ba_2TiO_4	$P112_1/n$	0	r.t.	Wu and Brown (1973)
19	Ca_2SiO_4	$P112_1/n$	0	r.t.	Jost et al. (1977)
20	Sr_2SiO_4	$P112_1/n$	0	r.t.	Catti et al. (1983)
21	Cs_2CdBr_4	$P112_1/n$	0	195	Altermatt et al. (1984)
22	Cs_2HgBr_4	$P112_1/n$	0	200	Altermatt et al. (1984)
23	Cs_2CdBr_4	$P\bar{1}$	0	120	Altermatt et al. (1984)
24	Rb_2ZnBr_4	$Pcmn(00\gamma)(ss\bar{1})$	0.294	r.t.	this thesis (chapter 3)
25	K_2SeO_4	$Pcmn(00\gamma)(ss\bar{1})$	0.31	113	Yamada and Ikeda (1983)
26	Cs_2FeI_4 #	$Pcmn(00\gamma)(ss\bar{1})$	0.384	133	Zandbergen (1981)
undistorted β-K_2SO_4 type structures:					
27	K_2SeO_4	$Pcmn$	-	r.t.	Kalman et al. (1970)
28	$(NH_4)_2ZnCl_4$	$Pcmn$	-	418	Matsunaga (1982)

* The reported structure is metastable at this temperature.

$ The symmetry is not correct (see text).

The reported structure is a 5-fold superstructure approximation. See the text for further remarks.

TABLE 4.3.1b. Cell parameters of the structures of table 4.3.1a. For incommensurate structures the cell parameters are those of the basic structure.

no.	compound	cell parameters a [Å]	b [Å]	c_s [Å]	α [°]	β [°]	γ [°]
1	$(NH_4)_2ZnCl_4$	12.661	7.236	37.116			
2	$(NH_4)_2ZnCl_4$	12.620	7.211	37.098		90.00	
3	$(NH_4)_2ZnCl_4$	12.629	7.213	37.118		89.992	
4	$(NH_4)_2ZnCl_4$	12.568	7.184	27.838			
5	K_2ZnCl_4	12.402	7.256	26.778			
6	K_2CoCl_4	12.406	7.262	26.838			
7	Rb_2ZnCl_4	12.627	7.242	27.505			
8	Rb_2ZnCl_4	12.542	7.201	27.439			
9	Rb_2ZnBr_4	13.198	7.549	28.842			
10	Rb_2ZnBr_4	13.184	7.599	28.869			
11	Ba_2TiO_4	10.540	6.107	22.952			
12	$(NH_4)_2BeF_4$	10.495	5.915	15.123			
13	$(NH_4)_2BeF_4$	10.482	5.910	15.105			
14	Ba_2SnS_4	12.613	7.359	17.823			
15	Sr_2CrO_4	10.100	5.788	14.182			
16	Cs_2FeI_4	14.318	8.287	21.459		90.14	
17	$(NH_4)_2SO_4$	10.61	5.967	7.837			
18	Ba_2TiO_4	10.545	6.096	7.681			92.99
19	Ca_2SiO_4	9.297	5.502	6.745			94.59
20	Sr_2SiO_4	9.767	5.663	7.084			92.67
21	Cs_2CdBr_4	13.949	7.856	10.201			90.0
22	Cs_2HgBr_4	13.796	7.813	10.162			90.0
23	Cs_2CdBr_4	13.898	7.788	10.200	90.0	90.0	90.0
24	Rb_2ZnBr_4	13.330	7.656	9.707			
25	K_2SeO_4	not reported					
26	Cs_2FeI_4	14.343	8.288	10.74			
undistorted β-K_2SO_4 type structures:							
27	K_2SeO_4	10.466	6.003	7.661			
28	$(NH_4)_2ZnCl_4$	12.745	7.275	9.295			

153K structure (reported by Misyul et al, 1980) is used in the comparison because it is based on more than twice as many reflections, resulting in smaller standard deviations of the atomic coordinates.

- The reported structure of K_2CoCl_4 is almost equal to the reported structure of K_2ZnCl_4 (maximal differences in atomic positions: 0.032Å). The differences between these two structures are much smaller than the differences between one of these structures and each of the other 3-fold superstructures of table 4.3.1a. Therefore, all conclusions made in this thesis for the room temperature structure of K_2ZnCl_4 are also valid for the structure of K_2CoCl_4.
- The structure of Cs_2HgBr_4 at 200K is also not considered explicitely, because of its very strong resemblence with the structure of Cs_2CdBr_4 at 195K (maximal differences in atomic positions: 0.070Å).
- The reported structure of the incommensurate phase of Cs_2FeI_4 (at 133K) is a 5-fold superstructure approximation with symmetry $P112_1/n$. The actual symmetry of the incommensurate phase is $Pcmn(00\gamma)(ss\bar{1})$ (Zandbergen, 1984). In the reported structure the second harmonics in the modulation functions are larger than the first harmonics. This is hardly possible, because Zandbergen (1981) reports that no second order satellite reflections could be observed. It is also not in accord with the other determined incommensurate structures (Rb_2ZnBr_4, K_2SeO_4), in which only first harmonics are found in the modulation functions, and with the reported 4-fold superstructures, in which the second harmonics are much smaller than the first harmonics. The strong second harmonics found by Zandbergen are probably caused by the fact that in the last stage of the structure refinement no second order satellites were included (Zandbergen, 1981, 1984). The amplitudes of the second harmonics of the modulation functions are then only very weakly fixed, since they depend chiefly on the second order satellites. Hence they can easily assume unrealistic values. Therefore the reported structure of Cs_2FeI_4 at 133K is considered not to be correct and will be ignored.
- Because the symmetry of Rb_2ZnCl_4 at 60K is not known, Quilichini and Pannetier (1983) used the symmetry of the compound at higher temperatures ($Pc2_1n$). The actual symmetry is lower because some of the reflections that should be systematically absent for space group $Pc2_1n$ are found to have non-zero intensity. Nevertheless, the agreement between observed and calculated intensities is very good. The reported 60K structure of Rb_2ZnCl_4 has a strong resemblence with the reported structure of the same compound at 100K (maximal difference in atomic positions: 0.062Å). Therefore the structure of Rb_2ZnCl_4 at 60K is not considered explicitely further.
- As will be discussed in section 4.6, the structure of Rb_2ZnBr_4 at room temperature is probably a 17-fold superstructure. Because this supercell is much larger than that of any other superstructure in table 4.3.1, the structure is treated as incommensurate in this and the next two sections.

To compare structures, they must be described with respect to the same set of axes, with the origin in corresponding positions. Also, the nomenclature of the atoms must be the same. These conditions are not satisfied by the data reported in the original publications. Therefore a computer program has been made that automatically puts the origin of the set of crystallographic axis at the proper position, generates the positions of all atoms in the unit cell and normalizes the (code) numbers of the atoms. For polar structures the position of the origin is chosen such that the centre of gravity of the unit cell contents is at position (0.5, 0.5, 0.5). The incommensurate structures are treated separately.

4.4. <u>Local structural details</u>.

4.4.1. Interatomic distances.

The first neighbour interatomic distances have been calculated from the atomic coordinates and the cell parameters (see table 4.3.1b) without applying corrections for the effect of thermal vibrations (see Cruickshank, 1956). These corrections would be very small in comparison with the differences in distances which will be considered here.

For the incommensurate structure of K_2SeO_4 the cell parameters have not been reported. The room temperature cell parameters are used instead. They are sufficiently precise.

For incommensurate structures the distances are found by approximating the structure by a large superstructure: a 23-fold superstructure is used for K_2SeO_4 and a 17-fold one for Rb_2ZnBr_4.

The interatomic distances in the BX_4 tetrahedra are not discussed here, because their variations are much smaller than the variations in other distances. They deviate only a few percent from those corresponding to regular and identical BX_4 tetrahedra.

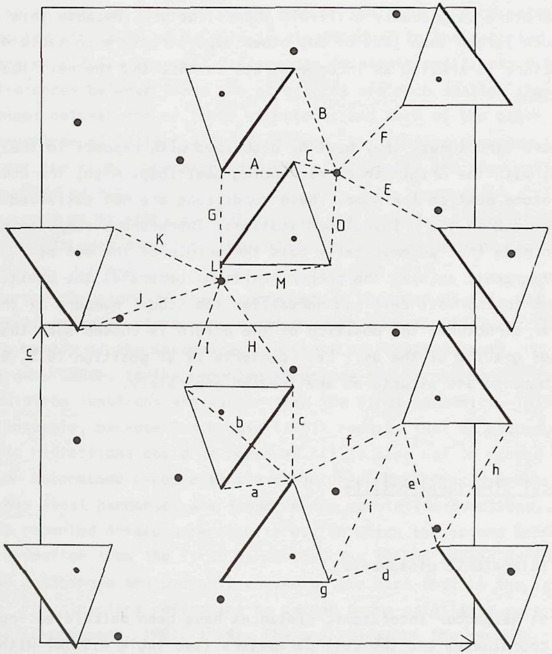

FIGURE 4.4.1. Nomenclature of the types of distances. The capitals denote A-X distances, whereas the lower-case letters denote X-X distances. Distance g is between two X atoms of two tetrahedra which coincide in the given projection.

The nomenclature of the distances is given in figure 4.4.1, showing a projection of a β-K_2SO_4 type structure. The A-X distances are denoted by a capital (A, ... F for A_1-X, and G, ... M for A_2-X) and the X-X distances by a lower case letter. The same letter is used for interatomic distances that are equivalent (related by symmetry) if the distortion with respect to the β-K_2SO_4 type structure is disregarded: each letter denotes a "type" of distance. Because in the β-K_2SO_4 type structure the A atoms are located on a mirror plane (perpendicular to b), most of the A-X distances around an A-atom occur in pairs of the same type, and hence with the same letter. The distances which do not occur in pairs are those of type A, B, E, G, H, J, g and h.

The interatomic distances for the crystal structures which are compared are given in figure 4.4.2.

Figure 4.4.2 also shows the A-X and X-X contact distances for each compound. These contact distances are calculated as the sum of the effective ionic radii, taken from Shannon (1976). The radii are those for atoms with a sixfold coordination. For the halogen ions, this is the largest coordination number for which radii are given. If for the A ions eight would have been chosen as coordination number, then each A-X contact distance would have been about 0.1Å larger.

The A_1 atoms are surrounded by nine X atoms. According to figure 4.4.2 only A_1-X distances of type C, corresponding to two distances per A_1 atom, have values covering a large range. The A_1-X distances of the other types have almost the same value within each structure. The values for these non-varying distance types are approximately equal to the minimum value of distance type C, and correspond to the contact distance of the atoms represented by A and X.

The A_2 atoms are surrounded by thirteen X atoms. As can be seen from figure 4.4.2, the A_2-X distances are in general larger then the A_1-X distances. Distances of only two types (G and H) always have about the same value; for G this value is close to the contact distance. The distances of the other types diverge considerably. It can be concluded that the A_2 atoms have more space than the A_1 atoms.

4.4.2. Displacements of individual atoms.

In the following the positions of the atoms in the distorted β-K_2SO_4 type structure will be considered with respect to the "related Pcmn structure".

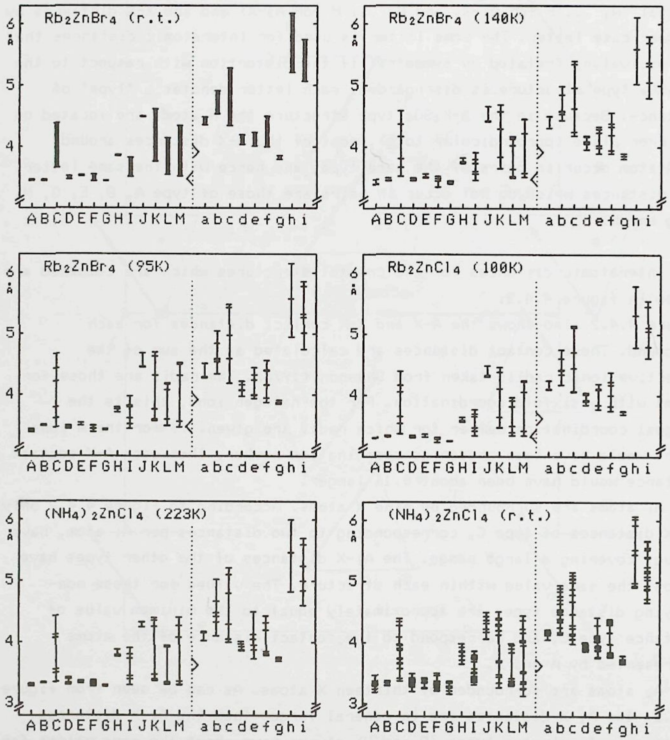

FIGURE 4.4.2. Distances in distorted β-K_2SO_4 type structures. See figure 4.4.1 for an explanation of the names of the distances.
The individual distances are indicated by horizontal bars, except for the incommensurate cases, where the range is indicated.
The marks on the vertical dotted lines indicate the sum of the effective ionic radii for the A-X and X-X distances, taken from Shannon (1976).
These radii are for ions with a sixfold coordination.

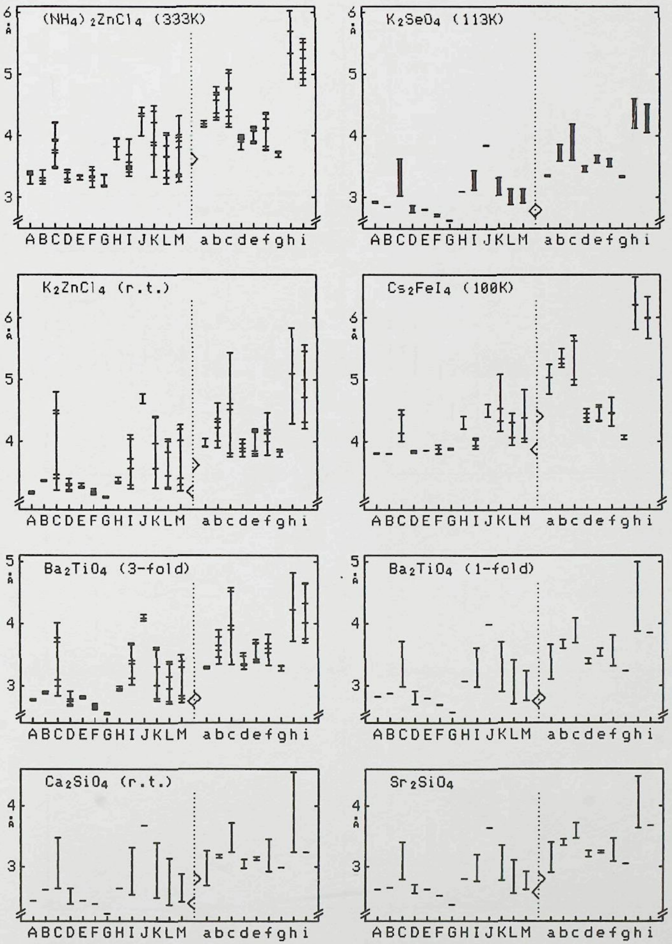

Figure 4.4.2 continued

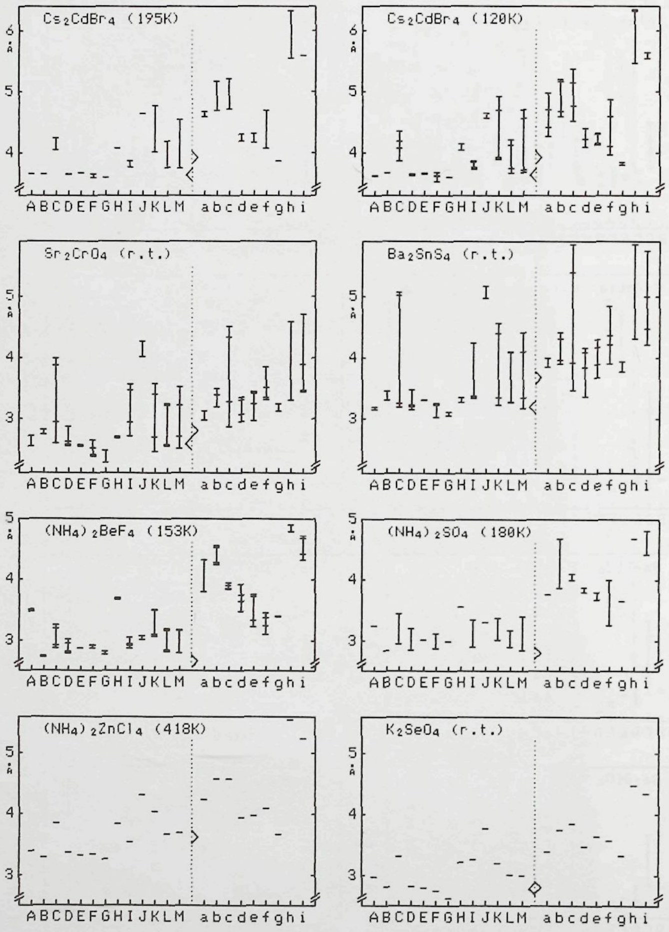

Figure 4.4.2 continued

For incommensurate structures with the prototype symmetry this is the basic structure. For superstructures, the related Pcmn structure is found in the following way. First the Pcmn symmetry operations of β-K_2SO_4 are made to act on the atomic coordinates of the superstructure, letting the corresponding symmetry elements coincide. These Pcmn operations are at least present in the superstructure as pseudo symmetry operations, so they yield clusters of atoms. The related Pcmn structure results from averageing the atomic coordinates of atoms in each cluster. For incommensurate structures of which the 4-dimensional space group is a proper subgroup of the prototype symmetry, the related Pcmn structure is found by applying the same recipe to its basic structure.

The displacements (in Å) of the atoms with respect to the positions in the related Pcmn structure are given in absolute value in figure 4.4.3. The nomenclature of the atoms is as given in chapter 1 (figure 1.4.1). For all structures shown in figure 4.4.3, the same pattern is found. The displacements of the atoms are mainly in the b direction for the A_1-, A_2-, B-, X_1- and X_2 atoms. Only the X_3 atoms have important components also in the a- and c directions.

The largest deviations are those of the X atoms. They mainly represent rotations of the tetrahedra, because the tetrahedra are rigid in good approximation and because the displacements of the B atoms are small. Because the displacements of the X_1- and X_2 atoms are mainly parallel to b, the rotation component around an axis parallel to b is zero in good approximation. The other two rotation components can be characterized by the displacements of the X_1- and X_2 atoms in the b direction. These displacements will be investigated in more detail.

For the superstructures, the displacements of the individual X_1- and X_2 atoms parallel to b are given in more detail in figure 4.4.4. These superstructures can be thought to consist of layers of BX_4 tetrahedra normal to c. The B atoms of both tetrahedra in such a layer have approximately the same z coordinates. Two such layers exist per c period. The A_2 atoms are located in these layers between the tetrahedra. Each A_1 atom is located between two layers.

For most layers the displacements of the two X_2 atoms are equal in good approximation. Therefore in figure 4.4.4 the corresponding triangles often form a single rhomb. The most important exceptions are found in the 2-fold superstructures of $(NH_4)_2BeF_4$, Ba_2SnS_4 and Sr_2CrO_4. In half of the layers in these structures the displacements of the two different X_2 atoms are opposite.

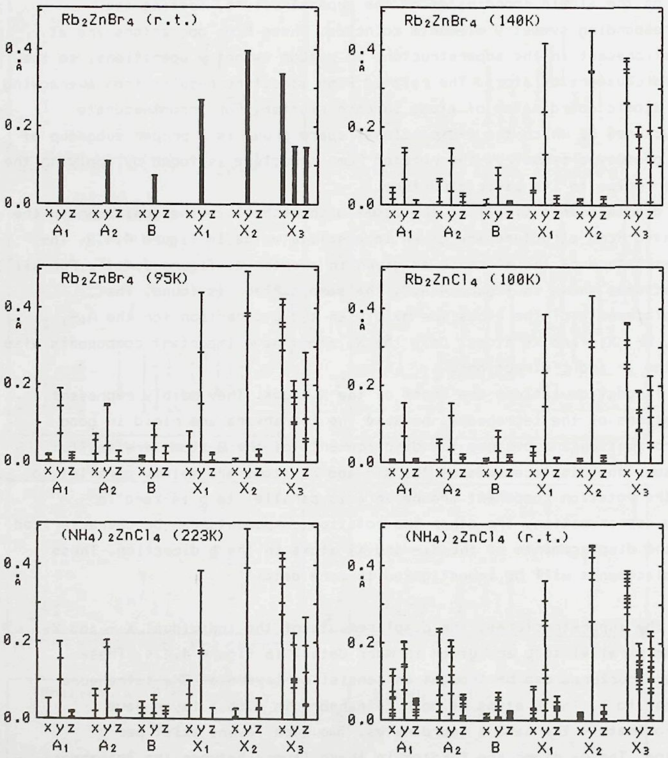

FIGURE 4.4.3. Components of the displacements of the atoms with respect to the related Pcmn structure.
The individual displacements are indicated by horizontal bars, except for the incommensurate case, where the range is indicated.

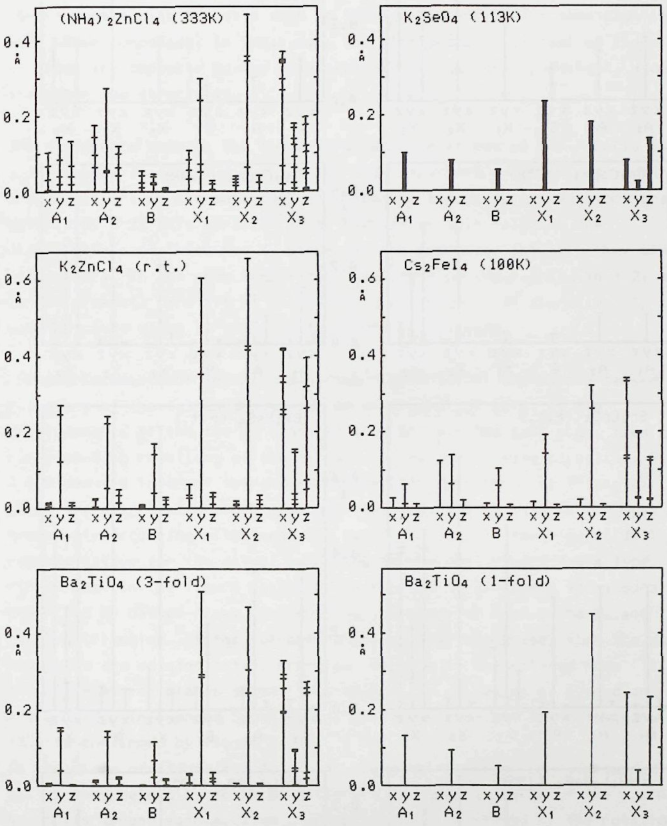

Figure 4.4.3 continued

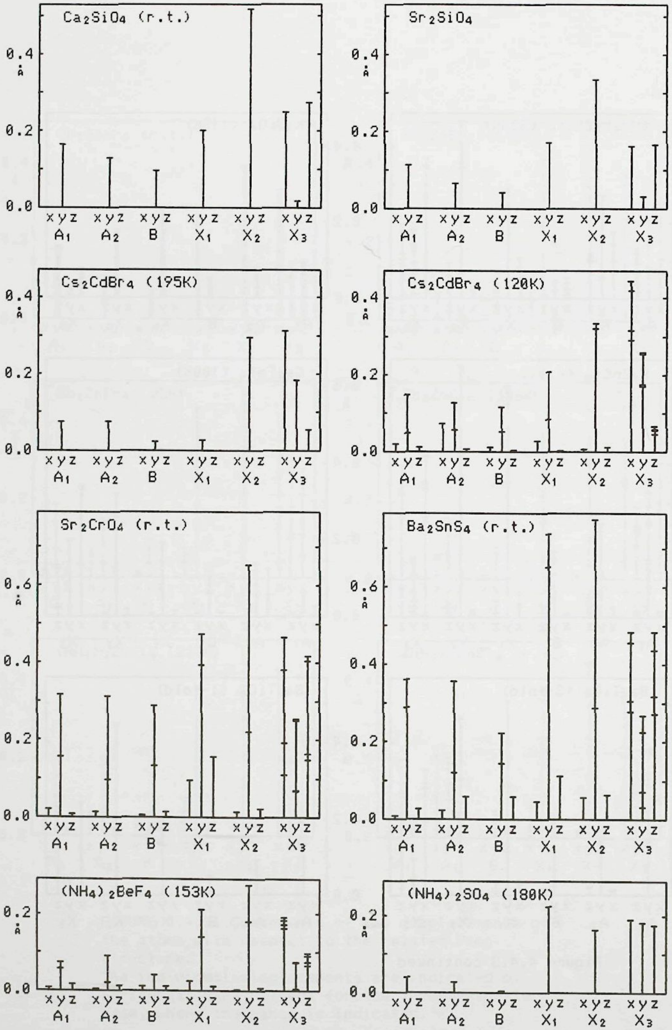

Figure 4.4.3 continued

The structure of $(NH_4)_2BeF_4$ strikingly differs from the structures of Ba_2SnS_4 and Sr_2CrO_4, despite the fact that these three structures have the same symmetry. X_1 atoms with approximately equal z coordinates have displacements with opposite sign in $(NH_4)_2BeF_4$, and of the same sign in both other compounds. In $(NH_4)_2BeF_4$ the displacements of four of the eight X_2 atoms are opposite to the displacements of the corresponding X_2 atoms in the other two structures.

The difference between the two 4-fold superstructures of $(NH_4)_2ZnCl_4$ is also visible in figure 4.4.4. In the 333K structure of this compound there are two layers in the supercell in which the two different X_2 atoms are related by a 2_1 axis parallel to a. Because of this relation the displacements of these two X_2 atoms must be opposite; actually they almost vanish here. In the room temperature structure of $(NH_4)_2ZnCl_4$ this 2_1 axis is not present. Here all X_2 atoms have displacements of approximately the same absolute value in the room temperature structure.

The displacements of the X_2 atoms (see figure 4.4.3) are mainly caused by rotations of the tetrahedra around an axis parallel to c. If the displacements of the two X_2 atoms in a layer have the same sign, then the corresponding rotations of the tetrahedra are in the same direction. Figure 4.4.5 shows a layer of tetrahedra (drawn with full lines as triangles) which are all rotated clock-wise over the same angle; this is the most frequently occurring situation. The rotation angle in the figure (10°) is representative for the actual rotations in the distorted β-K_2SO_4 type structures. In the figure neighbouring X atoms of different tetrahedra are connected by dashed lines representing distances of type d and g, and forming triangles. If the tetrahedra are rotated clockwise, then the dashed triangles are rotated anti clock-wise. Because in the related Pcmn structure mirror planes normal to b exist, the distances of type d and g are hardly influenced by the cooperative rotations of the tetrahedra; this is confirmed by figure 4.4.2.
In the plane of figure 4.4.5, the A_2 atoms in the layer are surrounded by six X atoms belonging to three different tetrahedra. Three of the six A_2-X distances around each A_2 atom are considerably shortened by the rotations of the tetrahedra, the other three are lengthened. In most of the layers shown in figure 4.4.4 the rotation angle of the tetrahedra is such that the shorter A_2-X distances are equal to the sum of the atomic radii. (These distances are the smaller K-, L- and M distances in figure 4.4.2.) In such a layer the rotation has reached the limit imposed by steric hindrance.

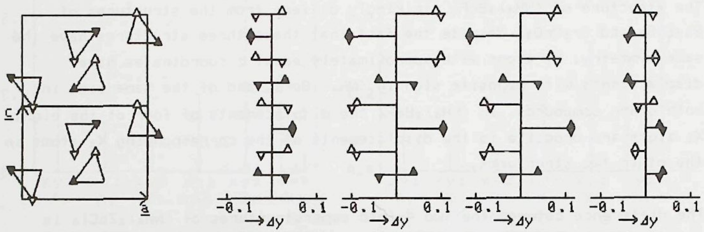

$(NH_4)_2BeF_4$ (153K) Ba_2SnS_4 Sr_2CrO_4 Cs_2FeI_4 (100K)

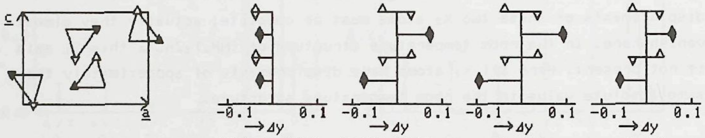

$(NH_4)_2SO_4$ (100K) Ba_2TiO_4 (1-f.) Ca_2SiO_4 Sr_2SiO_4

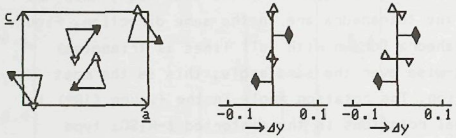

Cs_2CdBr_4 (195K) Cs_2CdBr_4 (120K)

FIGURE 4.4.4. Deviation of the y coordinates of the X_1- and X_2 atoms from those in the related Pcmn structure. The open and full triangles in the left figures represent X_1- and X_2 atoms respectively. For the superstructures the corresponding deviations of the y coordinates are given in the other drawings at the same horizontal levels. This page shows 1- and 2-fold superstructures.

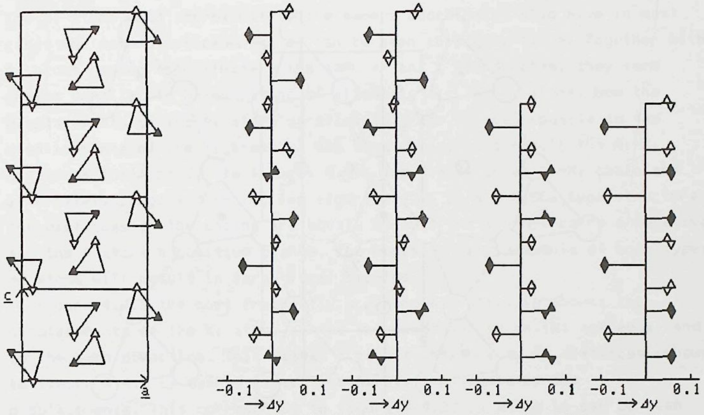

$(NH_4)_2ZnCl_4$ (333K) $(NH_4)_2ZnCl_4$ (r.t.) $(NH_4)_2ZnCl_4$ (223K) K_2ZnCl_4

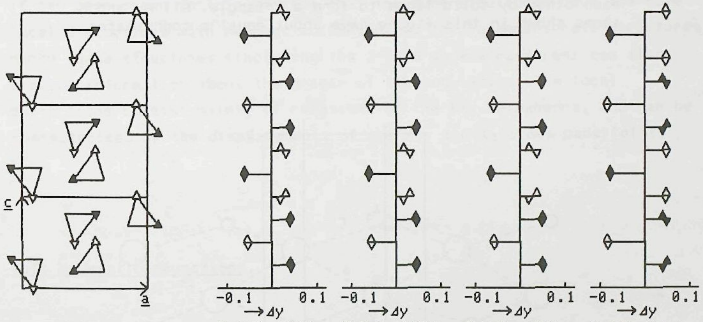

Rb_2ZnCl_4 (100K) Rb_2ZnBr_4 (140K) Rb_2ZnBr_4 (95K) Ba_2TiO_4 (3-f.)

Figure 4.4.4 continued with the 3- and 4-fold superstructures.

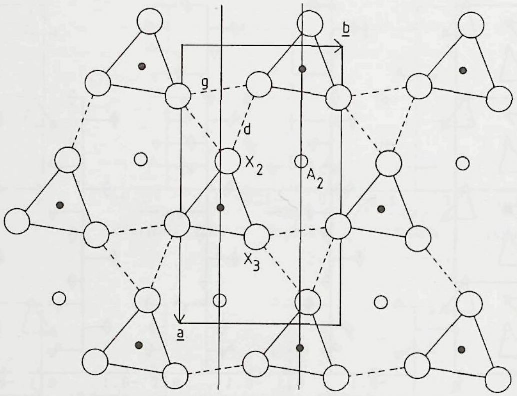

FIGURE 4.4.5. Layer of tetrahedra normal to c. Of each tetrahedron, three X atoms are shown, which are connected to each other by solid lines to form a triangle. All A- and X atoms shown in this figure have about equal z coordinates.

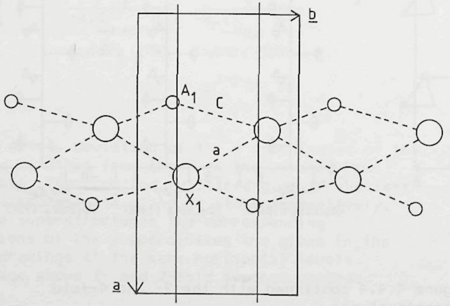

FIGURE 4.4.6. Two neighbouring X_1-A_1 chains parallel to b. The atoms shown have about equal z coordinates. All X_1 atoms are displaced in the positive b direction, the A_1 atoms in the negative b direction. As a corollary, the distances of type C in a chain are alternately longer and shorter.

The X_1 atoms with approximately the same z coordinates also have in most cases the same displacements, as can be seen in figure 4.4.4. Together with A_1 atoms having approximately the same x- and z coordinates, they form chains parallel to b consisting of alternate X_1- and A_1 atoms. Now the displacements of the A_1 atoms parallel to b are always opposite to the displacements of the X_1 atoms in the same chain. As a result the A_1-X_1 distances (of type C, see figures 4.4.1 and 4.4.2) in an A_1-X_1 chain are alternately large and small, see figure 4.4.6. In a β-K_2SO_4 type structure the distances in the chains are equal. Because the X atoms carry a negative and the A atoms a positive charge, the opposite displacements of both types of atoms will result in large local dipoles.
In figure 4.4.6 the most frequently occuring situation is shown: the displacements of the X_1 atoms in the two neighbouring chains are equal and in the same direction. This has as a result that the X_1-X_1 distances (shown in figure 4.4.6 as dashed lines) are hardly influenced by the displacements. This corresponds to figure 4.4.2, in which it can be seen that these distances (of type a) are almost equal within each structure.

It has been shown in this section that the superstructures have the same local distortions with respect to β-K_2SO_4 as the incommensurate structures. Hence these structures (including the 1-fold superstructures) can also provide information about the origin of the modulation. The local distortions consist mainly of rotations of the BX_4 tetrahedra, and can be characterized by the displacements of the X_1- and X_2 atoms parallel to b.

4.5. Modulation functions.

In this section the modulation functions of the incommensurate structures and the 3- and 4-fold superstructures will be compared. The modulation functions of superstructures have been obtained from the atomic coordinates by fourier analysis, using the standardized modulation wave vectors.
In that analysis, for a v-fold superstructure only the harmonics of orders *0 ... (v-1)/2 for v odd, or 0 ... v/2 for v even (with the minimum* amplitude of the v/2-th harmonic) were not assumed to vanish. So the highest order allowed for a 3-fold superstructure is the first, and for a 4-fold one it is the second harmonic.

Only the first harmonics will be discussed. The reported incommensurate structures do not contain higher harmonics. (The only exception is Cs_2FeI_4 at 133K, but the determination is probably not correct, as explained in section 4.3). In the reported 4-fold superstructures the second harmonics are smaller than 20% of the largest first-harmonic amplitude. Therefore, in the following the second and higher harmonics will be neglected. So for a given atom the modulation functions can be written as

$$d_i(t) = A_i \cos(2\pi(t-\varphi_i)) \quad (A_i \geqslant 0) \ . \qquad (4.5.1)$$

In this equation A_i is the amplitude of the displacement modulation function in direction i (i=1, 2 and 3 correspond to directions x, y and z respectively) and φ_i is the phase of this function. (Note that subscript i of A_i and φ_i has another meaning in chapter 5.) Figure 4.5.1 shows how these functions will be represented graphically. The modulation function in this figure can be represented by either one of two line segments of length A_i, which we shall call s_1 and s_2. The position of the line segment s_1, drawn above that axis at $t=\varphi_i$, gives the value of t at which $d_i(t)$ is maximal; s_2 is at the position $t=\varphi_i\pm0.5$ of the minimum and is drawn below the base line. Using for each modulation function one of these symbols, it is possible to represent many modulation functions in one drawing. Having two symbols available one can display more clearly the symmetry by choosing for each modulation function the most appropriate one.
In figure 4.5.2 the first harmonics of modulation functions in K_2ZnCl_4 are given, together with two projections of a β-K_2SO_4 type structure. For each modulation function the corresponding atom can be found in the projections by extending the horizontal line to which the symbol is connected into the projection and looking there for the same square, circle or triangle on that line. In the upper part of figure 4.5.2b the modulation functions $d_2(t)$ are given. In the lower part $d_1(t)$ and $d_3(t)$ are given for the X_3- and X_4 atoms. For the other atoms $d_1(t)$ and $d_3(t)$ are not shown because they have amplitudes smaller than 16% of the largest amplitude in the same structure. In the incommensurate structures with the prototype symmetry and in the superstructures with a c-glide plane normal to b the first harmonics of these modulation functions have zero amplitude because of symmetry, cf. section 2.3.
The functions $d_3(t)$ are longitudinal modulation functions. Therefore the line segments representing these functions are drawn horizontally. Figure 4.5.2c shows the nomenclature of the atoms used in the following discussion. In figure 4.5.3 the modulation functions of the other

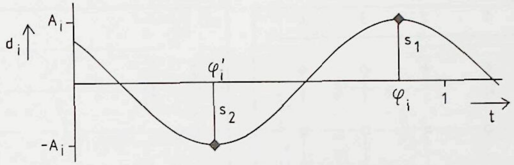

FIGURE 4.5.1. Function $d_i(t) = A_i\cos(2\pi(t-\varphi_i))$ can be represented by line segments s_1 or s_2.

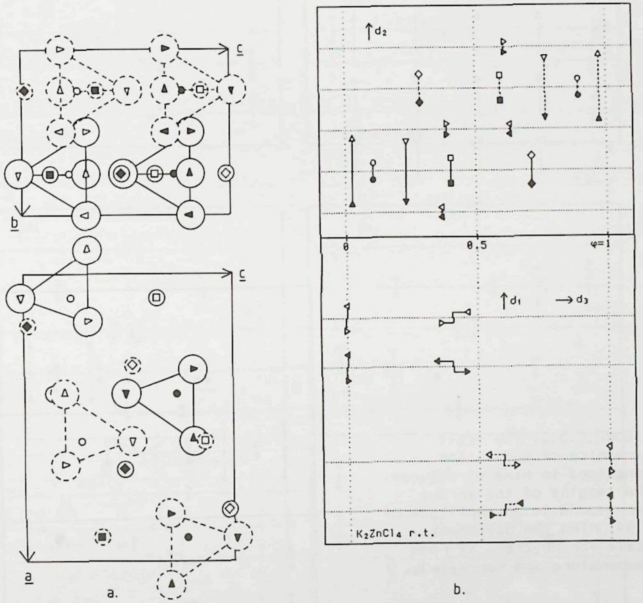

a.

b.

FIGURE 4.5.2a. Two projections of a β-K_2SO_4 type structure.
b. The first harmonics of modulation functions in K_2ZnCl_4, represented in the way shown in figure 4.5.1. The corresponding atoms lie on the same horizontal level in the projections of part a of this figure. The length of the arrows corresponds to an amplitude of 0.04.
c. Nomenclature of the atoms.

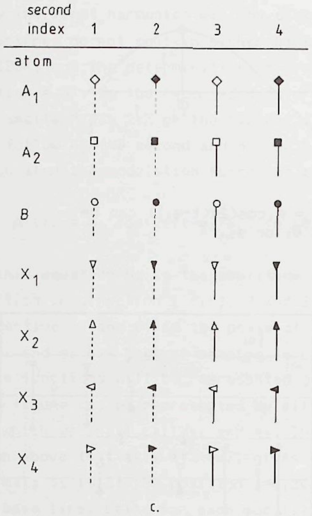

FIGURE 4.5.2c. Nomenclature of the atoms.

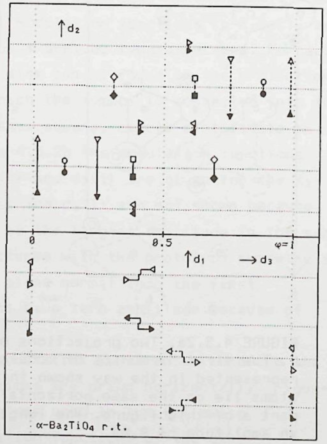

FIGURE 4.5.3. The first harmonics of modulation functions in nine structures. The lengths of the arrows correspond to an amplitude of 0.04. Mind the different scale for Rb_2ZnBr_4 at room temperature and for K_2SeO_4.

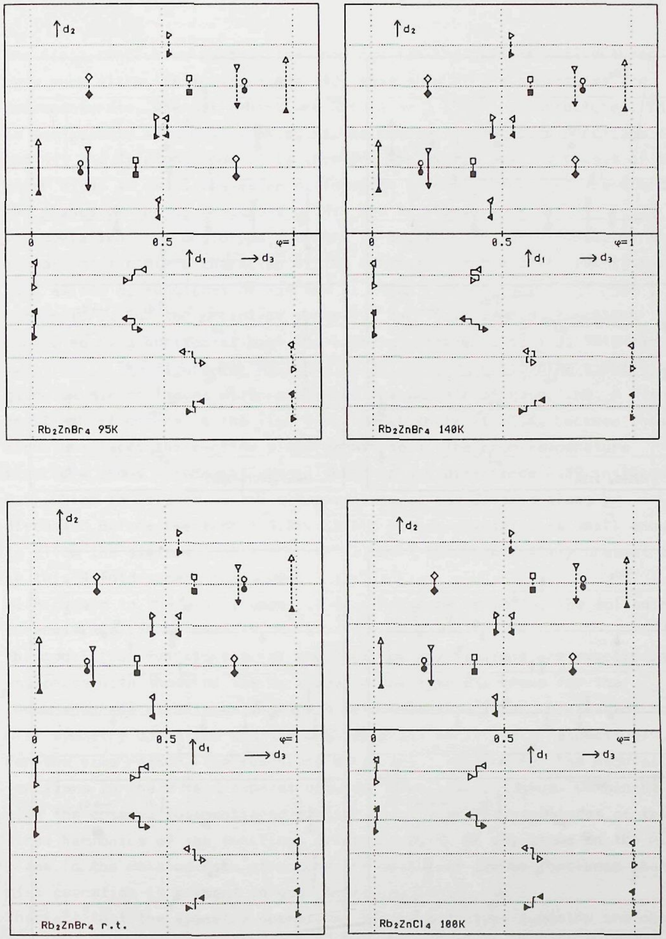

FIGURE 4.5.3. continued.

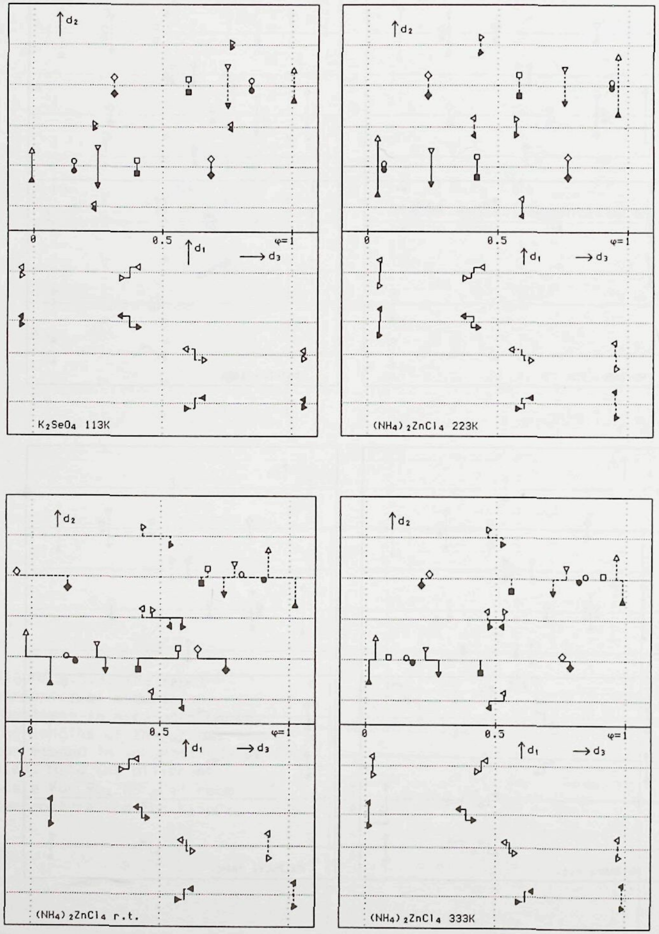

FIGURE 4.5.3. continued.

structures are given.

The first conclusion is that the drawings for the different structures are very much alike, in spite of the fact that some of the structures are incommensurate, whereas others are 3-fold or 4-fold superstructures. This is most easily seen when looking at the dominant modulation functions for the X_1- and X_2 atoms, but it is true for the amplitudes and phases of the other atoms as well. The major differences between structures are found in the phases of the d_2 functions of X_3- and X_4 atoms.

The deviation from prototype symmetry is small in all structures. As an example of the minor character of the deviations which still exist, one may look at the d_2 functions of X_3- and X_4 atoms for $(NH_4)_2ZnCl_4$ at room temperature. For the prototype symmetry, each pair (two d_2 functions connected by a horizontal bar) has a phase difference of 1/2. This can be verified in the figure for Rb_2ZnBr_4 because the corresponding symbols are pairwise mirror images with respect to the horizontal base line. A (very small) shift occurs in the figure for $(NH_4)_2ZnCl_4$ at 333K, because this structure lacks the c-glide plane normal to a. The room temperature structure shows a somewhat larger shift (phase difference 0.39 instead of 0.5) which is related to the disappearence of the 2_1 axis along a discussed before (section 4.4.2). Still, such a deviation is small enough to allow the statement that the c(s) element is approximately present even in this 4-fold superstructure.

With regard to the m(s) element of the prototype symmetry, the following observations can be made.

The modulation functions $d_1(t)$ and $d_3(t)$ of the X_3 atoms are exactly in antiphase with those of the X_4 atoms of the same BX_4 group for the incommensurate structures and the 4-fold superstructures, because of the m(s) symmetry operation and the c-glide plane normal to b respectively. For the same reason, the functions $d_2(t)$ are in phase. For the modulation functions in the 3-fold superstructures this is almost true. Combining this with the observation mentioned earlier, viz. that the amplitudes of the first harmonics of the functions $d_1(t)$ and $d_3(t)$ of the atoms on the mirror plane in the related Pcmn structure are small, it can be concluded that the m(s) operation is present in good approximation.

The fact that the symmetry operations of the prototype symmetry are obeyed in good approximation in the 4- and 3-fold superstructures again confirms that these superstructures have pseudo-prototype symmetry.

The translations of the BX_4 tetrahedra can be found from the modulation

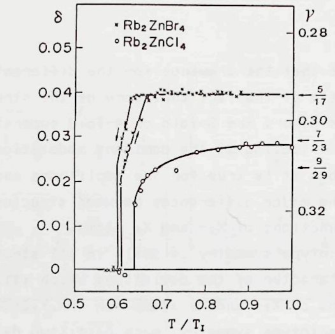

FIGURE 4.6.1. Modulation wavevector component γ as a function of the reduced temperature T/T_i for Rb_2ZnBr_4 (T_i=347K) and Rb_2ZnCl_4 (T_i=300K). The figure is taken from Gesi and Iizumi (1979b), including the curves. Only the γ-scale ($\gamma=1/3-\delta$) has been added.

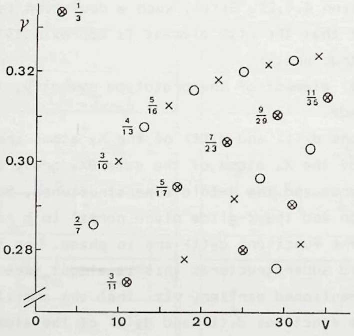

FIGURE 4.6.2. The possible rational values u/v of γ as a function of the supercell size v, for all three parity combinations: both u and v odd (crossed circles); u odd, v even (crosses); u even, v odd (open circles).

functions of the B atoms. Because the latter's amplitudes are small, it can be concluded that these translations are small as well.

For the structures of which the modulation functions are given in figures 4.5.3 and 4.5.2 the function $d_2(t)$ of atom A_{11} is approximately in antiphase with $d_2(t)$ of X_{14}. These two atoms have approximately the same x- and z coordinates and form a chain parallel to b̲. The same situation occurs for the atom pairs A_{13}-X_{12}, A_{12}-X_{13} and A_{14}-X_{11}. The fact that the modulation functions $d_2(t)$ of the two atoms in one chain are in antiphase means that if the A_1 atoms are displaced in the positive b̲ direction, then the X_1 atoms in the same chain are displaced in the negative b̲ direction. These chains have already been discussed in section 4.4.

Other observations made in section 4.4 which can be confirmed here are the cooperative displacements of the X_2 atoms of tetrahedra in the same layer of tetrahedra normal to c̲ and the cooperative displacements of X_1 atoms with approximately the same z coordinates. Two X_2 atoms of tetrahedra in the same layer are for example X_{21} and X_{23} (see figure 4.5.2). Indeed it can be seen from figures 4.5.3 and 4.5.2 that the modulation functions $d_2(t)$ of these atoms have the same phase in good approximation.

Two X_1 atoms with approximately the same z coordinates are for example X_{11} and X_{14}. These atoms also have modulation functions $d_2(t)$ with approximately the same phase, as expected.

4.6. Large superstructures.

In this section those structures will be discussed in which the measured value of γ as a function of temperature has one or more plateau's not corresponding to simple superstructures. As mentioned in chapter 1, this leaves some doubt as to whether the structure - within the range of such a plateau - is incommensurate or is a complex superstructure.

The temperature dependence of γ of Rb_2ZnBr_4 has been measured by De Pater et al. (1979) and by Gesi and Iizumi (1978), see figure 4.6.1. Both measurements reveal that from T_i down to about 210K the value of γ remains constant at 0.293(1). This value equals 5/17=0.2941 within the experimental error. *Iizumi and Gesi (1983) verified this by more precise measurements.* Gesi and Iizumi (1978) also found a clear anomaly in the intensities of satellite reflections at the temperature where γ leaves the constant region (at about 210K). They suggested that there is a phase transition at this temperature. By means of dielectric measurements, Van Kleef et al (1981) actually did find in some of there samples two successive phase transitions, 10 to 20K apart (depending on the sample) instead of one at T_c.

The temperature dependence of γ for Rb_2ZnCl_4 has been measured by Mashiyama et al. (1981) and by Gesi and Iizumi (1979a), whose results are reproduced in figure 4.6.1. The curve in that figure is smooth but the measured points allow the assumption of two intervals in which γ is constant. The first lies between 260K and 300K, the second between 200K and 220K. Gesi and Iizumi (1979a) also measured the intensity of a satellite reflection as a function of temperature. This curve has a shoulder around 210K, which seems to confirm the second plateau of $\gamma(T)$. The values which γ takes in the regions mentioned are 0.305 above 260K and 0.311 around 210K. The simplest fractions which equal these numbers within experimental error (estimated from the spreading of the data to be 0.001) are 7/23=0.3043 and 9/29=0.3103.

The measurements of Mashiyama et al. (1981) also show that γ has the value 0.305 between 260K and 300K. The other plateau is not found in their measurements. A narrow but well-established shoulder in their curve of $\gamma(T)$ suggest that γ also is constant with value 0.317 (13/41=0.3171) in a small temperature interval just above T_c.

Zandbergen (1981) reports that in Cs_2FeI_4 γ has the value 0.384(5) in the entire temperature region (123K-152K) of the so-called incommensurate phase. This value is equal to 5/13=0.3846 within the experimental error.

The rational values of γ mentioned above (5/13, 5/17, 7/23, 9/29, 13/41) all obey the same parity condition: u and v both odd. The same condition holds for the 3-fold superstructures found at lower temperatures in Rb_2ZnBr_4 and Rb_2ZnCl_4: $\gamma=1/3$.

As can be seen in figure 4.6.2, the values 1/3, 5/17, 7/23 and 9/29 are - among the fractions which obey this parity condition - the ones which give the smallest supercells in the region $0.29<\gamma<0.34$. Several fractions which do not obey this condition and correspond to smaller supercells (e.g. 3/10, 4/13. 5/16), are not observed. Therefore it can be concluded that Rb_2ZnBr_4 and Rb_2ZnCl_4 have a preference for commensurate modulation wave vectors with u and v both odd.

From figure 4.2.2 it can be seen that only under this condition the c(s) operation of the prototype symmetry can be present as a c-glide plane normal to a̲ in a rational subgroup of this symmetry. Hence the observed parity condition suggests that it is energetically favorable to keep this symmetry element in the structure.

The above-mentioned compounds are not the only ones with a preference for modulation wave vectors obeying such a parity condition. In thiourea a similar situation exists. This compound has an orthorhombic modulated phase with the modulation vector parallel to c̲. A careful neutron diffraction analysis of the p-T phase diagram of fully deuterated thiourea by Denoyer et al. (1981) has shown that there are stable superstructures for $\gamma=1/9$, 1/7 and 1/3, the latter two occuring at higher pressures only. In the p-T phase diagram, the stability regions for these superstructures border on, or are surrounded by a large area in which γ appears to change continuously. An earlier paper by Shiozaki (1971) deals with such an incommensurate phase. The conditions for reflections observed by X-ray diffraction are:

(i) 0klm present only for k=even,

(ii) h0lm present only for h+l+m=even.

Condition (ii) corresponds to an n(s)-glide plane normal to b̲.

Projected along a̲, this element yields exactly the same configuration as c(s) in figure 4.4.4d, and therefore yields the same condition, viz. u and v both odd. Hence also in thiourea the rational values for γ which are observed are just those for which a certain symmetry element can be present in a rational subgroup of a prototype symmetry.

Moudden et al. (1982) observed that in the presence of an electric field parallel to b̲, and hence normal to the n(s)-glide plane, also a superstructure with $\gamma=1/8$ exists in a certain temperature region. This electric field apparently destroys the n(s)-glide plane.

An attempt has been made to find more evidence for the 7/23 and 9/29 plateaus in Rb_2ZnCl_4 by neutron diffraction. γ has been determined from the position of the reflections 0200, 021-1, 0211 and 0220 at several temperatures between T_i and T_c.

The result is given in figure 4.6.3. Near T_c, which has been found to be 196K in this experiment, also higher order satellites can be observed. Figure 4.6.4 shows a complete scan parallel to c̲ between reflections 0200 and 0220 of Rb_2ZnCl_4 at 198K. For this temperature γ also has been calculated from the positions of the higher order satellite reflections. This value is in good agreement with the value calculated from the positions of the first order satellites, as can be seen in figure 4.6.3, where both values are given.

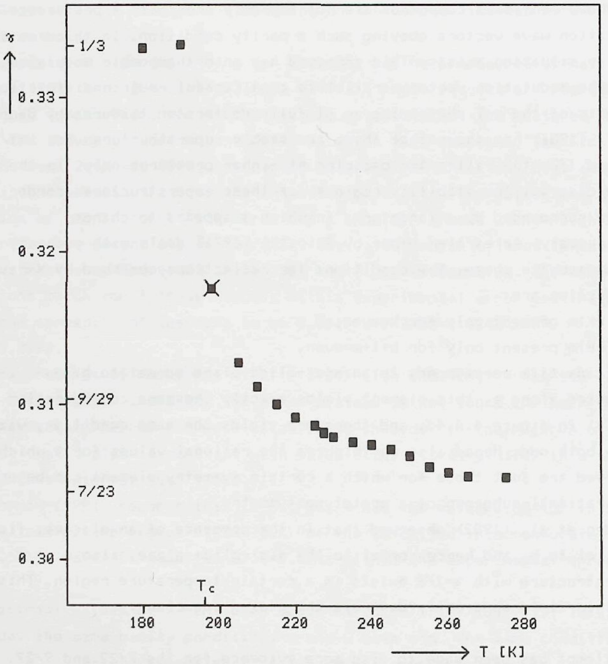

FIGURE 4.6.3. τ in Rb_2ZnCl_4 as a function of temperature.
■ : from first order satellites
X : from higher order satellites

In figure 4.6.3 it can be seen that our measurements do not give evidence for a plateau at τ=9/29. The plateau of the high temperature side of the incommensurate phase is at τ=0.3054(2). This value deviates significantly from 7/23=0.3043. The measured value is too large.

The reflections observed at 198 K in Rb_2ZnCl_4 on the line between reflections 0200 and 0220 are (see figure 4.6.4): 021-3, 0201, 02-15, 021-1, 023-7, 0210, 02-17, 0211, 022-2, 023-5 and 022-1. Note that the higher order satellite reflections are very weak with respect to the first order satellites 021-1 and 0211. Three of the observed reflections (0201, 0210 and 022-1) do not obey the rule for systematic absences of the c(s)-glide plane normal to $\underline{a}$: 0klm reflections are absent if l+m=odd. The observation of these three reflections is not due to half-wavelength contamination of the neutron beam.
The same "forbidden" reflections are present more pronouncedly in a similar scan made by Iizumi and Gesi (1983) for Rb_2ZnBr_4 at room temperature. Therefore it must be concluded that this c(s) symmetry element is not present in the incommensurate phase of Rb_2ZnCl_4 and in the 17-fold superstructure phase of Rb_2ZnBr_4. This contradicts the above hypothesis that this element is conserved - no explanation has yet been found.

Though the existence of superstructure phases in Rb_2ZnCl_4 is questionable, this is not the case for Rb_2ZnBr_4. Iizumi and Gesi (1983, see also chapter 3) confirmed that the room temperature phase of this compound has a 17-fold superstructure. Together with the value τ=0.384(5)≈5/13, found for a large temperature region in Cs_2FeI_4, this seems to show that these compounds in their large superstructures prefer τ=odd/odd above other kinds of fractions.

Acknowledgement. The measurements on Rb_2ZnCl_4 described in this section, have been performed in cooperation with dr. C. van Dijk of ECN (Netherlands Energy Research Foundation) in Petten.

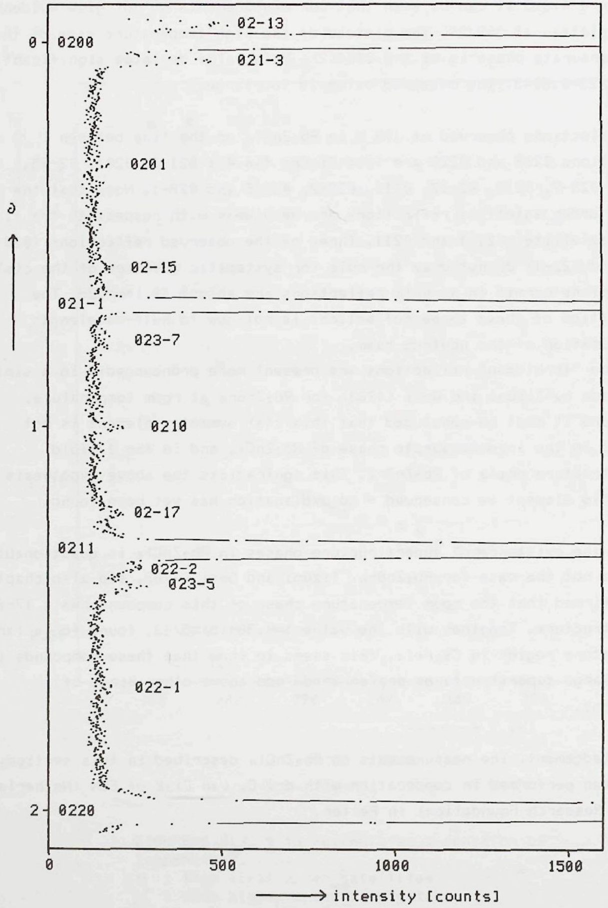

FIGURE 4.6.4. Measured neutron intensity as a function of the position in reciprocal space on the line 02∂ $(0<\partial<2)$ for Rb_2ZnCl_4 at 198K.

Chapter 5

THE ORIGIN OF THE MODULATION.

5.1. Introduction.

The origin of the modulation in distorted β-K_2SO_4 type crystal structures is still unclear, despite appreciable efforts of several authors. Phenomenologic theories, of the Landau type, have been put forward for the crystal structures of interest here. Though satisfactory explanations can be given for some of the phenomena, no insight is provided in the microscopic interactions causing the modulation of these structures (De Pater et al., 1979; Iizumi et al., 1977).

In relation to our detailed comparison of the crystal structures, we are especially interested in microscopic theories. An Ising model constructed by Yamada and Hamaya (1983a, 1983b) gives some hints towards the origin of the phase transitions. The interactions, however, bear no direct relation to the actual structural interactions. Janssen (1985) brings the model of Janssen and Tjon (1981, 1982, 1983) in connection with some of the crystal structures discussed in this thesis. The interactions which he assumes to exist are in our opinion not argumented adequately.

Haque and Hardy (1980) performed a theoretical lattice dynamical study of the normal to incommensurate phase transition of K_2SeO_4. All possible Coulomb interactions as well as 32 independent short range interactions were taken into account. The calculations showed the presence of a softening low frequency optical mode with a wave vector close to the observed modulation wavevector. The treatment regards the dynamics of the normal phase. Because of the complexity of the model it is very difficult to get insight in the mechanism which causes the modulation.

The purpose in the present chapter will be to calculate explicitly the static stability of the modulated phases, using the structural knowledge to sort out those interactions which are expected to play a dominant role in the stability. The word "interaction" will be used to indicate a simple interatomic force as well as the result of a combination of such forces.

The model will be presented in section 5.2, whereas in section 5.3 the

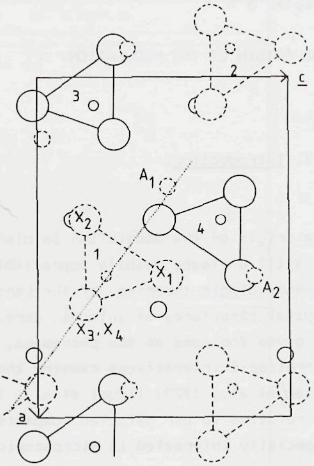

FIGURE 5.2.1. The numbering of the tetrahedra in a subcell, as used in this chapter. The dotted line indicates the plane containing the atoms shown in figure 5.3.3.

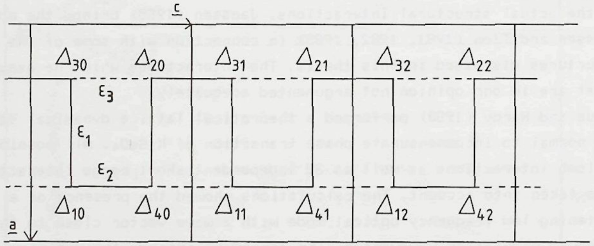

FIGURE 5.2.2. The interactions between the X_2 atoms in the model crystal structure. Δ_{ik} is the displacement parallel to $\underline{b}$ of the X_2 atom of tetrahedron i in subcell k. Each solid line indicates an interaction favouring equal displacements, whereas each dashed line indicates an interaction favouring opposite displacements.

relation of this model to the β-K_2SO_4 type crystal structure will be discussed. In section 5.4 it will be shown which structures are stable as a function of the interaction parameters in the model. In section 5.5 it will be assessed which of the observations can be explained by the model and which of them cannot. In the last section (5.6) the results will be discussed.

5.2. <u>The model</u>.

The model consists of an energy expression (5.2.1) derived from an assembly of interactions between first neighbours in an idealized structure. Although not exhaustive, this assembly is thought to be representative because the consequences of each interaction, taken separately, are reflected in systematic features present in the actual structures.
In the model it is assumed that $\underline{a}$ and $\underline{b}$ are true symmetry translation vectors. Hence, the modulation wave vector is parallel to $\underline{c}$, and it is sufficient to consider only a single row of subcells parallel to c. It is further assumed that a structure is completely determined by the displacements parallel to $\underline{b}$ of the X_2 atoms from the mirror planes in Pcmn. Hence, the model contains four parameters for the k-th subcell: the displacements Δ_{ik} of the X_2 atoms, i=1,2,3,4 denoting the tetrahedron number as indicated in figure 5.2.1.

The potential energy per subcell in the model is given by

$$F = \lim_{N\to\infty} \frac{1}{2N+1} \sum_{k=-N}^{N} [\sum_{i=1}^{4} (\Delta_{ik}^4-\sigma\Delta_{ik}^2) + \varepsilon_1((\Delta_{1k}-\Delta_{3k})^2+(\Delta_{2k}-\Delta_{4k})^2) +$$
$$+ \varepsilon_2((\Delta_{1k}-\Delta_{4k})^2+(\Delta_{2k}-\Delta_{3k+1})^2) +$$
$$+ \varepsilon_3((\Delta_{3k}+\Delta_{2k})^2+(\Delta_{4k}+\Delta_{1k+1})^2)] . \qquad (5.2.1)$$

In the following we shall refer to F as "the energy". The coefficients σ, ε_1, ε_2 and ε_3 are positive.
The term

$$(\Delta_{ik}^4-\sigma\Delta_{ik}^2) \qquad (5.2.2)$$

in equation 5.2.1 represents a double-well potential for Δ_{ik}. It is the only type of term in that equation which can have a negative value. The double well potential 5.2.2 has its minima at $\Delta_{ik}=\pm\surd(\sigma/2)$.
Each term of the form

$$(\Delta_{ik}-\Delta_{mn})^2 \tag{5.2.3}$$

describes an interaction between the X_2 atoms of tetrahedra i and m of subcell k and n respectively. If acting alone it would make $\Delta_{ik}=\Delta_{mn}$. In equation 5.2.1 the terms with coefficients ε_1 and ε_2 are of this type. The interactions represented by these terms are called ε_1- and ε_2 interactions respectively.
The terms of the form

$$(\Delta_{ik}+\Delta_{mn})^2 \tag{5.2.4}$$

describe another kind of interaction, tending to make $\Delta_{ik}=-\Delta_{mn}$. They all have coefficient ε_3 and are called ε_3 interactions.
In figure 5.2.2 all interactions in the model are represented graphically. Interactions of type 5.2.3 are shown as full lines, those of type 5.2.4 as dashed lines.

The model shows the feature of frustration: the interactions have counteracting tendencies. For instance, in figure 5.2.2 Δ_{20} is coupled to Δ_{30} by ε_1- and ε_2 interactions via Δ_{40} and Δ_{10}. The corresponding terms in the energy are smallest if

$$\Delta_{20} = \Delta_{40} = \Delta_{10} = \Delta_{30} \quad . \tag{5.2.5}$$

However, Δ_{20} is also coupled directly to Δ_{30} by a ε_3 interaction. This interaction has the tendency to make

$$\Delta_{20} = -\Delta_{30} \quad . \tag{5.2.6}$$

The crystal structure, represented by the model, must find a compromise for this conflict, assuming that σ in equation 5.2.1 is large enough (and hence the wells of the double well potential deep enough) to prevent vanishing of all displacements Δ_{ik}.
Such a competition of interactions is typical for the models that show incommensurate structures. An example is the model of Janssen an Tjon (1981, 1982, 1983).

The coefficient σ in equation 5.2.1 can be associated with the temperature: for a larger value of σ the wells of the potential are narrower and deeper. This can be interpreted as a decrease of the smoothing effect of thermal motion. Hence, a larger value of σ corresponds to a lower temperature. For low values of σ the energy (5.2.1) has its minimum at $\Delta_{ik}=0$ for each i and k, while for large values of σ the minimum will have nonzero displacements. Of course, the other coefficients in the model (ε_1, ε_2 and ε_3) may be temperature dependent as well, but presumably much less than σ.

5.3. Relation between model and crystal structure.

5.3.1. Introduction.

Four types of local atomic arrangements in distorted β-K_2SO_4 type crystal structures will be discussed in this section. The interatomic forces involved will lead to the energy expression 5.2.1. Before discussing the structural details, let us discuss the interatomic forces between two individual atoms. The interaction between two negative X atoms can be described by the usual potential energy expression

$$E(r) = \frac{c_1}{r} + \frac{c_2}{r^n} \quad (c_1,\ c_2 \text{ positive; } n\gg1, \text{ e.g. } n=12) \ , \tag{5.3.1}$$

in which r is the distance between the centres of both atoms. The first term is the Coulomb energy. The second one is an extra repulsive term, which is dominant for small values of r. Here the exact value of n is not relevant.
The first derivative of E with respect to r is negative, the second derivative is positive.

For the interaction of a negative X atom and a positive A-atom we write:

$$E'(r) = \frac{-c_3}{r} + \frac{c_4}{r^n} \quad (c_3,\ c_4 \text{ positive}) \ . \tag{5.3.2}$$

Often a Taylor series will be used, writing e.g. for E(r):

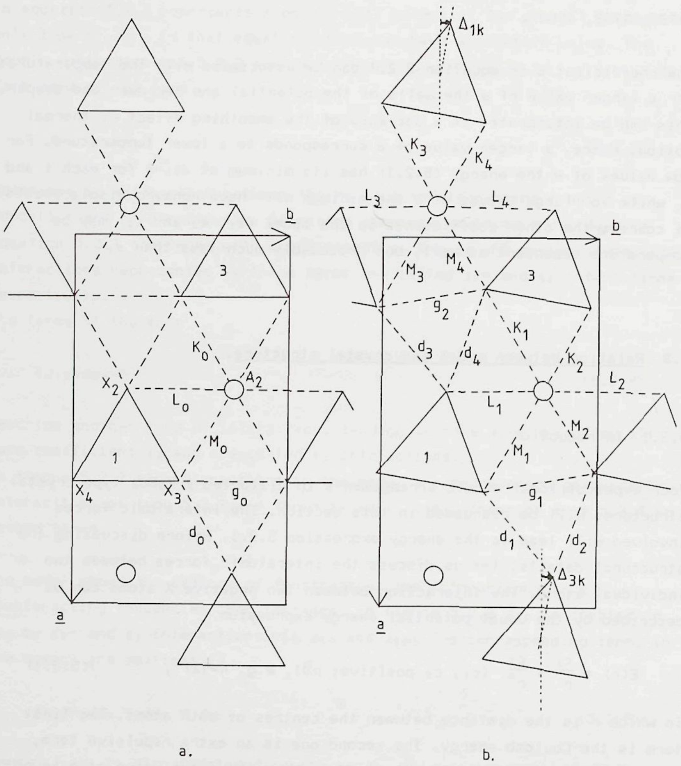

FIGURE 5.3.1. A layer normal to c̲ of X_2, X_3, X_4 and A_2 atoms. The X atoms are located at the corners of the triangles.

a. undistorted;

b. after rotation of the tetrahedra around an axis parallel to c̲.

$$E(r) = E(r_o) + \left(\frac{dE}{dr}\right)_{r_o} \Delta r + \left(\frac{d^2E}{dr^2}\right)_{r_o} \Delta r^2/2 + \ldots \qquad (5.3.3)$$

$$\text{with } r = r_o + \Delta r \ , \qquad (5.3.4)$$

where r_o is a distance in an undistorted β-K_2SO_4 type structure.

In chapter 4 it has been shown that the distortions of the structures with respect to Pcmn symmetry are mainly rotations of the tetrahedra, which can be characterized by displacements of the X_1- and X_2 atoms parallel to b̲. In this section this observation will be used as a starting point for the discussion: it will be assumed that the B atoms are not displaced, that the tetrahedra are regular and rigid and that the rotation of each tetrahedron has just two components, the component around an axis parallel to b̲ being zero (this component is very small in the actual structures, as discussed in section 4.4). We consider first a rotation around the line B-X_1, corresponding to a displacement of the X_2 atom parallel to b̲ (in first approximation). The second component, also about an axis lying in the a̲,c̲ plane, will be considered later.

5.3.2. Layer of tetrahedra normal to c̲.

The first one of the local atomic arrangements to be studied is the layer of tetrahadra normal to c̲ already discussed in section 4.4. Because a̲ and b̲ are translation vectors, only two non-equivalent tetrahedra exist in such a layer.

In figure 5.3.1a an undistorted layer is shown, whereas in figure 5.3.1b the tetrahedra are rotated. The atoms shown all have about equal z coordinates. Therefore the other rotation component (involving displacement of the X_1 atoms) does not have much influence on the distances between the atoms in the figure. The A_2 atoms are supposed to be fixed at the centra of the hexagons. In order to make equations simpler, it is further assumed that $a=b\sqrt{3}$ (hexagonal lattice), that the z coordinates of all atoms in figure 5.3.1 are equal and that the length of the tetrahedra edges is equal to b/2, so that

$$d_o = g_o = K_o = L_o = M_o = b/2 \ . \qquad (5.3.5)$$

These simplifications do not affect the conclusions which will be made later.
Only interactions between atoms which are connected by first neighbour distances (types d, g, K, L and M) are considered here.

For small rotation angles we find, developing orthogonal components of each distance up to Δ_{ik}^2:

$$d_1^2 = \frac{1}{4}\left(b+2\Delta_{1k}+4\Delta_{3k}+\frac{6\Delta_{1k}^2}{b}\right)^2 + \frac{3}{4}\left(b-2\Delta_{1k}+\frac{2\Delta_{1k}^2}{b}+\frac{4\Delta_{3k}^2}{b}\right)^2 , \qquad (5.3.6)$$

$$g_1^2 = \left(\frac{b}{2}+\frac{3\Delta_{1k}^2}{b}\right)^2 + 3\Delta_{1k}^2 , \qquad (5.3.7)$$

$$K_1 = \frac{b}{2} + \Delta_{3k} . \qquad (5.3.8)$$

From these equations and their analogues for d_2 etc one finds, in the same order of approximation:

$$d_1 = d_4 = \frac{b}{2} - \frac{\Delta_{1k}}{2} + \frac{\Delta_{3k}}{2} + \frac{9}{4b}(\Delta_{1k}^2+\Delta_{3k}^2) + \frac{3}{2b}\Delta_{1k}\Delta_{3k} , \qquad (5.3.9)$$

$$d_2 = d_3 = \frac{b}{2} + \frac{\Delta_{1k}}{2} - \frac{\Delta_{3k}}{2} + \frac{9}{4b}(\Delta_{1k}^2+\Delta_{3k}^2) + \frac{3}{2b}\Delta_{1k}\Delta_{3k} , \qquad (5.3.10)$$

$$g_1 = \frac{b}{2} + \frac{6}{b}\Delta_{1k}^2 , \qquad (5.3.11)$$

$$g_2 = \frac{b}{2} + \frac{6}{b}\Delta_{3k}^2 , \qquad (5.3.12)$$

$$K_1 = L_4 = M_3 = \frac{b}{2} + \Delta_{3k} , \qquad (5.3.13)$$

$$K_2 = L_3 = M_4 = \frac{b}{2} - \Delta_{3k} , \qquad (5.3.14)$$

$$K_3 = L_2 = M_1 = \frac{b}{2} + \Delta_{1k} , \qquad (5.3.15)$$

$$K_4 = L_1 = M_2 = \frac{b}{2} - \Delta_{1k} . \qquad (5.3.16)$$

Using 5.3.3 and the analogous equation for $E'(r)$, and neglecting third and higher order terms in Δ_{1k} and Δ_{3k}, the energy contribution of the interactions of these distances can be written as (leaving out the terms not depending on Δ_{1k} or Δ_{3k}):

$$F_1 = -\sigma_2(\Delta_{1k}^2+\Delta_{3k}^2) + \varepsilon_1'(\Delta_{1k}-\Delta_{3k})^2 \qquad (5.3.17)$$

$$\text{with } \sigma_2 = \frac{-18}{b}\left(\frac{dE}{dr}\right)_{b/2} - 3\left(\frac{d^2E'}{dr^2}\right)_{b/2} \qquad (5.3.18)$$

$$\text{and } \varepsilon_1' = \frac{-3}{b}\left(\frac{dE}{dr}\right)_{b/2} + \left(\frac{d^2E}{dr^2}\right)_{b/2} \qquad (5.3.19)$$

Now in the structures with space group Pcmn the distances of type K, L and M are larger than the A-X contact distance whereas in the other structures at least the average of the distances of each of these types is larger than that contact distance (as can be seen in figure 4.4.2). Therefore it can be assumed that the first term of 5.3.3 is dominant for small values of Δ_{1k} and Δ_{3k}. Hence

$$\left(\frac{d^2E'}{dr^2}\right)_{b/2} < 0 . \qquad (5.3.20)$$

The first derivative of E(r) (equation 5.3.1) is always negative, and its second derivative always positive. From this it follows that σ_2 and ε_1' are both positive.
So far it has been assumed that the rotation angles are small. For larger rotation angles the contact distance will be approached by some of the distances K, L or M. Then the repulsive second term in equation 5.3.2 becomes dominant, raising the energy. Therefore, in the model the terms

$$\sigma_4\Delta_{1k}^4 + \sigma_4\Delta_{3k}^4 \quad (\sigma_4 \text{ positive}) \qquad (5.3.21)$$

are included.

The energy of the layer then becomes

$$F_1' = \sigma_4\Delta_{1k}^4 - \sigma_2\Delta_{1k}^2 + \sigma_4\Delta_{3k}^4 - \sigma_2\Delta_{3k}^2 + \varepsilon_1'(\Delta_{1k}-\Delta_{3k})^2 . \qquad (5.3.22)$$

This energy has its minimum at

$$\Delta_{1k} = \Delta_{3k} = \pm\frac{\sqrt{\sigma_2}}{\sqrt{2}\sqrt{\sigma_4}} . \qquad (5.3.23)$$

The term with ε_1' in equation 5.3.22 accounts for the observation in section 4.4 that the X_2 displacements within a layer are very often almost equal and in the same sense.

Combining the energy of all layers in a structure gives

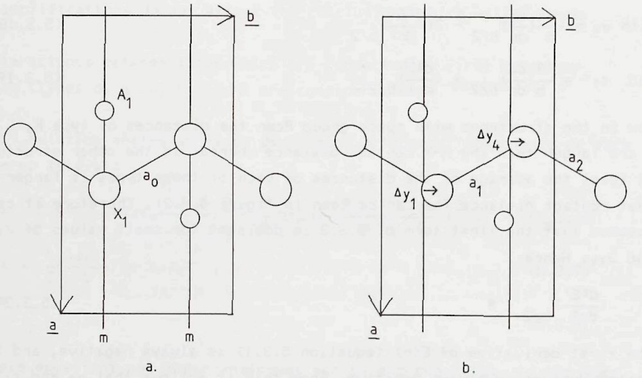

FIGURE 5.3.2. Chain of X_1 atoms parallel to b̲. The two non-equivalent X_1 atoms are of tetrahedra 1 and 4 respectively (in figure 5.2.1 the numbering of the tetrahedra is shown).
a. undistorted;
b. distorted: Δy_1 and Δy_4 are the two non-equivalent X_1 displacements in the chain.

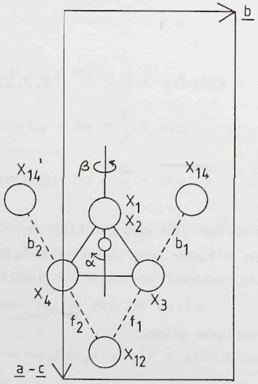

FIGURE 5.3.3. A tetrahedron with three surrounding X_1 atoms, lying in good approximation in one plane (indicated in figure 5.2.1). The forces between atoms connected by the indicated distances result in an effective interaction between atoms X_1 and X_2.

FIGURE 5.3.4. The interaction chain between two X_2 atoms via the X_1 atoms of the same tetrahedra. This chain can be replaced by a single interaction between the two X_2 atoms.

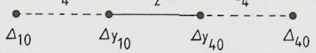

$$F_1'' = \sum_K \Big[\sum_{i=1}^{4} (\sigma_4 \Delta_{ik}^4 - \sigma_2 \Delta_{ik}^2) + \varepsilon_1'((\Delta_{1k}-\Delta_{3k})^2 + (\Delta_{2k}-\Delta_{4k})^2) \Big], \quad (5.3.24)$$

being the first part of the model energy expression, apart from the factor σ_4.

5.3.3. Interaction between layers involving X_1 atoms.

a. X_1 chains parallel to b̲.

In figure 5.3.2a an undistorted chain of X_1 atoms parallel to b̲ is shown (in subcell k). The atoms in the figure all have approximately equal z coordinates. In figure 5.3.2b a situation is shown in which tetrahedra 1 and 4 are rotated such that the X_1 atoms are displaced in the positive b̲ direction. Because b̲ is a translation vector, only two non-equivalent X_1 atoms exist in the chain.
The distances a_1 and a_2 can be written as

$$a_1 = a_o - \frac{b}{2a_o}(\Delta y_{1k} - \Delta y_{4k}) + \frac{a_o^2 - b^2/4}{2a_o^3}(\Delta y_{1k} - \Delta y_{4k})^2 \quad , \qquad (5.3.25)$$

$$\text{and} \quad a_2 = a_o + \frac{b}{2a_o}(\Delta y_{1k} - \Delta y_{4k}) + \frac{a_o^2 - b^2/4}{2a_o^3}(\Delta y_{1k} - \Delta y_{4k})^2 \quad , \qquad (5.3.26)$$

with Δy_{1k} and Δy_{4k} being the displacements of the X_1 atoms of tetrahedra 1 and 4 respectively, and a_o the length of the distances in the undistorted situation (figure 5.3.2a). Here and in all subsequent calculations we neglect third and higher powers of Δy_{ik}, and we omit constant terms in the energy.
The contribution to the energy of the interactions between the atoms connected by distances a_1 and a_2 can be obtained by substituting 5.3.25 and 5.3.26 into 5.3.3. The sum of the results is

$$F_2 = \varepsilon_2''(\Delta y_{1k} - \Delta y_{4k})^2 \qquad (5.3.27)$$

$$\text{with} \quad \varepsilon_2'' = \frac{a_o^2 - b^2/4}{a_o^3}\left(\frac{dE}{dr}\right)_{a_o} + \frac{b^2/4}{a_o^2}\left(\frac{d^2E}{dr^2}\right)_{a_o} . \qquad (5.3.28)$$

The coefficient ε_2'' is positive, as can be checked by substituting in 5.3.28 the first and second derivatives, which can be calculated from 5.3.1, and using

$$a_o^2 - b^2/4 < b^2/4 . \qquad (5.3.29)$$

The energy F_2 has a minimum ($F_2=0$) for

$$\Delta y_{1k} = \Delta y_{4k} \ . \qquad (5.3.30)$$

This corresponds to the observation (figure 4.4.4) that in most X_1 chains in distorted β-K_2SO_4 type structures the X_1 displacements within a X_1 chain parallel to b̲ are almost equal.

b. Effective interaction between X_1 and X_2 of the same tetrahedron.

Via this interaction the interaction between the X_1 atoms in the chain discussed above is transmitted to the X_2 atoms of the corresponding tetrahedra. Then, effectively, there is an interaction between the two X_2 atoms of the tetrahedra to which the X_1 atoms in the chain belong.

Figure 5.3.3 shows schematically part of the surrounding atoms of a tetrahedron. In real structures, the atoms shown in figure 5.3.3, except X_1 and X_2, lie in one plane in good approximation (see the dashed line in figure 5.2.1). Atoms X_1 and X_2 are approximately mirror images of each other with respect to this plane. X_1, X_{14} and X_{14}' are atoms of the same chain parallel to b̲.
For simplicity, the following assumptions are made: the atoms X_{14}, X_{14}' and X_{12} are fixed at their positions in the high temperature phase; the tetrahedron edges and the undistorted distances of type b and f have length b/2 (b being the length of translation vector b̲); the atoms B, X_3, X_4, X_{14}, X_{14}' and X_{12} lie in one plane.
In figure 5.3.3, two rotation components of the tetrahedron are indicated. Rotation component β corresponds to equal but opposite displacements of atoms X_1 and X_2, whereas component α corresponds to equal displacements of these atoms in the same direction. Together, these rotations take also into account the second non-zero component of the total rotation, mentioned in subsection 5.3.1.

The distances b_1, b_2, f_1 and f_2 as a function of the X_1- and X_2 displacements Δy and Δ (suppressing the indices giving the tetrahedron number and subcell number) can be written as

$$b_1 = \frac{b}{2} - \frac{\sqrt{6}+1}{4}(\Delta y+\Delta) - \frac{6\sqrt{3}-13}{16b}(\Delta y+\Delta)^2 + \frac{1}{2b}(\Delta y-\Delta)^2 \ , \qquad (5.3.31)$$

$$b_2 = \frac{b}{2} + \frac{\sqrt{6}+1}{4}(\Delta y+\Delta) - \frac{6\sqrt{3}-13}{16b}(\Delta y+\Delta)^2 + \frac{1}{2b}(\Delta y-\Delta)^2 \ , \qquad (5.3.32)$$

$$f_1 = \frac{b}{2} + \frac{\sqrt{6}+1}{4}(\Delta y+\Delta) - \frac{2\sqrt{6}-3}{16b}(\Delta y+\Delta)^2 \ , \qquad (5.3.33)$$

$$f_2 = \frac{b}{2} - \frac{\sqrt{6}+1}{4}(\Delta y+\Delta) - \frac{2\sqrt{6}-3}{16b}(\Delta y+\Delta)^2 \ . \qquad (5.3.34)$$

The contribution to the energy of the interactions between the atoms connected by the distances of type b and f shown in figure 5.3.3 can be obtained by substituting 5.3.31, 5.3.32, 5.3.33 and 5.3.34 into 5.3.3 respectively. The sum of the results is

$$F_r = \varepsilon_4(\Delta y+\Delta)^2 - X(\Delta y^2+\Delta^2) \qquad (5.3.35)$$

$$\text{with } \varepsilon_4 = \frac{-(\sqrt{6}+6)}{8b}\left(\frac{dE}{dr}\right)_{b/2} + \frac{2\sqrt{6}+7}{4}\left(\frac{d^2E}{dr^2}\right)_{b/2} \qquad (5.3.36)$$

$$\text{and } X = \frac{-2}{b}\left(\frac{dE}{dr}\right)_{b/2} \ . \qquad (5.3.37)$$

Both ε_4 and X are positive because the first derivative of E is negative and the second derivative is positive.
The first term of equation 5.3.35 gives the effective interaction between the displacements of the X_1- and X_2 atoms of the same tetrahedron.

c. Resulting effective interaction.

Between the X_2 atoms of tetrahedrons 1 and 4 of subcell 0 there is a chain of three interactions, as shown in figure 5.3.4. This chain can be replaced by a single interaction between the two X_2 atoms, as will be shown in the following.
The relevant terms of the energy are:

$$F_c = \varepsilon_2''(\Delta y_{10}-\Delta y_{40})^2 + \varepsilon_4((\Delta y_{10}+\Delta_{10})^2+(\Delta y_{40}+\Delta_{40})^2) -$$

$$- X(\Delta y_{10}^2+\Delta y_{40}^2+\Delta_{10}^2+\Delta_{40}^2) \ . \qquad (5.3.38)$$

The term with ε_2'' is taken from equation 5.3.27. The terms with ε_4 and X are from 5.3.35.
Because the X_1 displacements Δy_{ik} are not involved in other interactions, they can be eleminated in the energy expression by substituting the values of Δy_{10} and Δy_{40} for which the energy is minimal:

$$\frac{\partial F_c}{\partial \Delta y_{10}} = 2[(\varepsilon_2''+\varepsilon_4-X)\Delta y_{10}+\varepsilon_4\Delta_{10}-\varepsilon_2''\Delta y_{40}] = 0 \ , \qquad (5.3.39)$$

$$\frac{\partial F_c}{\partial \Delta y_{4o}} = 2[(\varepsilon_2''+\varepsilon_4-X)\Delta y_{4o}+\varepsilon_4\Delta_{4o}-\varepsilon_2''\Delta y_{1o}] = 0 \quad . \tag{5.3.40}$$

The solution of 5.3.39 and 5.3.40 (two linear equations, two unknowns: Δy_{1o} and Δy_{4o}) gives a minimum of F_c if

$$\frac{\partial^2 F_c}{\partial \Delta y_{1o}^2} > 0 \quad , \tag{5.3.41}$$

$$\frac{\partial^2 F_c}{\partial \Delta y_{4o}^2} > 0 \quad , \tag{5.3.42}$$

and
$$\frac{\partial^2 F_c}{\partial \Delta y_{1o}^2}\,\frac{\partial^2 F_c}{\partial \Delta y_{4o}^2} - \left(\frac{\partial^2 F_c}{\partial \Delta y_{1o}\partial \Delta y_{4o}}\right)^2 > 0 \quad . \tag{5.3.43}$$

Now from 5.3.38

$$\frac{\partial^2 F_c}{\partial \Delta y_{4o}^2} = \frac{\partial^2 F_c}{\partial \Delta y_{1o}^2} = \varepsilon_2'' + \varepsilon_4 - X \tag{5.3.44}$$

$$\frac{\partial^2 F_c}{\partial y_{4o}\partial y_{1o}} = (2\varepsilon_2''+\varepsilon_4-X)(\varepsilon_4-X) \quad . \tag{5.3.45}$$

Since $\varepsilon_2''>0$, conditions 5.3.41, 5.3.42 and 5.3.43 are fulfilled if

$$\varepsilon_4 - X > 0 \quad . \tag{5.3.46}$$

This condition is fulfilled for our simplified structure (figure 5.3.3), as can be checked by substituting 5.3.1 into 5.3.36 and 5.3.37, and 5.3.36 and 5.3.37 into 5.3.46.
From equations 5.3.39 and 5.3.40 it follows that

$$\Delta y_{1o} = \frac{\varepsilon_4(\varepsilon_2''+\varepsilon_4-X)\Delta_{1o} + \varepsilon_4\varepsilon_2''\Delta_{4o}}{\varepsilon_2''^2 - (\varepsilon_2''+\varepsilon_4-X)^2} \tag{5.3.47}$$

and
$$\Delta y_{4o} = \frac{\varepsilon_4(\varepsilon_2''+\varepsilon_4-X)\Delta_{4o} + \varepsilon_4\varepsilon_2''\Delta_{1o}}{\varepsilon_2''^2 - (\varepsilon_2''+\varepsilon_4-X)^2} \quad . \tag{5.3.48}$$

Substitution of 5.3.47 and 5.3.48 into 5.3.38 gives

$$F_c = \varepsilon_2'(\Delta_{1o}-\Delta_{4o})^2 - X'(\Delta_{1o}^2+\Delta_{4o}^2) \tag{5.3.49}$$

with
$$\varepsilon_2' = \frac{\varepsilon_2''\varepsilon_4}{(\varepsilon_2''+\varepsilon_4-X)^2 - \varepsilon_2''^2} \tag{5.3.50}$$

and
$$X' = \frac{X(2\varepsilon_4-X)}{\varepsilon_4-X} \quad . \tag{5.3.51}$$

Because of 5.3.46 and because ε_2'', ε_4 and X are positive, ε_2' and X' are also positive.

Combining the energy contributions of all X_1 chains parallel to $\underline{b}$ and all intra-tetrahedron interactions one gets from 5.3.49:

$$F_c' = \sum_{k} [\ \varepsilon_2'((\Delta_{1k}-\Delta_{4k})^2+(\Delta_{2k}-\Delta_{3k+1})^2) + \sum_{i=1}^{4} X'\Delta_{ik}^2\ ] \quad , \tag{5.3.52}$$

in which the summation over k is over all subcells.

5.3.4. Interaction between layers not involving X_1 atoms.

Figure 5.3.5 shows in a projection on the $\underline{a},\underline{b}$ plane the relevant atoms in subcell k. Part a of this figure shows the undistorted situation, whereas in part b the tetrahedra are rotated around an axis parallel to $\underline{c}$. The other rotation component, involving displacements of the X_1 atoms, is not considered here, since that would make the calculation much more complicated.

As in subsection 5.3.1 we assume that a=b/3 (hexagonal lattice) and that the edges of the rigid and regular tetrahedra have length b/2. Further, it is assumed that for each tetrahedron the three X atoms shown in figure 5.3.5 have equal z coordinates.
The distances e_1, e_2, e_3 and e_4 are

$$e_1 = e_4 = \frac{b}{2} + \frac{1}{2}(\Delta_{3k}+\Delta_{2k}) + \frac{1}{4b}(\Delta_{3k}+\Delta_{2k})^2 \quad , \tag{5.3.53}$$

$$e_2 = e_3 = \frac{b}{2} - \frac{1}{2}(\Delta_{3k}+\Delta_{2k}) + \frac{1}{4b}(\Delta_{3k}+\Delta_{2k})^2 \quad , \tag{5.3.54}$$

The undistorted distance e_o has been put equal to b/2 in these equations. The energy of the interactions of these distances can be obtained by substituting the distances in 5.3.3 respectively and summing the results:

$$F_3 = \varepsilon_3'(\Delta_{3k}+\Delta_{2k})^2 \tag{5.3.55}$$

with
$$\varepsilon_3' = \frac{1}{b}\left(\frac{dE}{dr}\right)_{b/2} + \frac{1}{2}\left(\frac{d^2E}{dr^2}\right)_{b/2} \quad . \tag{5.3.56}$$

ε_3' is positive. This can be seen by substituting the derivatives calculated from equation 5.3.1.
For the other pair of tetrahedra in the subcell, a similar energy expression can be derived.
The energy F_3 is smallest if $\Delta_{3k}=-\Delta_{2k}$. There indeed is such a tendency in

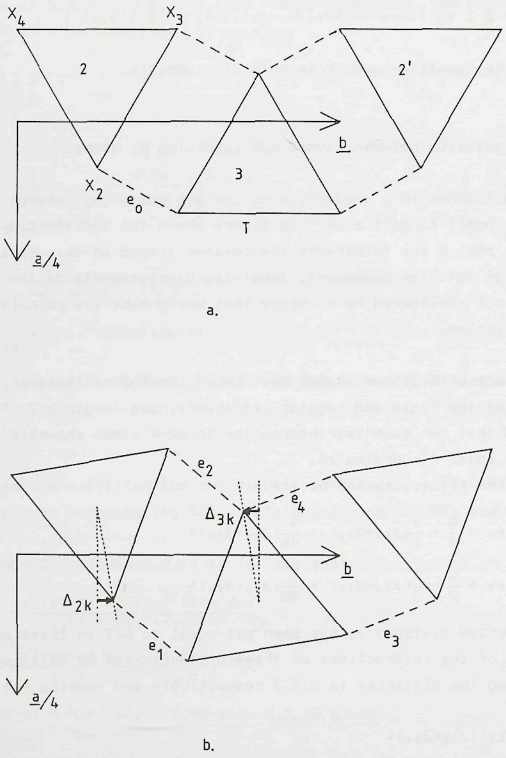

FIGURE 5.3.5. Projection of the X_2, X_3 and X_4 atoms of tetrahedra 2 and 3 on the $\underline{a}$,$\underline{b}$ plane.
a. undistorted;
b. after rotation of the tetrahedra around an axis parallel to $\underline{c}$. Δ_{2k} and Δ_{3k} are positive if the displacements are in the positive $\underline{b}$ direction.

the actual structures, cf. figure 4.4.4.
The sum of the energies of all interactions of this type is given by

$$F_3' = \sum_{k} \varepsilon_3'((\Delta_{3k}+\Delta_{2k})^2+(\Delta_{4k}+\Delta_{1k+1})^2) \quad . \qquad (5.3.57)$$

The summation is over all subcells.

5.3.5. Assembly.

Summing the energy contributions derived in the previous three subsections (F_1'', F_c' and F_3' in equations 5.3.24, 5.3.52 and 5.3.57 respectively) and averageing over the subcells gives

$$\begin{aligned} F' = \lim_{k\to\infty} \frac{1}{2N+1} \sum_{k=-N}^{N} [& \sum_{i=1}^{4} (\sigma_4\Delta_{ik}^4-(\sigma_2+X')\Delta_{ik}^2) + \\ & + \varepsilon_1'((\Delta_{1k}-\Delta_{3k})^2+(\Delta_{2k}-\Delta_{4k})^2) + \varepsilon_2'((\Delta_{1k}-\Delta_{4k})^2+(\Delta_{2k}-\Delta_{3k+1})^2) + \\ & + \varepsilon_3'((\Delta_{3k}+\Delta_{2k})^2+(\Delta_{4k}+\Delta_{1k+1})^2)] \quad . \end{aligned} \qquad (5.3.58)$$

Division by σ_4 gives the model energy given in section 5.2 (equation 5.2.1), with

$$\sigma = (\sigma_2+X')/\sigma_4 \quad , \qquad (5.3.59)$$

$$\varepsilon_1 = \varepsilon_1'/\sigma_4 \quad , \qquad (5.3.60)$$

$$\varepsilon_2 = \varepsilon_2'/\sigma_4 \quad , \qquad (5.3.61)$$

$$\varepsilon_3 = \varepsilon_3'/\sigma_4 \quad . \qquad (5.3.62)$$

The interatomic interactions included in the discussion above to derive the model are not the only nearest neighbour ones in the A_2BX_4 compounds. However, they are considered to be the most important ones. As will be shown in section 5.5, the resulting model indeed can explain most of the observations. Therefore, no extra interactions have been included.

5.4. Model calculations.

Using energy expression 5.2.1, one can calculate for which X_2 displacements Δ_{ik} the model structure is stable for certain values of σ, ε_1, ε_2 and ε_3. These calculations and their results will be discussed in this section.

For reasons of convenience it is assumed that the modulation functions do not contain second or higher harmonics:

$$\Delta_{ik} = B_i + A_i \cos 2\pi((z_{io}+k)\gamma - \varphi_i) \quad . \tag{5.4.1}$$

It should be noted that for 1-, 2-, or 3-fold superstructures only the first harmonic is relevant anyhow. In 4-fold superstructures only the second harmonic is excluded by our assumption.
A_i and φ_i are the amplitude and the phase of the first harmonic of the modulation function for the X_2 displacements of tetrahedra i (the numbering of the tetrahedra is as shown in figure 5.2.1; in chapter 3 and 4 subscript i in A_i and φ_i has another meaning). B_i is the average X_2 displacement for these tetrahedra. Δ_{ik} is the X_2 displacement of tetrahedron i in subcell k. z_{io} is the z coordinate of the X_2 atom of subcell 0. For i=1,2,3 and 4 this coordinate is 0, 0.5, 0 and 0.5 respectively.
The term modulation function has a slightly different meaning in this chapter: contrary to the definition in section 1.1, a modulation function can have a non-zero average (B_i) here. In this chapter the modulation functions give the displacements with respect to Pcmn symmetry, rather than with respect to the basic structure.
For an incommensurate structure and a 4-fold or 3-fold superstructure, the X_2 displacements are as given by 5.4.1 with γ=irrational, $\gamma=1/4$ and $\gamma=1/3$ respectively. For a 2-fold or a 1-fold superstructure, however, the expression can be simplified because the modulation function is determined by less than three points per modulation period, leading to

$$\Delta_{ik} = B_i + A_i \cos \pi k \tag{5.4.2}$$

and $\Delta_{ik} = B_i \quad .$ (5.4.3)

Because no higher harmonics are allowed in the modulation functions and the highest power of Δ_{ik} in equation 5.2.1 is 4, 5-fold and larger superstructures are not stable in the model.

The energy as a function of the parameters A_i, φ_i and B_i for a ν-fold superstructure can be found by substituting equation 5.4.1, 5.4.2 (for a 2-fold superstructure) or 5.4.3 (1-fold superstructure) into 5.2.1, and by replacing the summation

$$\lim_{N\to\infty} \frac{1}{2N+1} \sum_{k=-N}^{N} [\ \dots\ ] \tag{5.4.4}$$

by $\displaystyle \frac{1}{\nu} \sum_{k=0}^{\nu-1} [\ \dots\ ] \quad .$ (5.4.5)

For an incommensurate structure the energy as a function of A_i, φ_i , B_i and γ can be obtained by substituting 5.4.1 into 5.2.1, but a more convenient expression can be found by substitution of

$$\Delta_{ik} = B_i + A_i \cos 2\pi((z_{io}+k)\gamma - \varphi_i + \Psi) \tag{5.4.6}$$

instead of 5.4.1 into 5.2.1, and replacing the summation (5.4.4) by an integral:

$$\int_0^1 d\Psi\, [\ \dots\ ]_{k=0} \quad . \tag{5.4.7}$$

The extra term Ψ in the argument of the cosine in equation 5.4.6 is an overall phase shift of the modulation wave. This does not change the incommensurate crystal structure. The replacement of the summation by the integral is allowed, because shifting an incommensurate modulation wave over one modulation wavelength and integrating over all subsequent situations in one unit cell has the same result as summing over all unit cells for one phase (Ψ=0) of the modulation wave.

For each set of values for σ, ε_1, ε_2 and ε_3 we can determine which structure is stable. This has been done for each structure (incommensurate, 4-fold, 3-fold, 2-fold and 1-fold superstructure) by calculating the values of the parameters A_i, φ_i, B_i and γ (for the incommensurate structure only) for which the energy is minimal. If all A_i and B_i are found to be zero, then the stable stucture is the normal (undistorted) structure.
The energy functions to be minimized have 4, 8 or 12 arguments for the 1-fold, the 2-fold and the other structures respectively. For the incommensurate structure this number is not 13 since a phase shift in this case is irrelevant. In order to find the minimum, a steepest descent method (Scheid, 1968) has been used.

The structures which are compared do not have an imposed symmetry. However, it turns out that the parameters A_i, φ_i and B_i of the stable structures are such that they always describe a structure of which the pointgroup has order 4 (for the superstructures) or 8 (for the undistorted and incommensurate structures). These are the largest point group orders which are possible in each case.
Using the symmetry relations between the modulation functions, the number of parameters in the energy expressions can be reduced. The final number of parameters is 1, 2, 3, 4 and 3 respectively for 1-fold, 2-fold, 3-fold 4-fold and incommensurate structures.
The full set of structures which are stable in the model are represented schematically in table 5.4.1, together with the energy expressions. Apart from the normal structure the stable structure types include one type of incommensurate structure, four types of 4-fold superstructures, four types of 3-fold superstructures, two types of 2-fold superstructures and two types of 1-fold superstructures. The simplified energy expression for the incommensurate structure type is derived in appendix B. For the other types it can be found by substituting the X_2 displacements mentioned in table 5.4.1 into equation 5.2.1 (after replacing the summation by the one given in 5.4.5).

For the incommensurate structure type and the two 1-fold superstructure types the values of the parameters for which the energy has its minimum can be derived analytically without difficulties. In appendix B these calculations are perfomed for the incommensurate structure. The result of these calculations is that under condition

$$-1 < \frac{\varepsilon_1(\varepsilon_3-\varepsilon_2)}{4\varepsilon_3\varepsilon_2} < 1 \qquad (5.4.8)$$

and condition

$$\sigma > \sigma_0 \qquad (5.4.9)$$

$$\text{with } \sigma_0 = \varepsilon_1 + \varepsilon_2 + \varepsilon_3 - \frac{(\varepsilon_2+\varepsilon_3)\sqrt{\varepsilon_1{}^2+4\varepsilon_2\varepsilon_3}}{2\sqrt{\varepsilon_2\varepsilon_3}} \qquad (5.4.10)$$

the incommensurate structure is stable, provided that its energy is smaller than the minima for the superstructures. The energy then has its minimum

$$F = -2(\sigma-\sigma_0)^2/3 \;. \qquad (5.4.11)$$

for

TABLE 5.4.1. The stable structures in the model. Given are supercell size, space group, modulation wave vector length (γ, standardized according to subsection 4.2.3), X_2 displacements (Δ_{ik}) and energy (F).

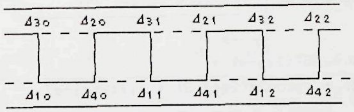

incommensurate structure
Pcmn(00γ)(ss$\bar{1}$)
$\Delta_{1k} = A\cos 2\pi(k\gamma-\varphi)$
$\Delta_{2k} = A\cos 2\pi((0.5+k)\gamma-\varphi+0.5)$
$\Delta_{3k} = A\cos 2\pi(k\gamma+\varphi)$
$\Delta_{4k} = A\cos 2\pi((0.5+k)\gamma+\varphi+0.5)$

$$F = 1.5A^4 + 2A^2[\varepsilon_1+\varepsilon_2+\varepsilon_3-\sigma - \varepsilon_1\cos 4\pi\varphi + \varepsilon_2\cos 2\pi(2\varphi+\gamma/2) - \varepsilon_3\cos 2\pi(2\varphi-\gamma/2)]$$

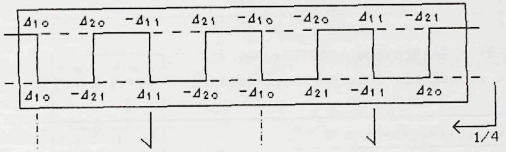

4-fold
superstructure
P2$_1$cn
γ = 1/4 or 3/4

$\Delta_{1k} = A_1\cos 2\pi(k\gamma-\varphi_1)$, $\Delta_{2k} = A_2\cos 2\pi((0.5+k)\gamma-\varphi_2)$

$$F = A_1{}^4(3+\cos 8\pi\varphi_1)/4 + A_2{}^4(3-\cos 8\pi\varphi_2)/4 + 2A_1A_2[\varepsilon_2\cos 2\pi(\varphi_1+\varphi_2+5\gamma/2) + \\ + \varepsilon_3\cos 2\pi(\varphi_1+\varphi_2-\gamma/2)] + \sum_{i=1}^{2} A_i{}^2[\varepsilon_1+\varepsilon_2+\varepsilon_3-\sigma - \varepsilon_1\cos 4\pi\varphi_i]$$

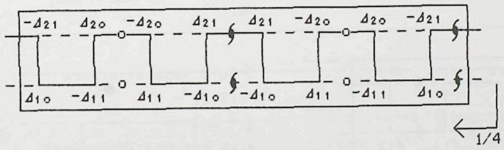

4-fold
superstructure
P12$_1$/c1
γ = 1/4 or 3/4

$\Delta_{1k} = A_1\cos 2\pi(k\gamma-\varphi_1)$, $\Delta_{2k} = A_2\cos 2\pi((0.5+k)\gamma-\varphi_2)$

$$F = A_1{}^4(3+\cos 8\pi\varphi_1)/4 + A_2{}^4(3-\cos 8\pi\varphi_2)/4 + 2A_1A_2\varepsilon_1\cos 2\pi(\varphi_1+\varphi_2+5\gamma/2) + \\ + \sum_{i=1}^{2} A_i{}^2[\varepsilon_1+\varepsilon_2+\varepsilon_3-\sigma + \varepsilon_2\cos 2\pi(2\varphi_i-\gamma) + \varepsilon_3\cos 4\pi\varphi_i]$$

Table 5.4.1. continued.

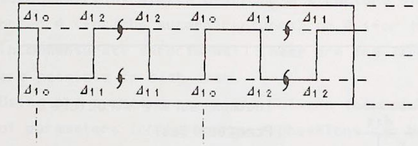

3-fold superstructure

$Pc2_1n$

$\gamma = 1/3$

$\Delta_{1k} = B + A\cos 2\pi(k/3-\varphi)$

$$F = 1.5A^4 + 4B^4 + 12A^2B^2 + 4A^3B\cos 6\pi\varphi + 4B^2(2\varepsilon_3-\sigma) + $$
$$+ 2A^2[-\varepsilon_1\cos 4\pi\varphi + \varepsilon_2\cos 2\pi(2\varphi+1/6) + \varepsilon_3\cos 2\pi(2\varphi+1/3) + \varepsilon_1+\varepsilon_2+\varepsilon_3-\sigma]$$

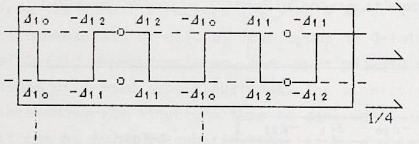

3-fold superstructure

$P112_1/n$

$\gamma = 2/3$

$\Delta_{1k} = B + A\cos 2\pi(2k/3-\varphi)$

$$F = 1.5A^4 + 4B^4 + 12A^2B^2 + 4A^3B\cos 6\pi\varphi + 4B^2(2\varepsilon_2-\sigma) + $$
$$+ 2A^2[-\varepsilon_1\cos 4\pi\varphi + \varepsilon_2\cos 2\pi(2\varphi+1/3) + \varepsilon_3\cos 2\pi(2\varphi+1/6) + \varepsilon_1+\varepsilon_2+\varepsilon_3-\sigma]$$

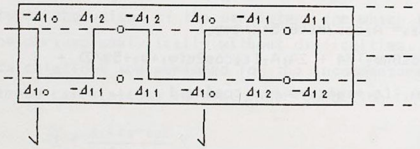

3-fold superstructure

$P2_1/c11$

$\gamma = 1/3$

$\Delta_{1k} = B + A\cos 2\pi(k/3-\varphi)$

$$F = 1.5A^4 + 4B^4 + 12A^2B^2 + 4A^3B\cos 6\pi\varphi + 4B^2(2\varepsilon_1+2\varepsilon_2-\sigma) + $$
$$+ 2A^2[\varepsilon_1\cos 4\pi\varphi + \varepsilon_2\cos 2\pi(2\varphi+2/3) + \varepsilon_3\cos 2\pi(2\varphi-1/6) + \varepsilon_1+\varepsilon_2+\varepsilon_3-\sigma]$$

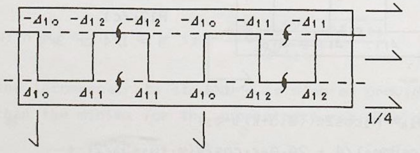

3-fold superstructure

$P2_12_12_1$

$\gamma = 2/3$

$\Delta_{1k} = B + A\cos 2\pi(2k/3-\varphi)$

$$F = 1.5A^4 + 4B^4 + 12A^2B^2 + 4A^3B\cos 6\pi\varphi + 4B^2(2\varepsilon_1+2\varepsilon_3-\sigma) + $$
$$+ 2A^2[\varepsilon_1\cos 4\pi\varphi + \varepsilon_2\cos 2\pi(2\varphi-1/6) + \varepsilon_3\cos 2\pi(2\varphi+2/3) + \varepsilon_1+\varepsilon_2+\varepsilon_3-\sigma]$$

Table 5.4.1. continued.

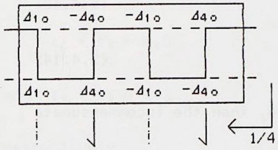

2-fold superstructure

$P2_1cn$, $\gamma = 1/2$

$\Delta_{10} = A_1$, $\Delta_{40} = A_4$

$$F = 2(A_1^4+A_4^4) + 2(A_1^2+A_4^2)(\varepsilon_2+\varepsilon_3-\sigma) + $$
$$+ 4A_4^2\varepsilon_1 - 4A_1A_4(\varepsilon_2+\varepsilon_3)$$

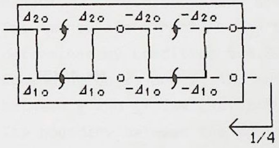

2-fold superstructure

$P12_1/c1$, $\gamma = 1/2$

$\Delta_{10} = A_1$, $\Delta_{20} = A_2$

$$F = 2(A_1^4+A_2^4) + 2(A_1^2+A_2^2)(\varepsilon_1-\sigma) + $$
$$+ 4A_2^2(\varepsilon_2+\varepsilon_3) - 4A_1A_2\varepsilon_1$$

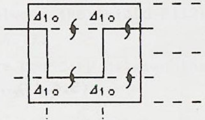

1-fold superstructure

$Pc2_1n$, $\gamma = 1$

$\Delta_{10} = B$

$$F = 4B^4 + 4B^2(2\varepsilon_3-\sigma)$$

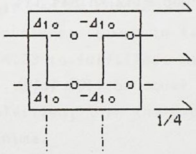

1-fold superstructure

$P112_1/n$, $\gamma = 0$

$\Delta_{10} = B$

$$F = 4B^4 + 4B^2(2\varepsilon_2-\sigma)$$

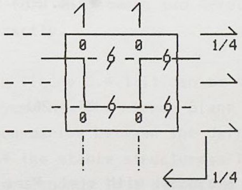

undistorted structure

$Pcmn$

$F = 0$

$$\gamma = \frac{1}{\pi} \arccos\left(\frac{\varepsilon_1(\varepsilon_3-\varepsilon_2)}{4\varepsilon_2\varepsilon_3}\right) , \qquad (5.4.12)$$

$$\varphi = \frac{1}{4\pi} \arctan\left(\frac{\sqrt{16\varepsilon_2{}^2\varepsilon_3{}^2-\varepsilon_1{}^2(\varepsilon_3-\varepsilon_2)^2}}{\varepsilon_1(\varepsilon_3+\varepsilon_2)}\right) , \qquad (5.4.13)$$

$$A = \sqrt{2(\sigma-\sigma_0)/3} \quad . \qquad (5.4.14)$$

If conditions 5.4.8 and 5.4.9 are not fulfilled, then the incommensurate structure is not stable.

The minimum of the energy for the 1-fold superstructure with space group $Pc2_1n$ (see table 5.4.1) is at

$$B = \sqrt{\sigma/2-\varepsilon_3} \qquad (5.4.15)$$

under condition

$$2\varepsilon_3 - \sigma < 0 \ . \qquad (5.4.16)$$

The value of the energy at this minimum is

$$F = -(2\varepsilon_3-\sigma)^2 \ . \qquad (5.4.17)$$

If condition 5.4.16 is not fulfilled, this 1-fold superstructure is not stable.
The energy of the 1-fold superstructure with space group $P112_1/n$ has its minimum at

$$B = \sqrt{\sigma/2-\varepsilon_2} \qquad (5.4.18)$$

if condition

$$2\varepsilon_2 - \sigma < 0 \qquad (5.4.19)$$

is fulfilled. In this minimum the energy is

$$F = -(2\varepsilon_2-\sigma)^2 \ . \qquad (5.4.20)$$

Figure 5.4.1 shows the $\varepsilon_2,\varepsilon_3,\sigma$ phase diagram for the model with $\varepsilon_1=1$. Part

a of this figure is a projection of lines at which regions of three phases meet each other. Part b and c are cross-sections through the $\varepsilon_2,\varepsilon_3,\sigma$ phase diagram. These cross-sections are the planes

$$\varepsilon_2 + \varepsilon_3 = 0.8 \qquad (5.4.21)$$

$$\text{and} \quad \varepsilon_2 + \varepsilon_3 = 1.2 \qquad (5.4.22)$$

respectively.
In figure 5.4.1a the regions with $\varepsilon_2,\varepsilon_3$ values for which the incommensurate structure cannot be stable are hatched. The region in which the incommensurate structure can be stable (for suitable values of σ) is determined by condition 5.4.8. (with $\varepsilon_1=1$).
Depending on ε_2 and ε_3 the modulation wave vector can have each value between $\underline{0}$ and $\underline{c}^*$, as indicated in figure 5.4.1b and 5.4.1c.
The boundary between the normal phase and the incommensurate one is determined by condition 5.4.9. The boundary between the 1-fold $Pc2_1n$ phase and the normal phase is determined by condition 5.4.16, and the boundary between the 1-fold $P112_1/n$ phase and the normal one is given by condition 5.4.19.
The boundary between the phases of both 2-fold superstructure types is given by

$$\varepsilon_2 + \varepsilon_3 = \varepsilon_1 \quad . \qquad (5.4.23)$$

This can be checked by comparing the energy expressions of these two structures (given in table 5.4.1). These equations are equal if condition 5.4.23 is fulfilled. Hence the energy of the minimum for such a set of $\varepsilon_2,\varepsilon_3,\varepsilon_1$ will be equal for both structure types. If condition 5.4.23 is not fulfilled, then the expressions are different, and will result in different minima.
The numerical calculations strongly suggest that each boundary between two 3-fold or between two 4-fold superstructure phases is also given by 5.4.23 exactly.

In figure 5.4.1 it can be seen that the $\varepsilon_2,\varepsilon_3,\sigma$ phase diagram has mirror symmetry. The mirror plane $\varepsilon_3=\varepsilon_2$ exists if one only considers the boundaries between the different phases, the supercell size and the energy of the stable structures. If an arbitrary point P in the phase diagram corresponds to a structure with modulation wave vector component γ

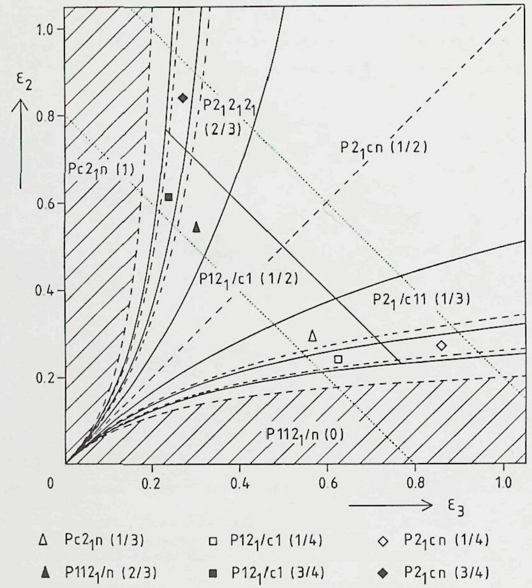

a.

FIGURE 5.4.1. The $\varepsilon_2,\varepsilon_3,\sigma$ phase diagram of the model ($\varepsilon_1=1$).

a. projection on the $\varepsilon_2,\varepsilon_3$ plane of lines at which three phases meet.
full lines: between two superstructure phases and the incommensurate phase.
dashed lines: between a superstructure phase, the incommensurate phase and the normal phase.
dotted lines: locations of the cross-sections shown in parts b and c of this figure.
In the hatched $\varepsilon_2,\varepsilon_3$ regions the incommensurate structure cannot be stable.

b. cross-section $\varepsilon_3=0.8-\varepsilon_2$. γ gives the modulation wave vector length ($\underline{q}=\gamma\underline{c}^*$) in the incommensurate regions;

c. cross-section $\varepsilon_3=1.2-\varepsilon_2$.

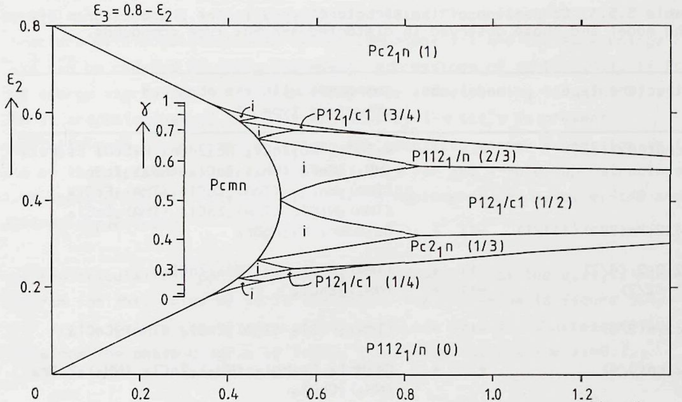

b.

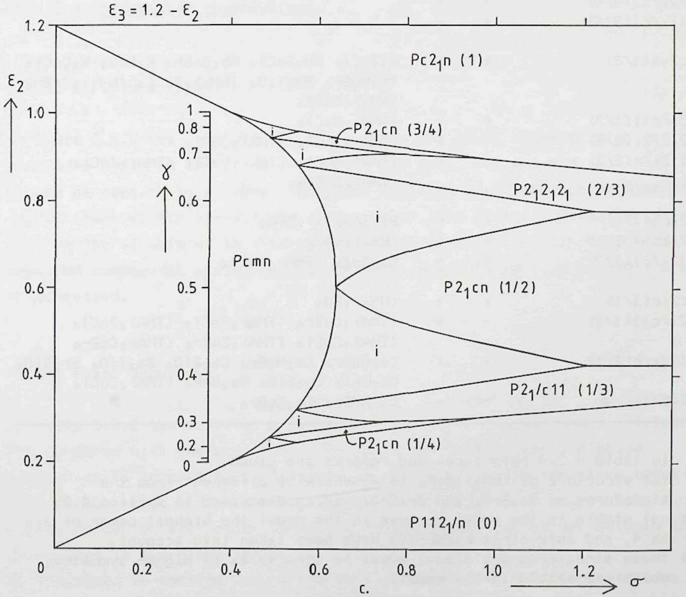

c.

Table 5.5.2. Comparison of observed phase sequences (in table 4.2.5 phase transition temperatures and references are given) with phase sequences possible in the model (m).

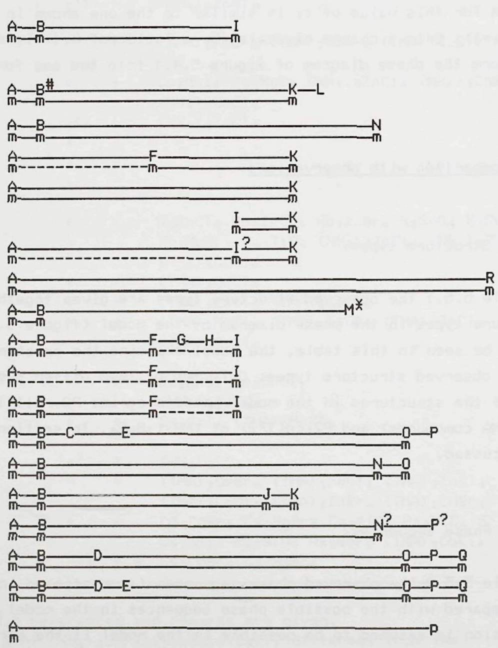

	Pcmn	incomm. $	$P2_12_12_1$ (4/7)	$Pc2_1n$ (3/5)	incomm. $	$P2_1cn$ (1/4)	P1c1 (1/4)	? (2/7)	$Pc2_1n$ (1/3)	$P2_1/c11$ (1/3)	$P112_1/n$ (0/1)	$P\bar{1}$ (0/1)	$P2_1cn$ (1/2)	$P12_1/c1$ (1/2)	$P112_1/n$ (2/3)	$P2_1/c11$ (1/1)	$P2_12_12_1$ (2/3)	$Pc2_1n$ (1/1)
	A	B	C	D	E	F	G	H	I	J	K	L	M	N	O	P	Q	R
K_2ZnCl_4 Rb_2ZnCl_4 Rb_2ZnBr_4 K_2SeO_4	A m	B m							I m									
Cs_2HgBr_4 Cs_2CdBr_4	A m	B# m									K m	L						
Cs_2FeI_4	A m	B m												N m				
Cs_2MnI_4	A m					F m					K m							
Sr_2SiO_4	A m										K m							
Ba_2TiO_4									I m		K m							
Ca_2SiO_4	A m								I? m		K m							
$(NH_4)_2SO_4$	A m																	R m
$(NH_4)_2BeF_4$	A m	B m											M*					
$(NH_4)_2ZnCl_4$	A m	B m				F m	G	H	I m									
$(NH_4)_2CoCl_4$	A m					F m			I m									
$(NH_4)_2ZnBr_4$	A m	B m				F m			I m									
$(TMA)_2FeCl_4$	A m	B m	C		E										O m	P		
$(TMA)_2MnCl_4$	A m	B m												N m	O m			
$(TMA)_2CuCl_4$	A m	B m								J m	K m							
$(TMA)_2NiCl_4$	A m	B m												N? m		P?		
$(TMA)_2ZnCl_4$	A m	B m		D											O m	P	Q m	
$(TMA)_2CoCl_4$	A m	B m		D	E										O m	P	Q m	
$(TMA)_2ZnBr_4$ $(TMA)_2CoBr_4$	A m															P		

$ The symmetry of the incommensurate structures is Pcmn(00γ)(ss1̄), except in one case.

The symmetry of the observed structures is $P112_1/n(00\gamma)(11\bar{1}/\bar{1})$.

? For this phases only the supercell size has been reported.

* This structure differs from the model structure $P2_1cn(1/2)$.

higher σ corresponds to a lower temperature. Therefore, compounds are expected to follow trajectories approximately parallel to the σ axis in the model phase diagram if their temperature is varied.
In table 5.5.2, for each compound mentioned in table 4.2.5 the observed phase sequence is given together with the most appropriate possible phase sequence in the model.

If the phases with structure types which cannot be stable in the model are disregarded, then the observed phase sequences for 19 of the 24 compounds can be explained by the model. In the remaining five compounds, phase transitions occur between structure types which border on each other at a line in the model phase diagram. Such a transition (indicated by a dashed line in table 5.5.2) *corresponds to a trajectory* in the model phase diagram (figure 5.4.1) going through this line of contact. It would be a coincidence if a compound would follow such a trajectory.

The unexplained phase transitions (indicated by dashed lines in table 5.5.2) are of two types. The first type is the phase transition between phases with structure types $P2_1cn(1/4)$ and $Pc2_1n(1/3)$ respectively. This transition type occurs in $(NH_4)_2CoCl_4$, $(NH_4)_2ZnBr_4$ and $(NH_4)_2ZnCl_4$. It might be that in these compounds an intermediate phase exists which has been overlooked, but no other indications exist for this assumption.
The second type is between the high temperature phase with space group Pcmn and a 4-fold or 3-fold superstructure. Such a phase transition is observed in Cs_2MnI_4, Ca_2SiO_4 and in $(NH_4)_2CoCl_4$. It might very well be that in these compounds an incommensurate phase has been overlooked. The observed phase sequences would match the model if an incommensurate phase would be added between the normal phase and the superstructure phase. In other words: the model predicts an incommensurate phase in these compounds. This conclusion is supported by the fact that in other models with competing interactions (e.g. Janssen and Tjon, 1981, 1982, 1983) the normal high temperature structure and a 4-fold or 3-fold superstructure are also separated by an incommensurate phase.

The model phase diagram suggests the existence of other phases and phase transitions, which have not been observed until now. Ba_2TiO_4 might show phase transitions from the 3-fold superstructure to an incommensurate structure and from the incommensurate structure to a normal structure on heating, just like e.g. K_2ZnCl_4.
For Ba_2SnS_4 and Sr_2CrO_4 only the room temperature structure has been

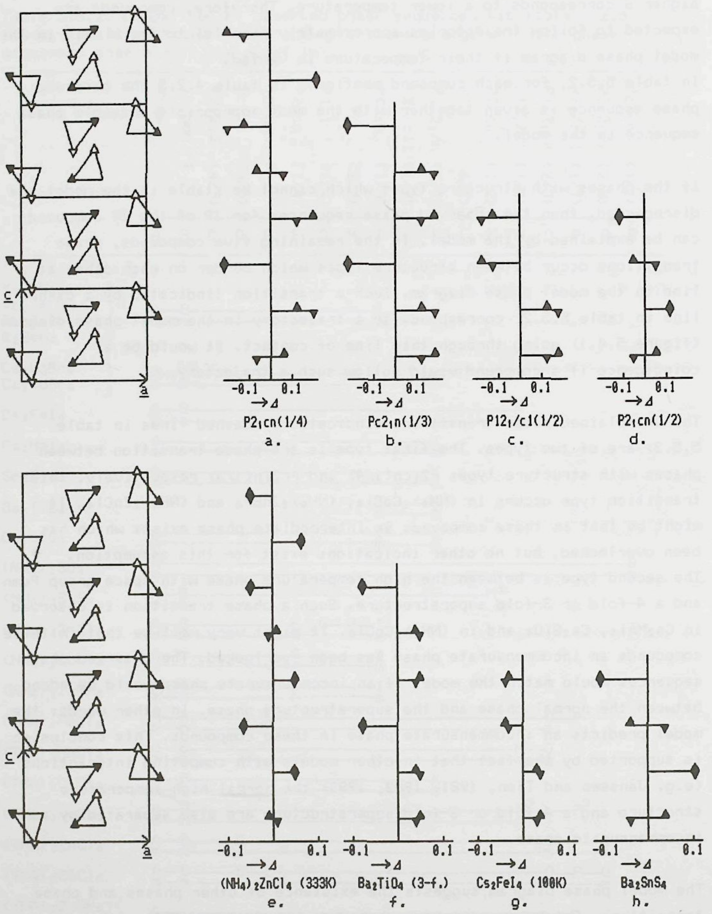

Figure 5.5.1. Examples of X_2 displacements (Δ) in the model for:
a. $\varepsilon_1=1$, $\varepsilon_2=0.25$, $\varepsilon_3=0.95$, $\sigma=0.56$;
b. $\varepsilon_1=1$, $\varepsilon_2=0.14$, $\varepsilon_3=0.2$, $\sigma=0.35$;
c. $\varepsilon_1=1$, $\varepsilon_2=0.16$, $\varepsilon_3=0.2$, $\sigma=0.3$;
d. $\varepsilon_1=1$, $\varepsilon_2=0.6$, $\varepsilon_3=0.6$, $\sigma=0.66$;
e-h. actual displacements, from figure 4.4.4.

reported (table 4.2.4). According to the model these compounds might show phase transitions from the room temperature phase to an incommensurate phase and from this phase to a normal phase.

5.5.3. X_2 displacements.

The X_2 displacements calculated in the model for several values of σ, ε_2 and ε_3 ($\varepsilon_1=1$) will be compared with the observed X_2 displacements, as discussed in section 4.4.
For incommensurate structures with space group Pcmn(00γ)(ss$\bar{1}$) the values of γ, φ and A of the model can be compared with those of actual crystal structures. For a certain value of γ and φ, A can always be adapted in the model to match the observed amplitude of the modulation function of the X_2 atoms in a real crystal structure. This can be achieved in two manners. The first one is multiplying the coefficients σ, ε_1, ε_2 and ε_3 by a suitable factor. The other manner is changing σ only, as can be seen in equation 5.4.14.
For a certain value of γ, φ can have each value between 0 and $\gamma/4$ for suitable choices of ε_1, ε_2 and ε_3. This can be derived from equations 5.4.12 and 5.4.13 in the following way. From equation 5.4.12 it follows that

$$\varepsilon_2 = \frac{\varepsilon_1\varepsilon_3}{\varepsilon_1+4\varepsilon_3\cos\pi\gamma} . \qquad (5.5.1)$$

Substitution of this in 5.4.13 gives

$$\varphi = \frac{1}{4\pi}\arctan\left(\frac{2\sin\pi\gamma}{\varepsilon_1/\varepsilon_3+2\cos\pi\gamma}\right) . \qquad (5.5.2)$$

From this equation it follows that for each γ between 0 and 0.5, φ can get each value between 0 and $\gamma/4$ by choosing a suitable ratio $\varepsilon_1/\varepsilon_3$.
For the room temperature structure of Rb_2ZnBr_4 and the structure of K_2SeO_4 at 113K the observed values of φ are 0.018 and -0.007 respectively, while $\gamma \approx 0.3$ for both structures. For Rb_2ZnBr_4, the value of φ can be realized in the model for suitable choices of ε_1, ε_2 and ε_3. But for K_2SeO_4 this is not possible. *The model value of φ can only be quite close to the negative* value of this compound by choosing the ratio $\varepsilon_1/\varepsilon_3$ large. Then φ gets a positive value close to zero.

The X_2 displacements of observed 1-fold superstructures with symmetry Pc2₁n or $P112_1/n$ can always be found in the model by choosing the parameters ε_2, ε_3 and σ properly, as can be seen in equations 5.4.15 and 5.4.18 respectively.

Because for 2-fold, 3-fold and 4-fold superstructures no analytical expressions are available for the amplitudes and phases of the modulation functions, numerical results will be compared with the observations. In figure 5.5.1 for some sets of values of ε_2, ε_3 and σ ($\varepsilon_1=1$), the X_2 displacements of the stable structure in the model are shown. These sets of *values are chosen such that the X_2 displacements resemble the observed ones* (figure 4.4.4). Of course, the values of the model X_2 displacements can be scaled to the observed ones by multiplication of the coefficients ε_1, ε_2, ε_3 and σ by a suitable factor.

As can be seen by comparing figure 5.5.1a-d with figure 4.4.4 (part of which has been reproduced in figure 5.5.1e-f), the resemblence is quite good.

5.6. Discussion.

From the results of the previous sections of this chapter, it can be concluded that

1. the model can explain most of the observations. No other model is known which explains as much as this one;
2. the interactions in the model are clearly present in the real crystal structures. Except for the complicated lattice dynamical model of Haque and Hardy (1980), no model has such realistic interactions as this one;
3. the model is a very simple one: the subcell containes only 4 atoms, which can displace only parallel to $\underline{b}$; only three types of interactions exist. The number of atoms cannot be smaller, because in that case the model crystal could not adopt all important space groups. Also the number of interactions cannot be smaller. If one of the interactions would be taken out of the model, the frustration would be gone;

With regard to point 1 the following can be remarked. As mentioned in section 5.5, only two deficiencies of the model are not readily explained: first the incapability to explain the existence of the 1-fold $P2_1/c11$ structure, (which appears in part of the TMA compounds) and the 2-fold superstructure of $(NH_4)_2BeF_4$; second, the incapability to explain the phase transition between the structure types $Pc2_1n(1/3)$ and $P2_1cn(1/4)$, occurring in part of the NH_4 compounds.

In connection with these deficiencies, two comments can be made. In the first place the A ions are not single atoms in these compounds, but NH_4 or $N(CH_3)_4$ groups. These ions cannot always be regarded as spheres, and will have preferential contact regions for the X atoms because of the charge *distribution on the positive ions and because of the shape of the groups.* The interatomic interactions will be different in both cases. This could be the cause of both types of deficiencies.

Secondly the approximation, made in section 5.3, viz. that the X-X distances in the tetrahedra as well as the shortest X-X distances between tetrahedra (e.g. distance type g) are equal to b/2, is not valid for $(NH_4)_2BeF_4$ and the TMA-compounds. In table 5.6.1 it can be seen that the inter-tetrahedra X-X distances are much larger than the intra-tetahedron ones for these compounds and for $(NH_4)_2SO_4$, while the two types of X-X distances are about equal for the other compounds. This shows that the former structures differ from the latter ones in this aspect. The interatomic interactions in the first group of compounds can be expected to differ from those in the other group. This could be the reason why the existence of the two structure types cannot be explained by the model.

Apart from the slight deficiencies, the model explains all observations for the structures discussed in this thesis. On the basis of the results of the model calculations, it can be concluded that the modulation in distorted β-K_2SO_4 type crystal structures is probably caused by the competing interactions discussed in section 5.3. As is shown in that section, all the interactions of the model are present in real crystal structures, whereas the correlations between X_2 displacements of neighbouring tetrahedra, as discussed in section 4.4 and in section 5.3, indicate that these interactions are important ones.

The model explains many things with regard to the distorted β-K_2SO_4 type crystal structures:

- the existence of incommensurate structures with modulation wave vectors from $\underline{0}$ to $\underline{c}^*$;
- the normal-to-incommensurate phase transition;
- the existence of many different superstructure types: four different

Table 5.6.1. Comparison of X-X distances intra BX_4 with X-X distance g (between tetrahedra).
av is the average X-X distance intra BX_4. g is the average of the distances of type g (as given in figure 4.4.2).

compound	temp. [K]	av [Å]	g [Å]	g/av	references
K_2ZnCl_4	r.t.	3.68	3.82	1.04	Mikhail and Peters (1979)
Rb_2ZnCl_4	100	3.69	3.72	1.01	Quilichini and Pannetier (1983)
Rb_2ZnBr_4	r.t.	3.88	3.84	0.99	this thesis
Cs_2CdBr_4	195	4.17	3.86	0.93	Altermatt et al. (1984)
Cs_2HgBr_4	200	4.19	3.81	0.91	Altermatt et al. (1984)
Cs_2FeI_4	100	4.28	4.07	0.95	Zandbergen (1981)
K_2SeO_4	113	2.69	3.34	1.24	Yamada and Ikeda (198)
Sr_2SiO_4	r.t.	2.67	3.05	1.14	Catti et al. (1983)
Ba_2TiO_4	r.t.	2.92	3.24	1.11	Wu and Brown (1973)
Ca_2SiO_4	r.t.	2.66	2.99	1.12	Jost et al. (1977)
$(NH_4)_2SO_4$	180	2.41	3.65	1.51	Schlemper and Hamilton (1966)
$(NH_4)_2BeF_4$	153	2.53	3.39	1.34	Misyul et al. (1980)
$(NH_4)_2ZnCl_4$	r.t.	3.68	3.72	1.01	Van Koningsveld (1983)
$(TMA)_2FeCl_4$	r.t.	3.74	5.25	1.40	Lauher and Ibers (1975)
$(TMA)_2NiCl_4$	r.t.	3.65	5.28	1.45	Wiesner et al. (1967)
$(TMA)_2ZnCl_4$	r.t.	3.67	5.32	1.45	Wiesner et al. (1967)
$(TMA)_2CoCl_4$	r.t.	3.67	5.28	1.44	Wiesner et al. (1967)
$(TMA)_2ZnBr_4$	r.t.	3.91	5.31	1.36	Trouelan et al. (1984)

4-fold-, four different 3-fold-, two different 2-fold- and two different 1-fold superstructure types.
If the shape of the double well potential would have been chosen in *another way* (e.g. $\Delta^8-\sigma\Delta^4$ instead of $\Delta^4-\sigma\Delta^2$) and/or higher harmonics were allowed in the modulation functions, then also larger superstructures would probably exist in the model.

- lock-in phase transitions to each of these superstructures;
- phase transitions between different superstructure types;
- phase transitions from the normal structure to each of the 1-fold superstructures directly, without an intermediate incommensurate phase;
- re-entering incommensurate phases. E.g. phase sequence normal - incommensurate ($\gamma<1/4$) - $P2_1cn(1/4)$ - incommensurate ($\gamma>1/4$). This phase sequence has not been observed, but two incommensurate phases with a 7-fold or a 5-fold superstructure phase in between have been observed in $(TMA)_2FeCl_4$ and $(TMA)_2CoCl_4$ respectively (table 4.2.5).

The two 1-fold superstructure types mentioned in the sixth point above are two extremes. As can be seen in section 5.4, $Pc2_1n(1)$ is stable for $\varepsilon_2 \gg \varepsilon_3$ and $P112_1/n(0)$ is stable for $\varepsilon_2 \ll \varepsilon_3$. The X_2 displacements of half of the tetrahedra in the latter structure type are opposite to those of the former. In $Pc2_1n(1)$ the interactions with ε_1 and ε_2 clearly have won the competition, while in the other structure type the interactions with ε_1 and ε_3 have won. The fact that the two different structures can both appear as a low temperature phase of the same high temperature stucture type, is thus explained by the presence of competing interactions.
Turning this argument around leads us to the following conjecture: if for a certain structure type two or more quite different low temperature structures have been observed (e.g. in different compounds) with the same kind of local distortions (e.g. rotation of a group of atoms around a certain axis), then competing interactions are present in structures of that type. This set of competing interactions can also cause incommensurate structures (e.g. in another compound) to occur for a *suitable balance of* the interactions.

Appendix A

CENTERING TRANSLATIONS IN SUPERSTRUCTURES.

In this appendix, which belongs to section 2.2, the largest common divisor of integers i_1, i_2, ... i_n will be denoted as LCD(i_1,i_2, ... i_n) and the smallest common multiple of these integers as SCM(i_1,i_2, ... i_n). The symbols u_i, v_i, e_{ki}, v, w and g denote integers as defined in section 2.2. In this appendix the index a (to denote the atom to which a quantity belongs) is omitted.

The following theorems, which are used in section 2.2, will be proved in this appendix. They refer to the superstructure described above equation 2.2.15.

Theorem 1: The dot-product of a subcell translation vector $\underline{e}_k$ and the modulation wave vector $\underline{g}$ can be written as

$$\underline{e}_k . \underline{g} = r/w \pmod 1 \quad (r=0,1,2, \ldots w-1) \quad , \qquad (A.1)$$

with $w = \mathrm{SCM}(v_1,v_2,v_3)$, (A.2)

and every value of r in A.1 occurs exactly g times, with

$$g = v/w \quad , \qquad (A.3)$$

if k runs from 1 to v (then $\underline{e}_k$ runs through all subcell translations in the supercell).

Theorem 2: Among the reflections given by equation 2.2.7, those which cannot be written as in 2.2.14, are systematically absent.

Before the proof of the above mentioned theorems will be started, the following theorem will be proved.

Theorem 3: For each set of integers I_1, I_2, ... I_n, N ($n \geq 2$) there is a set of integers i_1, i_2, ... i_n fulfilling

$$i_1I_1+i_2I_2+ \dots +i_nI_n = N \qquad (A.4)$$

$$\text{if} \quad \mathrm{LCD}(I_1,I_2, \dots I_n) = 1 \, . \qquad (A.5)$$

Proof of theorem 3:

For n=2 theorem 3 is an elementary theorem of the theory of numbers (see e.g. Deas, 1960). For n>2 theorem 3 can be derived from theorem 3 for n-1: If we put

$$J = \mathrm{LCD}(I_1,I_2, \dots I_{n-1}) \, , \qquad (A.6)$$

then, according to A.5

$$\mathrm{LCD}(J,I_n) = \mathrm{LCD}(\mathrm{LCD}(I_1,I_2, \dots I_{n-1}),I_n) =$$

$$= \mathrm{LCD}(I_1,I_2, \dots I_n) = 1 \, . \qquad (A.7)$$

According to theorem 3 for n=2, there is always a set of integers j,i_n fulfilling

$$jJ + iI_n = N \, . \qquad (A.8)$$

According to theorem 3 for n-1, there is always a set of integers $i_1,i_2,i_3, \dots i_{n-1}$ fulfilling

$$j = i_1\frac{I_1}{J} + i_2\frac{I_2}{J} + \dots + i_{n-1}\frac{I_{n-1}}{J} \qquad (A.9)$$

because (see A.6)

$$\mathrm{LCD}(\frac{I_1}{J} , \frac{I_2}{J} , \dots \frac{I_{n-1}}{J}) = 1 \, . \qquad (A.10)$$

Substituting A.9 into A.8 gives A.4.
Hence there is always a set of integers $i_1,i_2, \dots i_n$ fulfilling A.4 under condition A.5.

Proof of theorem 1:

According to equations 2.2.9 and 2.2.12 the dot-product in A.1 can be written as

$$\underline{e}_k.\underline{g} = \left[\sum_{i=1}^{3} e_{ki}\underline{a}_i\right] \cdot \left[\sum_{i=1}^{3} \frac{u_i}{v_i}\, \underline{a}_i{}^*\right] = \sum_{i=1}^{3} \frac{e_{ki}u_i}{v_i} = p/w \qquad (A.11)$$

with w given by A.2 and p integer.

Because always

$$p/w = r/w \pmod 1 \quad (r=0,1,2, \dots w-1) \, , \qquad (A.12)$$

$\underline{e}_k.\underline{g}$ can be written as in A.1.
If k runs from 1 to v, then the set e_{k1},e_{k2},e_{k3} runs through all possible combinations with (see 2.2.9)

$$0 \leq e_{ki} \leq v_i-1 \quad (i=1,2,3) \, . \qquad (A.13)$$

From A.1 it follows that

$$w\underline{e}_k.\underline{g} + ws = r \quad (s \text{ integer}) \, , \qquad (A.14)$$

or, written out:

$$e_{k1} \frac{u_1v_2v_3}{g} + e_{k2} \frac{u_2v_1v_3}{g} + e_{k3} \frac{u_3v_1v_2}{g} + sw = r \quad . \qquad (A.15)$$

with g given by A.3.
If

$$\mathrm{LCD}(\frac{u_1v_2v_3}{g} , \frac{u_2v_1v_3}{g} , \frac{u_3v_1v_2}{g} , w) = 1 \, , \qquad (A.16)$$

it can be concluded, using theorem 3 with n=4, that for each r there is a set of integers e_{k1},e_{k2},e_{k3},s which fulfils A.15. If the set x_1,x_2,x_3,s' is a solution of A.15, then suitable integers p_i (i=1,2,3) can be found such that

$$\begin{aligned} e_{k1} &= x_1+p_1v_1 \\ e_{k2} &= x_2+p_2v_2 \\ e_{k3} &= x_3+p_3v_3 \\ s &= s'-p_1u_1-p_2u_2-p_3u_3 \quad (p_i\text{: arbitrary integers}) \, , \end{aligned} \qquad (A.17)$$

satisfies both A.15 and A.13, as can be checked by substitution of A.17 in A.15.

From this it follows that for each r there is at least one vector $\underline{e}_k$ that fulfils A.1.
All vectors $\underline{e}_k$ for which r=0 are translation vectors (including $\underline{0}$) in the superstructure because, if we call these vectors $\underline{e}_c$,

$$\underline{e}_c.\underline{g} = 0 \pmod 1 \tag{A.18}$$

and hence for two position vectors $\underline{x}_1$ and $\underline{x}_2$ with

$$\underline{x}_2 = \underline{x}_1 + \underline{e}_c \ , \tag{A.19}$$

the arguments of the modulation functions are equal:

$$\underline{x}_2.\underline{g} = (\underline{x}_1+\underline{e}_c).\underline{g} = \underline{x}_1.\underline{g} + \underline{e}_c.\underline{g} = \underline{x}_1.\underline{g} \ . \tag{A.20}$$

Suppose there are g′ different vectors $\underline{e}_c$. Then each value of r occurs g′ times, because if it occurs for $\underline{e}_1$, then

$$\underline{e}_k = \underline{e}_1 + \underline{e}_c \tag{A.21}$$

gives the same value of r in A.1. Because the number of basic structure translation vectors $\underline{e}_k$ in the supercell is v, and w different values of r exist, we have g′=w/v=g: each value of r occurs exactly g times. This proves theorem 1 except for one point: A.16 must be proved.

A.16 is equivalent to

$$\mathrm{LCD}(u_1v_2v_3, u_2v_1v_3, u_3v_1v_2, v_1v_2v_3) = g \ . \tag{A.22}$$

According to the definition of u_i and v_i (see the text under equation 2.2.12):

$$\mathrm{LCD}(u_i, v_i) = 1 \quad (i=1,2,3) \ . \tag{A.23}$$

From this it follows that

$$\mathrm{LCD}(u_1v_2v_3, v_1v_2v_3) = v_2v_3 \ . \tag{A.24}$$

Hence the divisors of u_1 are not relevant in A.24. Because the left hand side of A.22 is a divisor of $\mathrm{LCD}(u_1v_2v_3, v_1v_2v_3)$, u_1 can be left out of it.

The same is true for u_2 and u_3. Hence in A.22 the factors u_1, u_2 and u_3 can be omitted giving

$$g = \mathrm{LCD}(v_2v_3, v_1v_3, v_1v_2, v_1v_2v_3) = \mathrm{LCD}(v_2v_3, v_1v_3, v_1v_2) \ . \tag{A.25}$$

Using only elementary rules for LCD and SCM, one gets

$$\begin{aligned} g &= \mathrm{LCD}(\mathrm{LCD}(v_2v_3, v_1v_3), v_1v_2) = \mathrm{LCD}(v_3\mathrm{LCD}(v_2,v_1), v_1v_2) = \\ &= \mathrm{LCD}(v_2,v_1).\mathrm{LCD}(v_3, v_1v_2/\mathrm{LCD}(v_1,v_2)) = \\ &= \mathrm{LCD}(v_2,v_1)\ \frac{v_3v_1v_2/\mathrm{LCD}(v_1,v_2)}{\mathrm{SCM}(v_3, v_1v_2/\mathrm{LCD}(v_1,v_2))} = \\ &= \frac{v_1v_2v_3}{\mathrm{SCM}(v_3, \mathrm{SCM}(v_1,v_2))} = \frac{v_1v_2v_3}{\mathrm{SCM}(v_1,v_2,v_3)} \ . \end{aligned} \tag{A.26}$$

According to A.2 and A.3 this is true, and hence A.16 is proved.

The proof of theorem 2:
This proof consists of three parts. First it will be proved that the centering translations do not cause one of the reflections given by 2.2.14 to be systematically absent. Next it will be proved that the number of satellite reflections given by 2.2.14 per main reflection is w-1. At the end it will be proved that the number of systematically present reflections is exactly the number of main reflections plus the number of satellite reflections given by 2.2.14. The rest of the reflections must be systematically absent then.

The first part:
Equation 2.2.15 can be written as

$$G(\underline{H}) = \exp(2\pi i\underline{H}.\underline{x}_0)\ \frac{1}{v} \sum_{K=1}^{v} \exp(2\pi i(\underline{H}.[\underline{e}_K+\underline{d}((\underline{x}_0+\underline{e}_K).\underline{g})]) \ , \tag{A.27}$$

with $\underline{H}$ given by 2.2.14.
Each of the subcell translation vectors $\underline{e}_K$ (K=1,2, ... v) can be written as

$$\underline{e}_K = \underline{e}_c + \underline{e}_r \quad (c=1,2, \ldots g \text{ and } r=1,2, \ldots w) \ , \tag{A.28}$$

where $\underline{e}_c$ is a centering translation and $\underline{e}_r$ is a basic structure translation vector with

$$\underline{e}_r.\underline{g} = r/w \pmod 1 \quad . \qquad (A.29)$$

Using A.28, the summation in A.27 can be written as

$$\sum_{r=1}^{w} (\exp(2\pi i\underline{H}.[\underline{e}_r+\underline{d}((\underline{x}_o+\underline{e}_r).\underline{g})]).\ \sum_{c=1}^{g} \exp(2\pi i\underline{H}.\underline{e}_c)) \qquad (A.30)$$

because (see A.18)

$$\underline{d}((\underline{x}_o+\underline{e}_r+\underline{e}_c).\underline{g}) = \underline{d}((\underline{x}_o+\underline{e}_r).\underline{g}) \quad . \qquad (A.31)$$

The second summation in A.30 gives the influence of the centering translations on the structure factor, and can be written as (using 2.2.14)

$$\sum_{c=1}^{g} (\exp(2\pi i\underline{h}.\underline{e}_c).\exp(2\pi im\underline{g}.\underline{e}_c)) \quad . \qquad (A.32)$$

Because $\underline{h}.\underline{e}_c$ and $m\underline{g}.\underline{e}_c$ are integer (see 1.1.6 , 2.2.9 and A.18), the result of this summation is g. Hence the centering translations do not cause systematic absences among the reflections given by 2.2.14.

The second part:
Because $\underline{g}$ is commensurate with the basic structure, there are values of m with m≠0 for which equation 2.2.1 represents main reflections. It can be verified, using 2.2.14, that each m given by m=nv (n integer) is such a value. In a superstructure with g>1, more such values for m exist. The number of satellite reflections of a main reflection is equal to m_1-1 if m_1 is the smallest value of m for which 2.2.14 represents a main reflection. m_1 represents a main reflection if the components of $m_1\underline{g}$ are multiples of $\underline{a}_1*$, $\underline{a}_2*$ and $\underline{a}_3*$.
$m_1\underline{g}$ can be written as (using 2.2.12)

$$m_1\underline{g} = m_1 \left(\frac{u_1}{v_1}\underline{a}_1* + \frac{u_2}{v_2}\underline{a}_2* + \frac{u_3}{v_3}\underline{a}_3* \right) \quad . \qquad (A.33)$$

In order to get integer multiples of the reciprocal basic structure vectors in A.33, m_1 must have divisors v_1, v_2 and v_3. Because of A.23 the smallest value of m for which 2.2.14 represents a main reflection is

$$m_1 = SCM(v_1,v_2,v_3) = w \quad . \qquad (A.34)$$

Hence the number of satellite reflections per main reflection is w-1.

The third part:
The volume V_s of the supercell is

$$V_s = vV \qquad (A.35)$$

if V is the volume of the subcell.
The volume V_s' of the primitive unit cell in the superstructure is

$$V_s' = V_s/g = Vv/g = wV \quad , \qquad (A.36)$$

since g centering translations (including $\underline{0}$) exist in the v-fold supercell.
The volume V_s*' of the cell spanned by the reciprocals of the primitive unit cell vectors is

$$V_s*' = 1/V_s' = 1/wV = V*/w \qquad (A.37)$$

if V* is the volume of the cell spanned by the reciprocals of the basic structure unit cell vectors.
Hence w reflections exist per main reflection. These must be the main reflection itself plus the w-1 satellites given by 2.2.14. The reflections not given by 2.2.14 are systematically absent because of the g centering translations. Theorem 2 has now been proved.

Appendix B

INCOMMENSURATE STRUCTURE WITH SYMMETRY $Pcmn(00\gamma)(ss\bar{1})$ IN THE MODEL.

This appendix belongs to section 5.4.

B.1. Energy expression.

For an incommensurate structure with symmetry $Pcmn(00\gamma)(ss\bar{1})$, the X_2-displacements Δ_{ik} in the model can be written as

$$\Delta_{1k} = A\cos 2\pi(k\gamma-\varphi+\Psi)\ , \qquad \text{(B.1.1)}$$

$$\Delta_{2k} = A\cos 2\pi((0.5+k)\gamma-\varphi+0.5+\Psi) \quad \text{(operation } c(s) \text{ on } \Delta_{1k}), \qquad \text{(B.1.2)}$$

$$\Delta_{3k} = A\cos 2\pi(k\gamma+\varphi+\Psi) \quad \text{(operation } n(\bar{1}) \text{ on } \Delta_{1k}), \qquad \text{(B.1.3)}$$

$$\Delta_{4k} = A\cos 2\pi((0.5+k)\gamma+\varphi+0.5+\Psi) \quad \text{(operation } 2_1(\bar{1}) \text{ on } \Delta_{1k}), \qquad \text{(B.1.4)}$$

in which A is the amplitude of the modulation functions, Ψ is the overall phase of the modulation wave, φ is the phase of the first modulation function, γ is the modulation wavevector component ($\underline{q}=\gamma\underline{c}^*$) and k is the subcell number. In Δ_{ik} i is the number of the tetrahedron in the subcell, as indicated in figure 5.2.1.
For an incommensurate structure the summation over all subcells in equation 5.2.1 can be replaced by an integration over Ψ between 0 and 1 for one subcell:

$$\lim_{N\to\infty} \frac{1}{2N+1} \sum_{k=-N}^{N} [\ \dots\ ] \quad \Rightarrow \quad \int_0^1 d\Psi [\ \dots\ ]_{k=0} \quad . \qquad \text{(B.1.5)}$$

This is possible because in a single subcell all possible subcell contents will be generated during the shifting of the modulation wave over one wavelength. The energy expression for the incommensurate structure is then:

$$F = \int_0^1 d\Psi \Big[\sum_{i=1}^{4} (\Delta_{i0}^4-\sigma\Delta_{i0}^2) + \varepsilon_1((\Delta_{10}-\Delta_{30})^2+(\Delta_{20}-\Delta_{40})^2) + $$
$$+ \varepsilon_2((\Delta_{10}-\Delta_{40})^2+(\Delta_{20}-\Delta_{31})^2) + \varepsilon_3((\Delta_{30}+\Delta_{20})^2+(\Delta_{40}+\Delta_{11})^2)\Big] \ . \qquad \text{(B.1.6)}$$

In the following the different kinds of terms in the integrand will be worked out successively.

After substitution of B.1.1 a term with σ in equation B.1.6 becomes

$$\int_0^1 \sigma \Delta_{io}^2 \, d\Psi = \sigma A^2/2 \quad (i=1,2,3,4) \; . \tag{B.1.7}$$

The second type of term to be worked out is the fourth order term. Using equation B.1.1 one gets by simple goniometry

$$\int_0^1 \Delta_{io}^4 \, d\Psi = 3A^4/8 \quad (i=1,2,3,4) \; . \tag{B.1.8}$$

In order to treat the other terms of equation B.1.6 together as one type of term, equations B.1.1 - B.1.4 are written as

$$\Delta_{ik} = A\cos(\alpha_{ik}+\Psi) \quad (i=1,2,3,4) \; . \tag{B.1.9}$$

The third type of term can be written as

$$\int_0^1 (\Delta_{ik}+s\Delta_{nm})^2 \, d\Psi \; , \tag{B.1.10}$$

in which s is +1 if it concerns a term with coefficient ε_3 and -1 if it concerns a term with coefficient ε_1 or ε_2.
Substituting B.1.9 into B.1.10 gives

$$\int_0^1 A^2[\cos 2\pi(\alpha_{ik}+\Psi)+s\cos 2\pi(\alpha_{nm}+\Psi)]^2 \, d\Psi =$$

$$= \int_0^1 A^2[\cos^2 2\pi(\alpha_{ik}+\Psi)+2s\cos 2\pi(\alpha_{ik}+\Psi)\cos 2\pi(\alpha_{nm}+\Psi)+\cos^2 2\pi(q_{nm}+\Psi)] \, d\Psi =$$

$$= \int_0^1 A^2[\cos 4\pi(\alpha_{ik}+\Psi)+1+2s\cos 2\pi(\alpha_{ik}+\alpha_{nm}+2\Psi)+$$

$$+2s\cos 2\pi(\alpha_{ik}-\alpha_{nm})+\cos 4\pi(\alpha_{nm}+\Psi)+1]/2 \, d\Psi =$$

$$= A^2[1+s\cos 2\pi(\alpha_{ik}-\alpha_{nm})] \; . \tag{B.1.11}$$

Using this result one can write out the terms in B.1.6 with coefficient ε_1:

$$\int_0^1 \varepsilon_1[(\Delta_{1o}-\Delta_{3o})^2-(\Delta_{2o}-\Delta_{4o})^2] =$$

$$= \varepsilon_1 A^2[2-\cos 2\pi(\alpha_{1o}-\alpha_{3o})-\cos(\alpha_{2o}-\alpha_{4o})] \; . \tag{B.1.12}$$

Substitution of the proper values of α_{ik} reduces the right hand side to

$$\varepsilon_1 A^2[2-\cos(-4\pi\varphi)-\cos(-4\pi\varphi)] = 2\varepsilon_1 A^2(1-\cos 4\pi\varphi) \; . \tag{B.1.13}$$

Analogously the terms in B.1.6 with coefficients ε_2 and ε_3 can be written respectively as

$$\int_0^1 \varepsilon_2[(\Delta_{1o}-\Delta_{4o})^2+(\Delta_{2o}-\Delta_{31})^2] = 2\varepsilon_2 A^2[1+\cos 2\pi(2\varphi+\gamma/2)] \tag{B.1.14}$$

and $$\int_0^1 \varepsilon_3[(\Delta_{3o}+\Delta_{2o})^2+(\Delta_{4o}+\Delta_{11})^2] = 2\varepsilon_3 A_2[1-\cos 2\pi(2\varphi-\gamma/2)] \; . \tag{B.1.15}$$

Substitution of B.1.7, B.1.8, B.1.13, B.1.14 and B.1.15 into B.1.6 gives

$$F = 3A^4/2 - 2\sigma A^2 + 2\varepsilon_1 A^2(1-\cos 4\pi\varphi) +$$

$$+ 2\varepsilon_2 A^2[1+\cos 2\pi(2\varphi+\gamma/2)] + 2\varepsilon_3 A^2[1-\cos 2\pi(2\varphi-\gamma/2)] =$$

$$= 3A^4/2 + 2A^2[\varepsilon_1 + \varepsilon_2 + \varepsilon_3 - \sigma - \varepsilon_1\cos 4\pi\varphi + \varepsilon_2\cos 2\pi(2\varphi+\gamma/2) -$$

$$- \varepsilon_3\cos 2\pi(2\varphi-\gamma/2)] \; . \tag{B.1.16}$$

This is the energy expresssion of the incommensurate structure with symmetry Pcmn(00γ)(ss$\bar{1}$) in the model, as mentioned in table 5.4.1.

B.2. Calculation of the minimum.

In this section the values of the parameters A, φ and γ for which the energy of the incommensurate structure in the model has its minimum will be calculated. First, the energy expression B.1.16 is rewritten to give

$$F = 3A^4/2 + 2A^2[\varepsilon_1 + \varepsilon_2 + \varepsilon_3 - \sigma - \varepsilon_1\cos 4\pi\varphi -$$

$$- (\varepsilon_3-\varepsilon_2)\cos 4\pi\varphi \cos\pi\gamma - (\varepsilon_3+\varepsilon_2)\sin 4\pi\varphi \sin\pi\gamma] \; . \tag{B.2.1}$$

As discussed in section 5.3, the coefficients ε_1, ε_2, ε_3 and σ are all positive. In the minimum the first derivatives of F with respect to A, φ and γ have to be zero. For φ this gives

$$\frac{\partial F}{\partial \varphi} = 8\pi A^2[\varepsilon_1 \sin 4\pi\varphi + (\varepsilon_3-\varepsilon_2)\ \sin 4\pi\varphi\ \cos\pi\gamma - (\varepsilon_3+\varepsilon_2)\ \cos 4\pi\varphi\ \sin\pi\gamma] = 0\ . \qquad (B.2.2)$$

For nonzero A and for $0<\gamma<1$ this gives

$$\frac{\cos 4\pi\varphi}{\sin 4\pi\varphi} = \frac{\varepsilon_1+(\varepsilon_3-\varepsilon_2)\cos\pi\gamma}{(\varepsilon_3+\varepsilon_2)\sin\pi\gamma}\ . \qquad (B.2.3)$$

Putting the first derivative of F with respect to γ equal to zero gives

$$\frac{\partial F}{\partial \gamma} = 2\pi A^2[(\varepsilon_3-\varepsilon_2)\ \cos 4\pi\varphi\ \sin\pi\gamma - (\varepsilon_3+\varepsilon_2)\ \sin 4\pi\varphi\ \cos\pi\gamma] = 0\ . \qquad (B.2.4)$$

For nonzero A and $0<\gamma<1$ (excluding the commensurate values 0 and 1) this is equivalent to

$$\frac{\cos\pi\gamma}{\sin\pi\gamma} = \frac{(\varepsilon_3-\varepsilon_2)\cos 4\pi\varphi}{(\varepsilon_3+\varepsilon_2)\sin 4\pi\varphi}\ . \qquad (B.2.5)$$

Substitution of B.2.3 into B.2.5 gives, after reworking:

$$\cos\pi\gamma = \frac{\varepsilon_1(\varepsilon_3-\varepsilon_2)}{4\varepsilon_3\varepsilon_2}\ . \qquad (B.2.6)$$

This equation only has a solution if (taken into account the exclusion of the commensurate values 0 and 1 for γ, see equation B.2.5)

$$-1 < \frac{\varepsilon_1(\varepsilon_3-\varepsilon_2)}{4\varepsilon_3\varepsilon_2} < 1\ . \qquad (B.2.7)$$

If as a solution

$$\gamma = \frac{1}{\pi}\arccos\left(\frac{\varepsilon_1(\varepsilon_3-\varepsilon_2)}{4\varepsilon_3\varepsilon_2}\right) \qquad (B.2.8)$$

is chosen, then γ covers the range $0<\gamma<1$ for suitable choices of ε_1, ε_2 and ε_3. All other solutions of B.2.6 (excluding 0 and 1) give modulation wave vectors $\underline{g}=\gamma\underline{c}^*$ which are equivalent (differing an integer multiple of $\underline{c}^*$ in length) to those given by B.2.8.

In equation B.2.3 γ can be eliminated by substituting B.2.6 in it. After reworking one gets

$$\tan 4\pi\varphi = \frac{\sqrt{16\varepsilon_3^2\varepsilon_2^2-\varepsilon_1^2(\varepsilon_3-\varepsilon_2)^2}}{\varepsilon_1(\varepsilon_3+\varepsilon_2)}\ . \qquad (B.2.9)$$

The square root is real if condition B.2.7 is fulfilled. From equation B.2.9 it follows that

$$\varphi = \frac{1}{4\pi}\arctan\left(\frac{\sqrt{16\varepsilon_3^2\varepsilon_2^2-\varepsilon_1^2(\varepsilon_3-\varepsilon_2)^2}}{\varepsilon_1(\varepsilon_3+\varepsilon_2)}\right) + \frac{n}{4} \quad (n \text{ integer}). \qquad (B.2.10)$$

In order to know for which values of n φ gives a minimum of F, the second order derivative has to be investigated:

$$\frac{\partial^2 F}{\partial \varphi^2} = 32\pi^2A^2[\varepsilon_1\cos 4\pi\varphi + (\varepsilon_3-\varepsilon_2)\ \cos 4\pi\varphi\ \cos\pi\gamma + (\varepsilon_3+\varepsilon_2)\ \sin 4\pi\varphi\ \sin\pi\gamma]\ . \qquad (B.2.11)$$

Substitution of B.2.6 gives

$$\frac{\partial^2 F}{\partial \varphi^2} = 32\pi^2A^2\left[\left(\varepsilon_1+\frac{\varepsilon_1(\varepsilon_3-\varepsilon_2)^2}{4\varepsilon_3\varepsilon_2}\right)\cos 4\pi\varphi + \frac{(\varepsilon_3+\varepsilon_2)\sqrt{16\varepsilon_3^2\varepsilon_2^2-\varepsilon_1^2(\varepsilon_3-\varepsilon_2)^2}}{4\varepsilon_3\varepsilon_2}\sin 4\pi\varphi\right]\ . \qquad (B.2.12)$$

Because according to equation B.2.9 and B.2.7 $\tan 4\pi\varphi$ is larger than 0, $\cos 4\pi\varphi$ and $\sin 4\pi\varphi$ are both positive or both negative. In the first case the second derivative (B.2.12) is positive, because the coefficients of $\cos 4\pi\varphi$ and $\sin 4\pi\varphi$ in B.2.12 are positive (because ε_1, ε_2 and ε_3 are positive). In the second case the second derivative is negative. Only the first case is compatible with a minimum. Hence n in equation B.2.10 has to be even.
For n=0 in equation B.2.10, the value of φ is between 0 and 1/8. For n=2 it is between 1/2 and 5/8. It can be checked in equations B.1.1 - B.1.4 that the resulting crystal structure is the same as for n=0 (differing only 0.5 in overall phase). Hence, the solution of B.2.9 can be limited to B.2.10 with n=0.

It can be checked that

$$\frac{\partial^2 F}{\partial \gamma^2} > 0 \qquad (B.2.13)$$

for γ and φ given by B.2.8 and B.2.10 (with n=0) respectively, as should be in a minimum.

The first derivative of F with respect to A is equal to

$$\frac{\partial F}{\partial A} = 6A^3 + 4A[\varepsilon_1 + \varepsilon_2 + \varepsilon_3 - \sigma - \varepsilon_1\cos 4\pi\varphi - (\varepsilon_3-\varepsilon_2)\cos 4\pi\varphi\ \cos\pi\gamma - (\varepsilon_3+\varepsilon_2)\sin 4\pi\varphi\ \sin\pi\gamma]\ . \qquad (B.2.14)$$

Putting this first derivative equal to zero and substitution of γ and φ from B.2.8 and B.2.10 (with n=0) gives

$$A[6A^2+4(\sigma_0-\sigma)] = 0 \qquad \text{(B.2.15)}$$

with $$\sigma_0 = \varepsilon_1 + \varepsilon_2 + \varepsilon_3 - \frac{(\varepsilon_2+\varepsilon_3)\sqrt{\varepsilon_1{}^2+4\varepsilon_2\varepsilon_3}}{2\sqrt{\varepsilon_2\varepsilon_3}} \quad . \qquad \text{(B.2.16)}$$

The solutions of B.2.15 are

$$A = 0 \qquad \text{(B.2.17)}$$

and $$A^2 = 2(\sigma-\sigma_0)/3 \quad . \qquad \text{(B.2.18)}$$

The second order derivative $\partial^2F/\partial A^2$ is equal to

$$\frac{\partial^2 F}{\partial A^2} = 18A^2 - 4(\sigma-\sigma_0) \quad . \qquad \text{(B.2.19)}$$

Accordingly, solution B.2.17 gives a minimum if $\sigma-\sigma_0 \leqslant 0$. The other solution (B.2.18) gives a minimum if $\sigma-\sigma_0 > 0$. Hence if

$$\sigma-\sigma_0 > 0 \quad , \qquad \text{(B.2.20)}$$

then the amplitude of the modulation is nonzero, and if this condition is not fulfilled, the amplitude is zero. In the first case the amplitude A is equal to

$$A = \pm\sqrt{2(\sigma-\sigma_0)/3} \quad . \qquad \text{(B.2.21)}$$

The two signs give crystal structures that are mirror images of each other with respect to the a,c plane. Hence, only the plus sign needs to be considered.

Concluding: we have found that the energy expression B.2.1 has a minimum for γ, φ and A given by B.2.8, B.2.10 (with n=0) and B.2.21 if conditions B.2.7 and B.2.20 are fulfilled (it has been checked numerically that for these values of γ, φ and A F has a minimum, and not e.g. a saddle point). The energy at the minimum is equal to

$$F = -2(\sigma-\sigma_0)^2 \quad , \qquad \text{(B.2.22)}$$

as can be verified by substituting B.2.8, B.2.10 and B.2.21 into B.2.1. Outside the region in $\varepsilon_1,\varepsilon_2,\varepsilon_3,\sigma$ space determined by conditions B.2.7 and B.2.20 the incommensurate structure cannot be the stable crystal structure in the model.

SUMMARY

This thesis concerns about 60 distorted β-K_2SO_4 type crystal structures. These structures are mainly incommensurately or commensurately modulated with a β-K_2SO_4 type basic structure. They occur in Rb_2ZnBr_4 and in many other compounds with the general chemical formula A_2BX_4.
After transformation to equivalent bases all known structures of the mentioned type are compared in detail. The comparison reveals a remarkable equivalence of the modulation wave functions among all structures reported in literature.
Detailed structural information from literature, supplemented with original structure determinations of Rb_2ZnBr_4 phases, leads to an ionic interaction model. This model explains and predicts the stability and phase sequence of the different distorted β-K_2SO_4 type structures fairly well.

In chapter 2 a new computer program, which has been used for the structure determinations, is described. It can handle superstructures as well as incommensurate structures.

Chapter 3 describes structure determinations of three different phases of Rb_2ZnBr_4. Two determinations are based on single crystal X-ray diffraction, the third one uses single crystal neutron diffraction. The phase at room temperature is the so-called incommensurate phase, the other two are 3-fold superstructures.
The results show that the modulations in the three phases are strikingly similar. For the room temperature phase the fact that the modulation wave vector is a constant fraction of $\underline{c}^*$ in a large temperature range suggests a superstructure. However the four dimensional space group $Pcmn(00\gamma)(ss\bar{1})$ gives the best agreement.

In chapter 4 the symmetry, the interatomic distances, the atomic displacements with respect to Pcmn symmetry and the normalized modulation functions of the distorted β-K_2SO_4 type structures are compared. It turns out that these structures have symmetry or pseudo-symmetry properties all corresponding to those of the same "prototype" symmetry: $Pcmn(00\gamma)(ss\bar{1})$. It also turns out that all structures considered have the same local distortions with respect to the β-K_2SO_4 type structure. The main component of these distortions is a rotation of the BX_4 tetrahedra around an axis

parallel to the pseudo-hexagonal $\underline{c}$ axis.

In chapter 5 a microscopic model is developed, which reveals the origin of the modulation. In the model the distortions of a structure are expressed in terms of displacements of certain X atoms out of the mirror plane; this displacement is a direct consequence of the above-mentioned rotation. The model takes into account the interactions between different pairs of nearest neighbours. One of the four parameters of the model can be *interpreted as a measure of the temperature.* The choice of these interactions is based on common features of the crystal structures. By minimizing the ensuing expression for the potential energy, most of the observations can be explained, such as the occurrence of the various types of distorted β-K_2SO_4 type structures, including incommensurate structures and superstructures, and the phase transitions between the different types of structure.
According to the model the origin of the modulation in Rb_2ZnBr_4 and related compounds resides in the fact that the BX_4 tertrahedra cannot rotate independently. Their rotations are interrelated in more than one way. These interrelations have counteracting tendencies (there is "frustration"), and the actual structure is the result of a compromise between the counteracting tendencies. This compromise may be an incommensurately modulated structure, a superstructure, or a structure with the same unit cell as the β-K_2SO_4 type structure, depending on the temperature and the relative strengths of the interactions.

SAMENVATTING.

Dit proefschrift betreft ongeveer 60 vervormde β-K_2SO_4-type kristalstrukturen. Deze strukturen zijn veelal incommensurabel of commensurabel gemoduleerd met een β-K_2SO_4-type basisstruktuur. Ze komen voor in Rb_2ZnBr_4 en in veel andere verbindingen met de algemene chemische formule A_2BX_4.
Na transformatie naar equivalente bases worden alle bekende strukturen van het genoemde type in detail vergeleken. De vergelijking laat een opmerkelijke overeenkomst zien tussen de modulatiegolf-functies van alle in de literatuur gerapporteerde strukturen.
Uit gedetailleerde gegevens van strukturen uit de literatuur, aangevuld met nieuwe struktuurbepalingen van Rb_2ZnBr_4-fasen, wordt een interactiemodel afgeleid. Dit model verklaart en voorspelt de stabiliteit en fase-volgorde van de verschillende β-K_2SO_4-type strukturen goed.

Hoofdstuk 2 beschrijft een nieuw computerprogramma, dat gebruikt is voor de struktuurbepalingen. Het kan zowel superstrukturen als incommensurabele strukturen behandelen.

In hoofdstuk 3 worden de struktuurbepalingen van drie verschillende fasen van Rb_2ZnBr_4 beschreven. Twee bepalingen zijn gebaseerd op eenkristal rontgendiffraktie-metingen, de derde op eenkristal neutronendiffraktie-metingen. De fase bij kamertemperatuur is de zogenaamde incommensurabele fase, de beide andere zijn 3-voudige superstrukturen.
De resultaten laten zien dat de modulaties in de drie fasen opvallend gelijkvormig zijn. Het feit dat de modulatiegolfvektor een constante fractie van $\underline{c}^*$ is in een groot temperatuurgebied, suggereert dat de struktuur van de kamertemperatuurfase een superstruktuur is. Toch geeft de vierdimensionale ruimtegroep $Pcmn(00\gamma)(ss\bar{1})$ de beste overeenstemming met de metingen.

In hoofdstuk 4 worden de symmetrie, de interatomaire afstanden, de atoomverplaatsingen ten opzichte van Pcmn-symmetrie en de genormaliseerde modulatiefuncties van de vervormde β-K_2SO_4-type strukturen vergeleken. Het blijkt dat deze strukturen symmetrie- of pseudo-symmetrie eigenschappen hebben, die corresponderen met dezelfde "prototype"-symmetrie: $Pcmn(00\gamma)(ss\bar{1})$.
Het blijkt ook dat alle bekeken strukturen dezelfde lokale vervormingen ten

opzichte van de β-K_2SO_4-type struktuur hebben. De voornaamste component van deze vervormingen is een rotatie van de BX_4-tetraeders rond een as evenwijdig aan de pseudo-hexagonale $\underline{c}$-as.

In hoofdstuk 5 wordt een microscopisch model ontwikkeld, dat de oorzaak van de modulatie aangeeft. In het model worden de vervormingen van de struktuur uitgedrukt in termen van verplaatsingen van bepaalde X-atomen uit het spiegelvlak. *Deze verplaatsing is een direct gevolg van de bovengenoemde* rotatie. Het model houdt rekening met interacties tussen verschillende paren van naaste buren. Een van de vier parameters van het model kan opgevat worden als een maat voor de temperatuur. De keuze van de interacties is gebaseerd op gemeenschappelijke kenmerken van de kristalstrukturen. Door de uitdrukking van potentiele energie die uit het model volgt te minimaliseren, kunnen de meeste waarnemingen verklaard worden, zoals het voorkomen van de diverse soorten vervormde β-K_2SO_4-type strukturen, inclusief incommensurabele strukturen en superstrukturen, en de fase-overgangen tussen de diverse struktuurtypen.
Volgens het model berust de oorsprong van de modulatie in Rb_2ZnBr_4 en verwante verbindingen op het feit dat de BX_4-tetraeders niet onafhankelijk kunnen roteren. Hun rotaties zijn gekoppeld op meer dan een manier. Deze *koppelingen werken elkaar tegen (er is "frustratie"), en de werkelijke* struktuur is het resultaat van een compromis tussen de elkaar tegenwerkende koppelingen. Dit compromis kan een incommensurabele struktuur zijn, een superstruktuur, of een struktuur met dezelfde eenheidscel als de β-K_2SO_4-type struktuur, afhankelijk van de temperatuur en de relatieve sterkte van de interakties.

LIST OF SYMBOLS

The units of the quantities represented by the symbols are given between square brackets. The position in the text where a symbol is defined or has been used for the first time, is given between braces. If a symbol is used only *in part ot the thesis, this part is indicated between triangular* brackets.

a, b, c [Å]	the lengths of $\underline{a}$, $\underline{b}$ and $\underline{c}$
$\underline{a}$, $\underline{b}$, $\underline{c}$	unit cell vectors of a β-K_2SO_4 type structure or of the basic structure of a distorted β-K_2SO_4 type structure
$\underline{a}^*$, $\underline{b}^*$, $\underline{c}^*$	the reciprocals of $\underline{a}$, $\underline{b}$ and $\underline{c}$
$\underline{a}_1$, $\underline{a}_2$, $\underline{a}_3$	equal to $\underline{a}$, $\underline{b}$ and $\underline{c}$ respectively
$\underline{a}_1^*$, $\underline{a}_2^*$, $\underline{a}_3^*$	equal to $\underline{a}^*$, $\underline{b}^*$ and $\underline{c}^*$ respectively
a, b, ... i	types of X-X distances {fig. 4.4.1}
a_i, b_i, d_k, e_k, f_i, g_i (i=0,1,2; k=0,1,2,3,4)	values of distances of respectively types a, b, etc., used for calculating interactions <ch. 5>
A	atom type in chemical formula A_2BX_4
A_i (i=1,2)	atom of type A at position i in a β-K_2SO_4 type structure {fig. 1.4.1}
A_{ik} (i=1,2; k=1,2,3,4)	atom of type A at position ik in a distorted β-K_2SO_4 type structure {fig. 4.5.2}
A_i (i=1,2,3)	amplitude of modulation function $d_i(t)$ {eq.3.5.3} <ch. 3 and 4 >
A_i or A (i=1,2,3,4)	*amplitude of modulation function* $d_2(t)$ of atom X_{2i} {eq. 5.4.1} <ch. 5>
A, B, ... M	types of A-X distances {fig. 4.4.1}
B	atom type in the chemical formula A_2BX_4
B_k	atom of type B at position k in a distorted β-K_2SO_4 type structure {fig. 4.5.2}
B_i or B (i=1,2,3,4)	constant part of modulation $d_2(t)$ of atom X_{2i} {eq. 5.4.1} <ch. 5>
c_1, c_2	positive coefficients in the expression for E(r) {eq. 5.3.1} <ch. 5>

c_3, c_4	positive coefficients in the expression for $E'(r)$ (eq. 5.3.2) <ch. 5>
c_s [Å]	length of $\underline{c}_s$
$\underline{c}_s$ or $\underline{C}$	supercell vector: $\underline{c}_s = \underline{C} = v\underline{c}$
$d_i(t)$ or $d_{ai}(t)$ ($i=1,2,3$)	modulation functions; components of $\underline{d}(t)$ or $\underline{d}_a(t)$ with respect to $\underline{a}_i$ ($i=1,2,3$)
d_{ic}, d_{is} ($i=1,2,3$)	*first harmonic fourier coefficients of modulation function $d_i(t)$ (eq. 3.5.2)*
$\underline{d}(t)$ or $\underline{d}_a(t)$	modulation displacement (of atom a) (eq. 1.1.2)
D [Å]	defined in equation 3.4.2 <ch. 3>
e_{ki} ($i=1,2,3$)	*components of $\underline{e}_k$ with respect to $\underline{a}_i$ ($i=1,2,3$)* <ch. 2>
$\underline{e}_k$	subcell translation vector in a supercell (k is an identification number) (eq. 2.2.9) <ch. 2>
$E(r)$	potential energy of the interaction between two X atoms as a function of the interatomic distance r (eq. 5.3.1) <ch. 5>
$E'(r)$	potential energy of the interaction between an A atom and a X atom as a function of the interatomic distance r (eq. 5.3.2) <ch. 5>
$f_a(\lvert\underline{H}\rvert)$	atomic scattering factor of atom a for the reflection with diffraction vector $\underline{H}$ (eq.2.2.1) <ch. 2>
F	potential energy of the model structure (eq. 5.2.1) <ch. 5>
F_o or F_{or}	observed structure amplitude (of reflection r)
F_{cr}	calculated structure factor of reflection r
$F(\underline{H})$	calculated structure factor of the reflection with diffraction vector $\underline{H}$ (eq.2.2.1)
F', F_1, F_1', F_1'', F_2, F_r, F_c, F_c', F_3, F_3'	potential energies of (idealized) parts of a crystal structure <ch. 5>
g	v/w (eq. 2.2.18) <ch. 2>
$G_a(\underline{H})$ or $G_{as}(\underline{H})$	*geometrical part of the structure factor of the* reflection with diffraction vector $\underline{H}$ for atom a (or as) (eq. 2.2.1) <ch. 2>
h, k, l, m	*reflection indices of a reflection with respect to* $\underline{a}^*$, $\underline{b}^*$, $\underline{c}^*$ and $\underline{q}$ (eq. 1.1.5, 1.1.6)
h_i ($i=1,2,3$)	equal to h, k and l respectively <ch. 2>

$\underline{h}$	diffraction vector of a main reflection (eq. 1.1.6)
$\underline{h}'$	defined in equation 2.2.7 <ch. 2>
H_i ($i=1,2,3$)	components of $\underline{H}$ with respect to $\underline{a}_i^*$ ($i=1,2,3$); $H_i = h_i + mq_i$
$\underline{H}$	diffraction vector; $\underline{H} = \underline{h} + m\underline{q}$ (eq. 1.1.5)
I	measured diffraction intensity <ch. 3>
K_k, L_k, M_k ($i=0,1,2,3,4$)	values of distances of respectively types K, L and M, used for calculating interactions <ch. 5>
m	satellite order (1.1.5)
$\underline{n}$	position vector of unit cell n (eq. 1.1.1)
p_a	multiplicity of atom a (eq. 2.3.1) <ch. 2>
q_i ($i=1,2,3$)	components of $\underline{q}$ with respect to $\underline{a}_i^*$ ($i=1,2,3$) <ch. 2>
$\underline{q}$	modulation wave vector (eq. 1.1.3)
r	distance between two atoms <ch. 5>
r_o	interatomic distance in an undistorted β-K_2SO_4 type structure <ch. 5>
R [m]	effective radius of a crystal <ch. 3>
R_w	residual (eq. 3.4.1)
R or R_s	3x3 rotation matrix of a 3- or 4-dimensional symmetry operation (operation s) (eq. 1.3.1)
R_{ik} ($i,k=1,2,3$)	*element of rotation matrix R*
s_i ($i=1,2,3$)	component of $\underline{s}$ with respect to $\underline{a}_i$ ($i=1,2,3$)
$\underline{s}$ or $\underline{s}_s$	shift of the 3-dimensional (part of a) symmetry operation (operation s) (eq. 1.3.1)
t	argument of a modulation function; $t = (\underline{n} + \underline{x}_o).\underline{q}$ (eq. 1.1.2)
T_i [K]	normal-to-incommensurate phase transition temperature; for Rb_2ZnBr_4: T_i = 374K
T_c [K]	incommensurate-to-commensurate phase transition temperature; for Rb_2ZnBr_4: T_c = 190K
T_3, T_4, T_5 [K]	phase transition temperatures of Rb_2ZnBr_4 at respectively 112K, 77K and 50K
$T_a(\underline{H})$ or $T_{as}(\underline{H})$	temperature factor of the reflection with diffraction vector $\underline{H}$ for atom a (or as) (eq. 2.2.1) <ch. 2>
TMA	tetramethylammonium, $N(CH_3)_4$
u, v	numerator and denominator of a rational value of γ:

	$\gamma = u/v$
u_i, v_i (i=1,2,3)	numerator and denominator of a rational value of q_i: $q_i = u_i/v_i$ (eq. 2.2.12) <ch. 2>
U_a	isotropic temperature parameter of atom a (eq. 2.2.2)
U_{ik} or U_{aik} (i,k=1,2,3)	anisotropic temperature parameters (of atom a) (eq. 2.2.3)
v	$v_1v_2v_3$ <ch. 2>
w	the smallest common multiple of v_1, v_2 and v_3 <ch. 2>
w_r	weight of reflection r in a structure refinement (eq. 2.1.1)
x, y, z	fractional coordinates of an atom with respect to $\underline{a}$, $\underline{b}$ and $\underline{c}$
x_{si} (i=1,2,3)	fractional coordinates of an atom with respect to $\underline{a}$, $\underline{b}$ and $\underline{c}_s$ <table 3.5.5>
x_{oi} or x_{oia} (i=1,2,3)	components of $\underline{x}_o$ or $\underline{x}_{oa}$ with respect to $\underline{a}_i$ (i=1,2,3)
$\underline{x}_o$ or $\underline{x}_{oa}$	the position vector of an atom (atom a) in the basic structure (eq. 1.1.1)
X	atom type in chemical formula A_2BX_4
X_i (i=1,2,3,4)	atom of type X at position i in a β-K_2SO_4 type structure (fig. 1.4.1)
X_{ik} (i,k=1,2,3,4)	atom of type X at position ik in a distorted β-K_2SO_4 type structure (fig. 4.5.2)
z_{io} (i=1,2,3,4)	z coordinates of the X_2 atoms in subcell 0 in the model: 0, 0.5, 0 and 0.5 respectively for i=1,2,3 and 4 (eq. 5.4.1) <ch. 5>
α, β, γ	components of $\underline{q}$ with respect to $\underline{a}^*$, $\underline{b}^*$ and $\underline{c}^*$; equal to respectively q_1, q_2 and q_3 (eq. 1.1.3)
α, β, γ [°]	angles between, $\underline{b}$ and $\underline{c}$, $\underline{a}$ and $\underline{c}$ and $\underline{a}$ and $\underline{b}$ respectively <table 4.3.1b>
δ	1/3 − γ <fig. 4.6.1>
∂	$\underline{a}_3^*$ component of a position in reciprocal space <fig. 4.6.4>
Δ_{ik} or Δ (i=1,2,3,4)	displacement of the X_2 atom of tetrahedron i in subcell k (eq. 5.2.1) <ch. 5>
Δy_{ik} or Δy (i=1,2,3,4)	displacement of the X_1 atom of tetrahedron i in subcell k (eq. 5.3.25) <ch. 5>
ε or ε_s	factor in the 4-th dimension of a symmetry operation (operation s) (eq. 1.3.1)
ε_1, ε_2, ε_3	coefficients in the model potential energy expression (eq. 5.2.1) <ch. 5>
ε_1', ε_2', ε_2'', ε_3', ε_4	coefficients in potential energy expressions <ch. 5>
μ [m^{-1}]	linear absorption coefficient of X-rays or neutrons in Rb_2ZnBr_4 <ch. 3>
σ	calculated standard deviation of a model parameter <ch. 3>
σ	coefficient in the model potential energy expression (eq. 5.2.1) <ch. 5>
$\sigma(F_o)$	standard deviation of F_o <ch. 3>
σ(I)	standard deviation of I <ch. 3>
σ_o	defined in equation 5.4.10 <ch. 5>
σ_2, σ_4	coefficients in potential energy expressions <ch. 5>
τ or τ_s	shift of the modulation wave in a 4-dimensional symmetry operation (operation s) (eq. 1.3.1)
φ_i (i=1,2,3)	phase of modulation function $d_i(t)$ (eq. 3.5.3) <ch. 3 and 4>
φ_i or φ (i=1,2,3,4)	phase of modulation function $d_2(t)$ of atom X_{2i} (eq. 5.4.1) <ch. 5>
φ_{ka}	$(\underline{x}_{ok} + \underline{e}_k).\underline{q}$; argument of the modulation function (eq. 2.2.11) <ch. 2>
χ, χ′	coefficients in potential energy expressions <ch. 5>

LIST OF REFERENCES

Aalst, W. van, Hollander, J. den, Peterse, W.J.A.M. and Wolff, P.M. de (1976): Acta Cryst. B 32, 47

Altermatt, D., Arend, H., Gramlich, V., Niggli, A. and Petter, W. (1984): Acta Cryst. B 40, 347

Azaroff, L.V. (1955): Acta Cryst. 8, 701

Belobrova, I.A., Aleksandrova, I.P. and Moskalev, A.K. (1981): Phys. Stat. Sol. (a) 66, K17

Boer, J.L. de (1984): private communication

Broda, H. (1984): Phys. Stat. Sol. (a) 82, K117

Catti, M., Gazzoni, G. and Ivaldi, G. (1983): Acta Cryst. C 39, 29

Cowley, J.M., Cohen, J.B., Salamon, M.B. and Wuensch, B.J. (1979): editors of "Modulated Structures", AIP Conference Proceedings 53

Cruickchank, D.W.J. (1956): Acta Cryst. 9, 754

Dam, B. and Janner, A. (1983): Z. Kristallogr. 165, 247

Deas, H.D. (1960): Z. Kristallogr. 114, 310

Denoyer, F., Moudden, A.H., Bellamy, A., Currat, R.. Vettier, C. and Lambert, M. (1981): C.R. Acad. Sc. Paris II 292, 13

Eysel, W. (1971): "Strukturelle und kristallchemische Verwantschaft bei Verbindungen $A_2(BX_4)$ und $A_2(BX_3)$", Habilitationsschrift, Aachen

Flack, H.D. (1974): Acta Cryst. A 30, 569

Flack, H.D. (1975): J. Appl. Cryst. 8, 520

Gesi, K. (1982): J. Phys. Soc. Jap. 51, 2532

Gesi, K. and Iizumi, M. (1978): J. Phys. Soc. Jap. 45, 1777

Gesi, K. and Iizumi, M. (1979a): J. Phys. Soc. Jap. 46, 697

Gesi, K. and Iizumi, M. (1979b): AIP Conference Proceedings 53, 211

Gunter, J.R. and Jameson, G.B. (1984): Acta Cryst. C 40, 2074

Hamilton, W. (1965): Acta Cryst. 18, 502

Haque, M.S. and Hardy, J.R. (1980): Phys. Rev. B 21, 245

Hasebe, K., Mashiyama, H., Tanisaki, S. and Gesi, K. (1982): J. Phys. Soc. Jap. 51, 1045

Hasebe, K., Mashiyama, H., Tanisaki, S. and Gesi, K. (1984): J. Phys. Soc. Jap. 53, 1866

Herbert, I.R. and Campbell, S.J. (1977): J. Appl. Cryst. 10, 18

Hogervorst, A.C.R. (1984): MRS Symposium Proceedings 21, 137

Hogervorst, A.C.R. and Wolff, P.M. de (1982): Sol. St. Comm. 43, 179

Iizumi, M., Axe, J.D., Shirane, G. and Shimaoka, K. (1977): Phys. Rev. B 15, 4392

Iizumi, M. and Gesi, K. (1977): Sol. St. Comm. 22, 37

Iizumi, M. and Gesi, K. (1983): J. Phys. Soc. Jap. 52, 2526

International Tables for Crystallography (1983): Vol. A, Dordrecht, Boston: D. Reidel Publishing Company

International Tables for X-ray Crystallography (1959): Vol. II, Birmingham: Kynoch Press

International Tables for X-ray Crystallography (1962): Vol. III, Birmingham: Kynoch Press

International Tables for X-ray Crystallography (1974): Vol. IV, Birmingham: Kynoch Press

Jager, G. de (1980): internal report, Delft

Janner, A. and Janssen, T. (1979): Physica 99A, 47

Janssen, T. (1985): to appear

Janssen, T. and Tjon, J.A. (1981): Phys. Rev. B 24, 2245

Janssen, T. and Tjon, J.A. (1982): Phys. Rev. B 25, 3367

Janssen, T. and Tjon, J.A. (1983): J. Phys. C 16, 4789

Jost, K.H., Ziemer, B. and Seydel, R. (1977): Acta Cryst. B 33, 1696

Kalman, A., Stephens, J.S. and Cruickshank, D.W.J. (1970): Acta Cryst. B 26, 1451

Kleef, R.P.A.R. van, Rasing, Th., Stoelinga, J.H.M. and Wyder, P. (1981): Sol. St. Comm. 39, 433

Koester, L. and Yelon, W.B. (1982): Neutron Diffraction Newsletter, december

Koningsveld, H. van (1983): Acta Cryst. C 39, 15

Lauher, J.W. and Ibers, J.A. (1975): Inorg. Chem. 14, 384

Lopez Echarri, A., Tello, M.J. and Gili, P. (1980): Sol. St. Comm. 36, 1021

Maeda, M., Honda, A. and Yamada, N. (1983): J. Phys. Soc. Jap. 52, 3219

Marion, G. (1981): J. Physique 42, 469

Marion, G., Almairak, R., Lefebvre, J., Ribet, M. (1981): J. Phys. C 14, 3177

Mashiyama, H. and Tanisaki, S. (1981): J. Phys. Soc. Jap. 50, 1413

Mashiyama, H. and Tanisaki, S. (1982): J. Phys. C 15, L455

Mashiyama, H. Tanisaki, S. and Hamano, K. (1981): J. Phys. Soc. Jap. 50, 2139

Matsunaga, H. (1982): J. Phys. Soc. Jap. 51, 864

Matsunaga, H., Itoh, K. and Nakamura, E. (1982): Acta Cryst. B 38, 898

McGinnety, J.A. (1972): Acta Cryst. B 28, 2845

Mikhail, I. and Peters, K. (1979): Acta Cryst. B 35, 1200

Misyul, S.V., Kruglik, A.I. and Simonov, M.A. (1980): Sov. Phys. Cryst. 25, 273

Moudden, A.H., Svensson, E.C., Shirane, G. (1982): Phys. Rev. Lett. 49, 557

Muller, O. and Roy, R. (1974): "The Major Ternary Structural Families", Berlin: Springer-Verlag

Nelder, J.A. and Mead, R. (1965): The Computer Journal 7, 308

Nomoto, K., Atake, T., Chaudhuri, B.K. and Chihara, H. (1983): J. Phys. Soc. Jap. 52, 3475

Onodera, A. and Shiozaki, Y. (1979): J. Phys. Soc. Jap. 46, 157

Pater, C.J. de (1978): "An experimental study of the incommensurate phase transformations in Rb$_2$ZnBr$_4$ and Na$_2$CO$_3$", Thesis, Delft

Pater, C.J. de (1979): Acta Cryst. B 35, 299

Pater, C.J, de, Axe, J.D. and Currat, R. (1979): Phys. Rev. B 19, 4684

Peterse, W.J.A.M. and Palm, J.H. (1966): Acta Cryst. 20, 147

Plesko, S. (1981): "Neue Folge von kommensurablen und inkommensurablen Phasen in Kristallen vom β-K$_2$SO$_4$ Typ", Thesis, Zuerich

Quilichini, M. and Pannetier, J. (1983): Acta Cryst. B 39, 657

Rasing, Th.H.M. (1982): "Experimental investigation of 4-dimensional superspace crystals", Thesis, Nijmegen

Saalfeld, H. (1975): American Minerologist 60, 824

Saalfeld, H. and Klaska (1981): Z. Kristalogr. 155, 65

Sato, T., Osaka, T. and Makita, Y. (1983): J. Phys. Soc. Jap. 52, 3297

Sato, T., Osaka, T. and Makita, Y. (1984): J. Phys. Soc. Jap. 53, 1907

Sawada, S., Shiroishi, Y., Yamamoto, A., Takashige, M. and Matsuo, M. (1977): J. Phys. Soc. Jap. 43, 2101

Scheid, F. (1968): "Numerical Analysis" (McGraw-Hill Book Co.)

Schlemper, E.O. and Hamilton, W.C. (1966): J. Chem. Phys. 44, 4498

Seifert, H.-J. and Wasel-Nielen, J. (1977): Revue de Chimie Minerale 14, 503

Shannon, R.D. (1976): Acta Cryst. A 32, 751

Shiozaki, Y. (1971): Ferroelectrics 2, 245

Shuvalov, L.A., Gridnev, S.A., Prasolov, B.N. and Sannikov, V.G. (1983): Ferroelectrics Letters 1, 85

Smid, R. (1984): internal report, Delft

Sugiyama, J., Wada, M., Sawada, A. and Ishibashi, Y. (1980): J. Phys. Soc. Jap. 49, 1405

Suza, K. and Steinfink, H. (1971): J. Sol. St. Chem. 3, 75

Suzuki, K. and Yamaguchi, G. (1968): Proc. Fifth Int. Symp. on the Chemistry of Cement, Tokyo, part I, p.67

Tanisaki, S. and Mashiyama, H. (1980): J. Phys. Soc. Jap. 48, 339

Trouelan, P., Lefebvre, J. and Derollez, P. (1984): Acta Cryst. C 40, 386

Tsakalakos, T. (1984): editor of "Modulated Structure Materials", NATO ASI Series E 83

Tuinstra, F. and Berg, A.J. van den (1983): Phase Transitions 3, 275

Ueda, T., Ikeda, S. and Terauchi, H. (1982): J. Phys. Soc. Jap. 51, 3953

Vermin, W.J., Verschoor, G.C. and IJdo, P.J.W. (1976): Acta Cryst. B 32, 3325

Wiesner, J.R., Srivastava, R.C., Kennard, C.H.L.. DiVaira, M. and Lingafelter, E.C. (1967): Acta Cryst. 23, 565

Wilhelmi, K.-A. (1966): Arkiv For Kemi 26, 157

Wolff, P.M. de (1974): Acta Cryst. A 30, 777

Wolff, P.M. de (1980): private communication

Wolff, P.M. de (1984): Acta Cryst. A 40, 34

Wolff, P.M. de, Janssen, T. and Janner, A. (1981): Acta Cryst. A 37, 652

Wu, K.K. and Brown, I.D. (1973): Acta Cryst. B 29, 2009

Yamada, N. and Ikeda, T. (1983): concept article

Yamada, Y. and Hamaya, N. (1983a): J. Phys. Soc. Jap. 52, 3466

Yamada, Y. and Hamaya, N. (1983b): Ferroelectrics 52, 243

Yamaguchi, T., Sawada, S., Takashige, M. and Nakamura, T. (1982): Jap. J. Appl. Phys. 21, L57

Yamamoto, A. (1981): Acta Cryst. A 37, 838

Yamamoto, A. (1982): Acta Cryst. A 38, 79

Yamamoto, A. (1983): Acta Cryst. B 39, 17

Zandbergen, H.W. (1981): "On ternary iodides", Thesis, Leiden

Zandbergen, H.W. (1984): private communication

NAWOORD

Graag wil ik op deze plaats iedereen bedanken die bijgedragen heeft aan het in dit proefschrift beschreven werk.

CURRICULUM VITAE

9 maart 1956	geboren te Pijnacker
1974	*diploma Atheneum B, St. Stanislas College te Delft*
1974 - 1979	studie Technische Natuurkunde, Technische Hogeschool Delft propadeutisch examen: 17 november 1976 Kandidaatsexamen : 17 oktober 1978 doctoraal examen : 30 oktober 1979 afstudeerrichting : Fysische Kristallografie
1979 - 1984	in dienst bij de Stichting voor Fundamenteel Onderzoek der Materie, werkzaam op het Laboratorium voor Technische Natuurkunde van de Technische Hogeschool Delft, promotieonderzoek onder leiding van prof.dr.ir. P.M. de Wolff en prof.dr.ir. F. Tuinstra
1985	*vanaf 1 januari in dienst bij het Kunststoffen en Rubber* Instituut van TNO.

STELLINGEN
behorend bij het proefschrift van
A.C.R. Hogervorst
13 mei 1986

1.
Effekten bij een lock-in faseovergang, zoals het breder worden van satellietreflekties, kunnen ook verklaard worden, als men aanneemt dat in het kristal makroskopische incommensurabele en commensurabele domeinen naast elkaar bestaan (R. Blinc, B. Lozar, F. Milia, R. Kind: J. Phys. C 17 (1984) 241; H. Mashiyama, S. Tanisaki, K. Hamano: J. Phys. Soc. Jap. 50 (1981) 2139).

2.
Een superstruktuur beschreven met een 4-dimensionale ruimtegroep die voor dit geval niet als een 3-dimensionale symmetrie opgevat kan worden, kan hooguit een goede benadering van de echte struktuur zijn (A. Yamamoto: Acta Cryst. B 38 (1982) 1446; K.D. Bronsema: proefschrift, Groningen, 1985; dit proefschrift).

3.
De door Hasebe et al. als funktie van de temperatuur gemeten modulatiegolfvectorlengte in $(N(CH_3)_4)_2CuBr_4$ wijst sterk op de aanwezigheid van superstruktuurfasen in het temperatuurgebied waarin volgens Hasebe et al. de kristalstruktuur incommensurabel is. Plateau's in deze funktie zijn verenigbaar met een 5-voudige en een 21-voudige superstruktuur (K. Hasebe, H. Mashiyama, S. Tanisaki, K. Gesi: J. Phys. Soc. Jap. 51 (1982) 1045).

4.
Incommensurabele strukturen kunnen verklaard worden met een model voor een ruimtelijke struktuur, zelfs wanneer er alleen interacties tussen naaste buren aanwezig zijn.

5.
Resultaten verkregen uit verfijningen die tot nevenminima leiden, bevatten informatie over de juiste struktuur.

6.
Het feit, dat er nog voor weinig kristallen met verplaatsingsmodulatie een mikroskopische verklaring is gevonden voor de modulatie, komt voort uit het feit, dat er nog maar weinig struktuurbepalingen van dergelijke strukturen zijn uitgevoerd.

7.
Van polaire materialen kunnen kristallen met een gemoduleerde struktuur gemaakt worden door ze te laten kristalliseren in een geschikt periodiek wisselend elektrisch veld.

8.
Het is aan te bevelen om de onderzoeksinspanning op het gebied van elektrostatische kontaktoplading, die in de kunststoffenindustrie veel problemen veroorzaakt, te vergroten.

9.
Mensen kunnen voor iedere verstandelijke taak computer(programma')s maken, die deze taak beter kunnen uitvoeren dan zijzelf.

10.
De berichtgeving over akties voor salarisverhoging zou objektiever zijn, als ook het huidige salaris van de aktievoerders vermeld werd.

11.
Uit het feit, dat hondenbezitters hun honden bijna nooit voor eigen voordeur of in eigen tuintje hun behoefte laten doen, blijkt, dat ook zij uitwerpselen van honden vies vinden.